



**UNIVERSIDADE FEDERAL DO PARÁ
INSTITUTO DE TECNOLOGIA
PROGRAMA DE PÓS-GRADUAÇÃO EM ENGENHARIA ELÉTRICA**

**A Radio Propagation Model for Mixed Paths in Amazon
Environments for the UHF Band**

LESLYE ESTEFANIA CASTRO ERAS

TD: 01/2019

**UFPA / ITEC / PPGEE
Belém - Pará - Brazil
January 2019**

UNIVERSIDADE FEDERAL DO PARÁ
INSTITUTO DE TECNOLOGIA
PROGRAMA DE PÓS-GRADUAÇÃO EM ENGENHARIA ELÉTRICA

LESLYE ESTEFANIA CASTRO ERAS

**RADIO PROPAGATION MODEL FOR MIXED PATHS IN AMAZON
ENVIRONMENTS FOR THE UHF BAND**

TD: 01/2019

Thesis submitted to the Examining Board of the Programa de Pós-Graduação em Engenharia Elétrica from Universidade Federal do Pará for obtaining PhD degree in Electrical Engineering, with emphasis on Telecommunications.

UFPA / ITEC / PPGEE
Belém - Pará - Brazil
January 2019

**Dados Internacionais de Catalogação na Publicação (CIP) de acordo com ISBD
Sistema de Bibliotecas da Universidade Federal do Pará
Gerada automaticamente pelo módulo Ficat, mediante os dados fornecidos pelo(a) autor(a)**

C355r Castro Eras, Leslye Estefania.
A Radio Propagation Model for Mixed Paths in Amazon Environments for the UHF Band / Leslye Estefania Castro Eras, . — 2019.
xxi, 87 f. : il. color.

Orientador(a): Prof. Dr. Gervásio Protásio dos Santos Cavalcante
Coorientador(a): Prof. Dr. Luis Manuel de Jesús Sousa Correia
Tese (Doutorado) - Programa de Pós-Graduação em Engenharia Elétrica, Instituto de Tecnologia, Universidade Federal do Pará, Belém, 2019.

1. trajeto misto, Televisão Digital, Teoria uniforme da Difração, Teoria geométrica da difração.. I. Título.

CDD 384

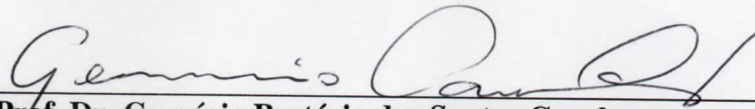
**“A RADIO PROPAGATION MODEL FOR MIXED PATHS IN AMAZON
ENVIRONMENTS FOR THE UHF BAND”**

AUTORA: LESLYE ESTEFANIA CASTRO ERAS

TESE DE DOUTORADO SUBMETIDA À BANCA EXAMINADORA APROVADA PELO
COLEGIADO DO PROGRAMA DE PÓS-GRADUAÇÃO EM ENGENHARIA ELÉTRICA, SENDO
JULGADA ADEQUADA PARA A OBTENÇÃO DO GRAU DE DOUTORA EM ENGENHARIA
ELÉTRICA NA ÁREA DE TELECOMUNICAÇÕES.

APROVADA EM: 22/01/2019

BANCA EXAMINADORA:

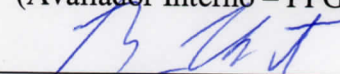


Prof. Dr. Gervásio Protásio dos Santos Cavalcante
(Orientador – PPGEE/UFPA)

Prof. Dr. Luis Manuel De Jesus Sousa Correia
(Co-Orientador – IST/UL)



Prof. Dr. Fabrício Jose Brito Barros
(Avaliador Interno – PPGEE/UFPA)



Prof. Dr. Bruno Souza Lyra Castro
(Avaliador Externo ao Programa – CCAST/UFPA)

Prof.^a Dr.^a Fernanda Carla Lima Ferreira
(Avaliadora Externa – UNIFESSPA)

Prof. Dr. António Manuel Restani Graça Alves Moreira
(Avaliador Externo – IST/UL)

VISTO:

Prof.^a Dr.^a Maria Emília de Lima Tostes
(Coordenadora do PPGEE/ITEC/UFPA)

DEDICATION

This work is dedicated to Gonzalo (+), Leslye, Adriana, Jonathan, Panchita, Diego, teachers and friends.

ACKNOWLEDGMENT

In our life we found people whom we have to thank because they directly or indirectly helped our goals come to an end. One of those goals for me is this thesis. I thank God for giving me the life and opportunity to meet incredible people. I begin by thanking my dad who once said that I would be a researcher; you were right dad, a giant hug to the sky, for always trusting me. Then my grandfather who always encourage me to study, although we could not see each other to say goodbye, I'm happy knowing that you were happy when I started the first publications. My dear mom, whom your cousins call an "iron woman", I am your admirer, I will never understand how you did so much with so little. Thank you for teaching me to be strong, but especially for your unconditional love. To Panchita for her uninteresting love, that few people can have and I have had; I'm very grateful for that. My brothers, Adriana and Jonathan, I love you very much, thank you for always giving me a word of encouragement, making me laugh, rebuke me, show me the great people that have become. To Diego Kasuo, thank you for supporting me, for always being with me, to make my ice heart beat again, God bless us always, my beloved fiancé.

None of this would be possible without the excellent opportunity afforded by the Organization of American States of scholarships between Ecuador and Brazil. Thanks to Professor Iracilda Sampaio, who received scholarship recipients with great affection in Belém do Pará. Thanks to Professor Evaldo Peláes and Professor Emilia Tostes for receiving me at UFPA's Electrical Engineering program. And to the emeritus advisor Prof. Gervásio Cavalcante, who received me at LCT, to all LCT members, teachers Fabricio, Jasmine, Josiane, Bruno, Miercio, my colleagues, Nelson, Allan(2), Iury, Andrea, Victor, Edemir, Tiago, Charlene, Walter, Brenda, Alexis, Fabio , Helio, Michele, Sidnir, Rita, Andre, Cristiane, Davison, Hugo, Ramz, Simone, Herminho and Wirlan.

Thank you very much to Professor Luis Correa, who received me in Portugal as a guest researcher for sharing his knowledge and contributing greatly to this thesis. To my new friends of INESC Kenan, Behnam, Morgan and Ramona; knowing their cultures was incredible, but more incredible meeting excellent people..

Thank you to my family and family of Kasuo who are always taking care of me, thanks for the affection. My grandparents (father) for their prayers and Mrs. Estelita for her words of esteem and for being the complement of my grandpa.

EPIGRAPH

“Things are not impossible, they only are more difficult.”

Miguel Angel Eras Soto (Dear grandpa)

Table of Contents

List of Figures.....	XIII
List of Tables.....	XV
List of Acronyms.....	XVI
List of Symbols.....	XVII
ABSTRACT.....	XXI
RESUMO.....	XXII
Chapter 1 – Introduction.....	1
1.1. Television in Brazil.....	1
1.2. Motivation.....	2
1.3. Objectives.....	3
1.4 Technics used to develop the model.....	3
1.5. Contributions.....	4
1.6. Organization of the thesis.....	6
Chapter 2 – Related papers.....	7
Chapter 3 – Fundamentals of Radio Propagation.....	11
3.1 – Introduction.....	11
3.2 – Radio propagation models.....	11
3.2.1 Okumura-Hata.....	11
3.2.2 Cost 231 model -Walfish-Ikegami.....	12
3.2.3 Recommendation ITU-R-P.1546.....	13
3.3 – Plane wave.....	15
3.4 – Fresnel zones.....	15
3.5 Geometrical Optics.....	17
3.5.1 Field of direct wave.....	18
3.5.2 Reflected field.....	18
3.5.3 Refracted/Transmitted field.....	21
3.6 Uniform Theory of Diffraction.....	24
3.7 Ray Tracing.....	27
3.8 Lateral Wave.....	28
3.8 Final considerations.....	30
Chapter 4 – Proposed Model: Mixed Path.....	31
4.1 Introduction.....	31
4.2 Scenario.....	31
4.3 Formulation.....	33
4.3.1 Formulation for City Path for M-DTV.....	34
4.3.2 Formulation for Water1 Path for M-DTV.....	36

4.3.3 Formulation for Water2 Path for M-DTV	37
4.3.4 Formulation for City Path for H-DTV	41
4.3.5 Formulation for Forest1 Path for H-DTV	41
4.3.6 Formulation for Forest2 Path for H-DTV	42
4.3.7 Summary of Mixed Path model formulation for M-DTV	43
4.4 Final considerations	44
Chapter 5 – Results of the proposed model	45
5.1 Introduction	45
5.2 Analysis of Mixed Path model parameters	45
5.3 Measurement Campaign	65
5.4 Results for Mixed Path model	68
5.4.1 Results for M-DTV City	68
5.4.2 Results for M-DTV City-Water1-Forest1-Water2	70
5.4.2 Results for H-DTV	79
5.4.3 Comparison between H-DTV and M-DTV	82
5.5 Final Considerations	82
Chapter 6 – Conclusions and Future Works	83
References	85

List of Figures

Fig. 1. Capitals of cities where Analogical TV was switched off	1
Fig. 2. A plane wave propagation trough space at a single moment in time.....	15
Fig. 3. Successive Fresnel zones	16
Fig. 4. Infinitesimally narrow diverging astigmatic ray tube, for which both ρ_1 and ρ_2 are positive (ρ is the astigmatic difference).....	17
Fig. 5. Reflected wave for : a) Vertical polarization, b) Horizontal polarization [33].....	19
Fig. 6. - Reflection coefficient magnitude for a frequency of 100MHz with $\epsilon_r=4$ and $\epsilon_r=12$, a) Vertical Polarization and b) Horizontal Polarization	20
Fig. 7. Refraction of a wave	21
Fig. 8. Diffracted wave	24
Fig. 9. Fresnel Transition function: a) Magnitude b) Phase	26
Fig. 10. Scattered field from a wedge with plane using UTD diffraction coefficients: a) Scattered field, b) Scattered field recalculated by the author	27
Fig. 11. Image method is used to find the difference between direct ray and reflected ray....	28
Fig. 12. Critical angle that produces a lateral wave	29
Fig. 13. Critical angle for Mixed Path.....	30
Fig. 14. Scenario for Mixed Path model for the services of M-DTV and H-DTV.	31
Fig. 15. Width of street and width of building.	32
Fig. 16. Rays used in Mixed Path for calculation of total electric field for M-DTV and H-DTV.....	32
Fig. 17. Rays used in Mixed Path for calculation of total electric field for M-DTV and H-DTV.....	46
Fig. 18. Variation of α when the receiver is in the same street from a top view.....	47
Fig. 19. Electric field for the variation of alpha when the receiver is in the same street.	47
Fig. 20. Variation of angle α using the same distance between transmitter and receiver from a top view.	48
Fig. 21. Angle α vs Electric field.....	48
Fig. 22. Height of building vs Electric field.....	49
Fig. 23. Width of the city vs Electric field.....	50
Fig. 24. Height of transmitter antenna vs Electric field.....	51
Fig. 25. Height of receiver antenna vs Electric field.....	52
Fig. 26. Values electric field vs receiver antenna height from 9.65 m to 12.2m.....	53
Fig. 27. Values electric field vs receiver antenna height from 1 m to 5 m.....	53
Fig. 28. Values of electric field for a receiver antenna of 1 m height in different distances...54	
Fig. 29. Distance over the water vs Electric field.....	55
Fig. 30. Level of water for a 5 m receiver height over the water vs Electric field.....	56
Fig. 31. Electric field vs level of water for a 10 m receiver height	56
Fig. 32. Electric field vs incidence angle Forest-Air.....	57
Fig. 33. Electrical parameters for forest vs Electric field.....	58
Fig. 34. Amplitude of each ray of total electrical field for sparse forest.....	59
Fig. 35. Amplitude of each ray of total electrical field for medium forest.....	59
Fig. 36. Amplitude of each ray of total electrical field for dense forest.....	60
Fig. 37. Electrical parameters for buildings vs Electric field.....	61
Fig. 38. Electrical parameters for water vs Electric field.....	62
Fig. 39. Radiation Diagram of Transmitter Antenna.....	63
Fig. 40. Radiation Diagram of Receiver Antenna.....	63
Fig. 41. Electric field vs azimuth of transmitter antenna	64
Fig. 42. Reception points for the first measurement campaign in City.....	65

Fig. 43. Reception points for the second measurement campaign for City-River-Forest-River.	66
Fig. 44. City-river path in Belém of Pará.	66
Fig. 45. River-Forest path in Belém of Pará.	67
Fig. 46. Spectrum analyzer and GPS.	67
Fig. 47. Receiver antenna over Curupira Ship.	68
Fig. 48. Electric field amplitude of each ray for total electric field in City	69
Fig. 49. Results of different Radio Propagation models over Belém City for M-DTV.	69
Fig. 50. Electric field amplitude of each ray for total electric field calculated for Radial 1 over Water1 and Water2.	71
Fig. 51. Results for Radial 1 over Water 1 and over Water 2.	72
Fig. 52. Electric field amplitude of each ray for total electric field calculated for Radial 2 over Water1 and Water2.	73
Fig. 53. Results for Radial 2 over Water 1 and over Water 2.	74
Fig. 54. Electric field amplitude of each ray calculated for Radial 3 over Water1 and Water2.	75
Fig. 55. Results for Radial 3 over Water 1 and over Water 2.	76
Fig. 56. Results in annuli for Mixed Path.	77
Fig. 57. Radio propagation models results for H-DTV - Radial 1.	80
Fig. 58. Radio propagation models results for H-DTV - Radial 2.	81
Fig. 59. Radio propagation models results for H-DTV - Radial 3.	81
Fig. 60. Comparison of Mixed Path model results for Radial 2 between M-DTV and H-DTV	82

List of Tables

Table I- Parameters for Mixed Path model	33
Table II- Rays used in Mixed Path model	34
Table III- Values for parameters used in Mixed Path model	46
Table IV- Angle of incidence Forest-Air and transmitted angle forest ar.....	57
Table V- Electrical parameters for different types of concrete [39].....	61
Table VI- Electrical parameters for water	62
Table VII. RMSE for Radial 1- M-DTV	73
Table VIII. RMSE for Radial 2- M-DTV	75
Table IX. RMSE for Radial 2- M-DTV.	77
Table X-RMSE for M-DTV	78
Table XI- Comparison between electric field from City and Water2	78
Table XII- RMS Error for H-DTV	80

List of Acronyms

E	<i>Electric Field</i>
ERP	<i>Effective Radiated Power</i>
EIRP	<i>Effective Isotropic Radiated Power</i>
GO	<i>Geometrical Optics</i>
GPS	<i>Global Positioning System</i>
GTD	<i>General Theory of Diffraction</i>
HF	<i>High Frequency</i>
H-DTV	<i>Home Digital Television</i>
IEEE	<i>Institute of Electrical and Electronics Engineers</i>
ITU	<i>International Telecommunication Union</i>
MF	<i>Medium Frequency</i>
M-DTV	<i>Mobile Digital Television</i>
RMS	<i>Root Mean Square</i>
UFPA	<i>Universidade Federal do Pará (Federal University of Para)</i>
UHF	<i>Ultra-High Frequency</i>
UTD	<i>Uniform Theory of Diffraction</i>

List of Symbols

L_b :	Path loss
E :	Electric Field
f :	Frequency
L_{sub} :	Path loss for suburban areas
E_{sea} :	Electric field over the sea
E_{land} :	Electric field on the land
d_F :	Distance of Fraunhofer
λ :	Wavelength
r_n :	Number of radio of Fresnel
d_1 :	Distance between the transmitter and the obstacles
d_2 :	Distance between the obstacle and the receiver.
v :	Fresnel Kirchoff diffraction parameter
e^{-ks} :	Phase shift along the ray path
$A(s)$:	Spreading factor
E_{LOS} :	Electric field for direct ray
P_T :	Transmission Power.
G_T :	Gain of transmitter antenna
L :	Loss for connectors, cable, etc
k :	Free space propagation constant
Γ_V :	Coefficient of reflection for Vertical polarization
Γ_H :	Coefficient of reflection for Horizontal polarization
η_i :	Intrinsic impedance of media i
σ :	Conductivity in (S/m)
ϵ :	Permittivity (F/m)
R_{Tp_r} :	Distance between the transmitter and the point of reflection
R_{p_rR} :	Distance between the receiver and the point of reflection
τ_V :	Coefficient of refraction/transmission for Vertical polarization
τ_H :	Coefficient of refraction/transmission for Horizontal polarization
E_t :	Electric field of transmission
R_{Tp_t} :	Distance between the transmitter and the point of transmission.
E_r :	Electric field of reflection
n :	Incidence point of transmission forest-air.
$R_{p_t n}$:	Distance inside the forest between p_t and n , the point of incidence of refraction forest-air
R_{nR} :	Distance between n and the receiver
τ_{af} :	Transmission coefficient air-forest
τ_{fa} :	Transmission coefficient forest-air
β :	Phase constant
μ :	permeability
α :	Attenuation constant
ω :	Angular frequency
D :	Diffraction coefficient
ϕ' :	Incidence angle of diffraction
ϕ :	Angle between the 0 face and the diffracted ray
s :	Distance between the fount (F) and the point of incidence of diffraction.

s' :	Distance between point of incidence of diffraction and the observation point (O)
G_0 :	Value to include the grazing effects in the surface 0.
G_n :	Value to include the grazing effects in the surface n.
E_d :	Diffacted electric field.
b :	Point of diffraction
R_{TB} :	Distance between transmitter and b.
θ_c :	Critical Angle
h_T :	Height of transmitter over ground
h_R :	Height of receiver
h_b :	Height of building over ground
h_g :	Height of ground
h_f :	Height of forest
d_{TR} :	Distance between transmitter and receiver over the ground
R_{TR} :	Direct distance between transmitter and receiver
W_s' :	Width of the street considering α (top view)
$W_{w1,2}$:	Width of Water1 or Water2
$W_{F1,2}$:	Width of Forest1 or Forest2
W_c :	Width of city with constructions
W_b' :	Width of the building considering α (top view).
α :	Angle between transmitter-receiver and the street or building (top view) Fig.15
W_s :	Width of the street from top view Fig. 15
W_b :	Width of the building from top view Fig. 15
p_t :	Incidence point of transmission
b :	Incidence point of diffraction
θ_{rv} :	Grazing angle for reflection on a vertical surface
θ_{rh} :	Grazing angle for reflection on a horizontal surface
θ_D :	Angle of direct ray
ψ_{iaf} :	Incidence angle for transmission air-forest
ψ_{taf} :	Transmission angle for air-forest
ψ_{ifa} :	Incidence angle for transmission forest-air
ψ_{tfa} :	Transmission angle for forest-air
z :	Point of transmitter placement
g :	Point of the base of the building
E_{rh} :	Electric field for a reflection on a horizontal surface.
E_{rv} :	Electric field for a reflection on a vertical surface.
E_{d-} :	Electric field for a diffraction on the left.
E_{d+} :	Electric field for a diffraction on the right.
E_{d-rh} :	Electric field for a diffraction on the left, reflection on a horizontal surface.
E_{d+rh} :	Electric field for a diffraction on the right, reflection on a horizontal surface
E_{d-rv} :	Electric field for a diffraction on the left, reflection on a vertical surface
E_{d+rv} :	Electric field for a diffraction on the right, reflection on a vertical surface
h :	Height of the obstacle for the calculation of the Fresnel parameter
$E_{\Sigma MC}$:	Total electric field for MDTV in City
d_{W1} :	Distance only over Water 1
C_{W1} :	Correction factor for City-Water
$E_{\Sigma MPW1}$:	Total electric field for MDTV over Water 1
d_{TF1} :	Distance between the transmitter and Forest 1
d_{W2} :	Distance only for MDTV over Water 2
d_{TF2} :	Distance between the transmitter and Forest 2

d_g :	Distance of grazing diffraction
C_{W2} :	Correction Factor for Water 2
$E_{\Sigma MPW2}$:	Total electric field for MDTV over Water 2
$E_{\Sigma HC}$:	Total electric field for HDTV in City
$E_{\Sigma HF1}$:	Total electric field for HDTV in Forest 1
d_b :	Break point distance

ABSTRACT

The present work proposes a radio propagation model for the Amazon region called Mixed Path. The techniques used for Mixed Path model are Geometrical Optics (GO) and the Uniform Theory of Diffraction (UTD). Only ten rays are considered the main contributors to calculate the total electric field. Increasing the number of rays does not improve the accuracy of Mixed Path model since the scenario is for receivers located in long distances. Then slope diffraction or multiple reflections means a low electric field that does not contribute significantly to the total electric field. The parameters of Mixed Path model such as electrical constants, antennas height, buildings height among others, are analyzed in order to know the influence of them in the received electric field. Measured data in the central frequency of 521 MHz of a Digital Television station in the city of Belem of Pará are used to validate Mixed Path model. This city is located in the Amazon region of Brazil and presents mixed routes formed by city, river, and forest. Because digital television has a wide coverage and reception flexibility, Mixed Path was designed for receivers at the user's level for the service of Mobile Digital Television (M-DTV) and for fixed receivers on the rooftops of homes for Home digital television (H-DTV). Finally, the proposed model and other models in the literature are compared with the data measured for M-DTV, being Mixed Path the model with the lowest RMS error with a value of 3.15 dB for a receiver over the river behind the city and behind the forest.

Key words: mixed path, Digital Television, Uniform Theory of Diffraction, Geometric Theory of diffraction.

RESUMO

O presente trabalho propõe um modelo de radio propagação para a região Amazônica denominado Mixed Path. As técnicas usadas pelo modelo proposto são a ótica geométrica (GO) e a teoria uniforme da difração (UTD). Adicionalmente, para melhorar o desempenho do modelo são escolhidos unicamente dez raios, que são considerados os principais para o cálculo do campo elétrico total recebido. Aumentar o número de raios não melhora a precisão de Mixed Path porque os receptores estão localizados em grandes distancias do transmissor, portanto, uma difração dupla ou várias reflexões não contribuem significativamente ao campo elétrico total. Os parâmetros usados no modelo tais como constantes elétricas, altura das antenas, altura dos prédios, entre outros, são analisados para conhecer a influência dos mesmos no campo elétrico total. Para validar este modelo, são usadas medidas na frequência central de 521 MHz de uma estação de televisão digital na cidade de Belém do Pará. Esta cidade está localizada na Região Amazônica do Brasil e apresenta percursos mistos formados por cidade, rio e floresta. Devido ao fato de que a televisão digital tem uma ampla cobertura e flexibilidade de recepção, o modelo Mixed Path foi projetado para receptores na altura dos usuários, no caso do serviço de Televisão Digital Móvel (M-DTV) e, para receptores fixos sobre os telhados das casas, para o serviço de televisão digital em casa (H-DTV). Finalmente o modelo proposto e outros modelos existentes na literatura são comparados com os dados medidos para M-DTV, sendo o modelo proposto o modelo com o menor erro RMS com um valor de 3.15 dB, para um receptor localizado sobre a água após a cidade e após a floresta.

Palavras chaves: trajeto misto, Televisão Digital, Teoria uniforme da Difração, Teoria geométrica da difração.

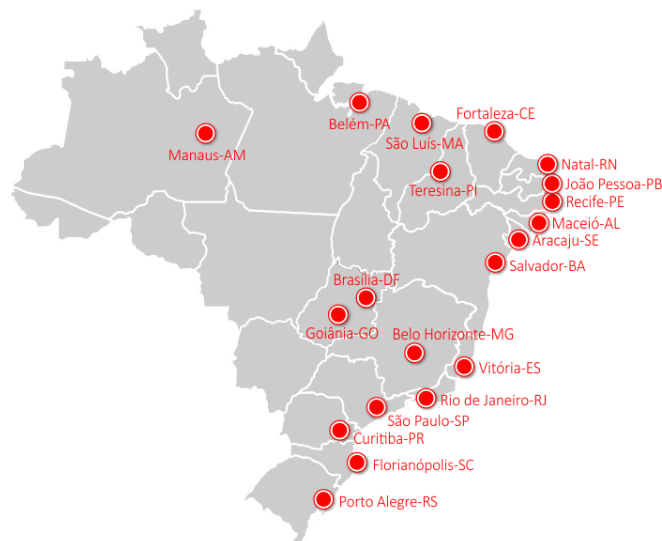
Chapter 1 – Introduction

1.1. Television in Brazil

In 1960 radio was the most popular telecommunication system in Brazil; television was beginning its popularization in São Paulo, Rio de Janeiro, Belo Horizonte, Porto Alegre and Salvador. However, with the military regime, since 1964, the State boosts television service to increase its popularization, as part of a national security policy, then television quickly enters in the majority of the Brazilian homes. Even when the military regime ended in 1985, the political relationships between the state and the television broadcasters were conserved until these days[1].

During the last years is being developed the transition between Analogical Television and Digital Television (DTV). To switch off the Analogical TV at least 93% of each state has to have access to the service of free DTV. Analogical Television was switched off in 861 cities [2]. The Brazilian System of Digital Terrestrial Television (SBTVD-T) uses the Japanese standard which is called Integrated System Digital Broadcasting (ISDB-T)[3]. Fig. 1 illustrates the capitals of the cities where the analogical signal was switched off until these days.

Fig. 1. Capitals of cities where Analogical TV was switched off



Source: [2]

The most popular channels of free DTV are Bandeirantes, Globo, Record, Rede TV, and SBT. The transmission channels in the UHF band are from number 14 to 59, it means from

470 MHz to 746 MHz. However, the 700 MHz band is being released and used to expand the fourth generation (4G) telephone and internet service in Brazil.

According to the norm NBR154604 of the Brazilian Association of Technical Standards (ABNT) [4], there are two types of receivers, the one segment, and the full segment. The one segment receivers are the portable ones which have screens smaller than 7 inches and have a bandwidth of 0.43 MHz. The full segment receivers are destined for fixed and mobile services and have a bandwidth of 5.7 MHz. The middleware for the Brazilian standard is called Ginga, created for applications with multi-user interactions. It supports Wifi, Bluetooth, Ethernet, and others. The version of Ginja-J is compatible with Globally Executable MHP (GEM) [5].

1.2. Motivation

Radio propagation models are important for planning and optimization of telecommunication systems. In Brazil, the most extended service of telecommunication is Television with coverage of 90%. Furthermore, there are not radio propagation models for the Amazon region formed by city-water and forest. In the literature can be found many papers about radio propagation for mobile digital TV (M-DTV) and fixed digital TV. In this study fixed digital TV is called Home digital TV (H-DTV) because the receiver antenna is over the rooftops of the houses. For M-DTV many scenarios have been studied including urban scenario[6], under ducts [7], mixed path land-sea[8] and indoor scenarios [9]. For the fixed DTV in [10] a study for different heights for the receiver, in different cities of Brazil for a suburban environment was presented while in [11] an indoor study to know the loss due to different materials of the constructions was analyzed.

The mixed paths currently studied are City-sea or City Forest. For City-sea most of the works are for low frequencies, the HF [12],[13], and MF bands [14], [15], [16] for vertical polarization. ITU-R Recommendation P.1546 [17], addresses the UHF band, but it does not differentiate if the first path is over land or sea, unlike the Okumura model [18], that establishes the correction for mixed path considering the first path is over water or land. However, Okumura and ITU-R P.1546 do not consider obstacles in the transition zone from land to water.

There are radio propagation models that consider mixed City-Forest path for mobile services, in [7] and [19] loss caused by forest is calculated using knife diffraction. Furthermore, the recommendation ITU-R P. 833 [20] gives an attenuation factor for forest of different countries. In the case of Brazil, the forest attenuation factor is only for Rio of

Janeiro city. Furthermore, there are some studies in the Amazon Region as in [21] where were applying dyadic green functions using four layers for air, treetop, trunk, and land for vertical polarization. Another work uses parabolic equations to calculate the electric field but has limitations with large propagation angles [22].

A less study scenario for mixed path involves land-river as in [23], which analyses propagation over water with the presence of obstacles, like buildings and bridges; however, it does not study the interaction between diffraction from a city and reflection over water, and it presents results for distances larger than 1km. Earlier works for mixed path formed by city-water do not study the transition zone city-river.

1.3. Objectives

General objective

- Develop a radio propagation model for UHF band for a mixed path in the Amazon Region, using geometrical optics and the uniform theory of diffraction for H-DTV and M-DTV.

Specific objectives

- Study the transition zone city-water, for distances less than 1 km.
- Use only the principal rays to obtain the total electric field.
- Analyze the influence of the parameters of the proposed model in the calculation of electric field.
- Compare the results of the proposed model with measured data.
- Compare the attenuation caused by the city and for the forest.
- Determine electrical parameters of forest.
- Validate the model with measured data.

1.4 Technics used to develop the model

This work is focused on outdoor radio propagation for M-DTV and H-DTV in a mixed path formed by city-water-forest not studied before. Since for planning and optimizing radio communication services, radio propagation models are necessary.

The techniques to calculate the electrical field are Geometrical Optics (GO) and Uniform Theory of Diffraction (UTD) [24]. UTD considers obstacles with finite conductivity

then it is more accurate than (Geometrical Theory of Diffraction) GTD according to [25]. Considering the electrical parameters allow characterizing each of the paths since all of them have different electrical parameters.

Earlier works implement ray reflection and diffraction for urban scenarios as the Ikegami, [26], and Walfish-Bertoni,[27] , models: the former considers grazing knife diffraction and the latter models buildings as several half-screens edges, the combination of the two being the COST231 Walfish-Ikegami model [28], duly assessed in Europe.

The proposed model called Mixed Path uses a different number of rays in each environment over study for M-DTV and H-DT. In the case of M-DTV, for the City path Mixed Path model uses eight rays: direct ray, reflected ray on the building, diffracted rays, and diffracted-reflected rays. For Water 1 four rays are necessary: direct ray, reflected ray over the water, a diffracted ray and a diffracted reflected ray. For Water 2 ten rays are necessary: direct ray, reflected ray on the forest, diffracted rays, diffracted-reflected rays and a transmitted/refracted ray. In the case of H-DTV, for City path three rays used direct ray, reflected ray on the top of the building and a diffracted ray on the building. For Forest 1 and Forest 2, four rays are necessary, direct ray, reflected ray on the building, reflected ray over the water and diffracted ray on the building.

Furthermore a correction factor is proposed to add the attenuation caused by the city when the electrical field is calculated over the water, the effect of the city was observed in [12] where a correction factor was proposed, however, this work was for low frequencies and does not consider obstacles on the border of the river. Additionally, using ray tracing as a deterministic model is possible to predict the electric field for various frequencies in the UHF band. Then, cities that have mixed paths formed by city-river-forest, the model can be used.

1.5. Contributions

This thesis presents a new radio propagation Model for a mixed path formed by City-River and Forest, not studied before. The proposed model is called Mixed Path, it calculates the electrical field for two types of reception: Mobile digital television, and Home Digital Television.

Furthermore, the electric field is calculated in the transition zone City-River in contrast to models from literature such as ITU-R. P.1546-5, Okumura Hata and Inland model. Mixed Path model considers constructions on the border of the river and the interaction of the

principal rays that arrive at the receiver located near the city over the water or near the forest over the water.

Finally, electrical parameters for the forest in Belém of Pará are calculated using a genetic algorithm (GA) from Matlab.

List of publications

1. Eras, L. E. C.; Almeida, M. ; Silva, D. K. N. ; Ferreira, H. R. O. ; Santos N. ; Barros, F. J. B. ; Cavalcante, G. P. S. “Evaluation of Radio Models Propagation for Digital TV in Mixed Paths (In Portuguese)”. *Simpósio Brasileiro de Telecomunicações e Processamento de Sinais*, Santarém, Brasil, Sept. 2016.
2. Eras, L. E. C, Luis M. Correia, Silva, D. K. N, Cavalcante, G. P. S, Barros, F. J. B. “Radio Propagation Model for Mixed paths in Amazon environments for UHF band”. *IRACON*, Graz Austria, Sept. 2017.
3. Eras, L. E. C, Silva, D. K. N, Barros, F. J. B, Luis M. Correia, Cavalcante, G. P.S “A Radio Propagation Model for Mixed Paths in Amazon Environments for the UHF Band,” *Wireless and Mobile Communication*, vol.2018, Article ID 2850830, 15 pages.
4. Silva. D.K.N, Eras. L.E.C, Antonio A. Moreira, Luis M. Correia, Barros. F. J. B, Calvacante. G.P.S, “A Propagation Model for Mixed Paths Using Dyadic Green's Functions: A Case Study over the River for a City-River-Forest Path,” *IEEE Antennas and Wireless Propagation Letters*, v. 17, Oct. 2018, p. 1-1.
5. Barbosa. B, Trindade. I, Eras. L. E. C., Aldebaro B.R.K, Barros. F. J. B, Araujo. J. P, “Methodology to Obtain Power Delay Profile in the 10 GHz, (In portuguese)”. In: *VIII Conferência Nacional em Comunicações e Rede*,. Anais da VIII Conferência Nacional em Comunicações, Redes e Segurança da Informação, Bahia p. 39-40, 2018.

1.6. Organization of the thesis

The proposal of the thesis is divided in 7 chapters:

Chapter 1: Describes the introduction, motivation and objectives and contribution of the present work.

Chapter 2: Presents earlier works about digital television and radio propagation models for mixed paths.

Chapter 3: Mention the literature in which the proposed radio propagation model is based.

Chapter 4: Development of the proposed model called Mixed Path and analysis of its parameters.

Chapter 5: Results of Mixed Path compared with measurement data and radio propagation models from literature to validate it.

Chapter 6: Conclusions and future works.

Chapter 2 – Related papers

This section describes different papers related to Digital Television and Radio Propagation models for mixed paths. It allows knowing the studied scenarios and those that were not analyzed yet. Furthermore, knowing about earlier studies allows improving the proposed solutions for mixed paths and present new solutions. Some related works are described next.

N. A. Pérez García *et al.*, “**Improved ITU-R Model for Digital Terrestrial Television Propagation Path Loss Prediction,**” *Electronics Letters*.

The Recommendation ITU-R P. 1812-4 was optimized using the bioinspired technique particular swarm optimization (PSO) [29]. A measurement campaign was carried out in Caracas Venezuela, for fixed reception in outdoor environments.

When ITU-R P.1812-4 is applying, it shows an optimistic estimation comparing with the measurement data in Caracas. There were not applied corrections effects of the land surrounding because the height of the transmitter exceeds the height for a dense urban area that is 20 m. The RMSE of ITU-R P.1812 is 21.09 dB. In order to improve the accuracy of ITU-R P.1812-4 is modified the path loss distance exponent and the independent term. After several tests, the value using PSO for x_1 was 0.9332 and for x_2 was 0.3692.

ITU-R P.1812 using optimization presents a better RMSE value, it is 10.41 dB.

W. Zhongyuan, R. Jin, and G. Junping, “**Finite Mixture Noise Models for Mobile Digital Television Channel on Urban Terrestrial Broadcasting,**” *IEEE Transactions on Broadcasting*.

In [6], three transportation environments were studied, viaduct, road, and river, because Digital TV service, is used while traveling in signal covered regions. The purpose of this work is studying the influence of average noise power of Digital TV channel in a UHF band on public transportation. The average noise power in viaducts is the highest and the most scattered of the environments according to this study. Furthermore, the average noise power in the river was higher and more discrete than on the ground roads. In addition, ISDB-T standard with the option of using a long time interleave is the most robust to impulsive noise

J. Yan and J. Bernhard, “**Investigation of the Influence of Reflective Insulation on Indoor Reception in Rural Houses,**” *IEEE Antennas and Propagation Letters*.

In [11], studies how metal affects the signal reception of DTV inside the houses and the effectiveness of using directional antennas. Generally, indoor antennas have a small aperture. Wireless Insite was used to simulate a typical house in North America, the points inside the house are distributed uniformly on a 30 cm grid. There were evaluated four transmitter positions with LOS and NLOS situations. Furthermore, the house was insulated and no insulated. From the simulations was observed that with LOS situation the reflective isolation is insignificant. However, in NLos situations, the reflective insulations can cause a significant signal fluctuation.

With path loss obtained by simulation was applying linear regression technique and were obtained four different equations for the four positions of the transmitter. The four proposed equations are evaluated with the simulated data and provide a good estimation of the average signal of path loss. Furthermore, the directional antennas for indoor TV can deteriorate the signal significantly under NLOS situations, being necessary using a 15 dB amplifier.

F. Ikegami, S. Yoshida, T. Takeuchi, and M. Umehira, **“Propagation Factor Controlling Mean Field Strength on Urban Street,”** *IEEE Transactions on Antennas & Propagation*.

A radio propagation model for an urban environment using geometrical optics and grazing knife diffraction is proposed [26]. After an analysis of model parameters, was found that building height, street width, street orientation, and mobile station antenna height affects the mean field strength. This model represents the urban environment as a city with uniform constructions. The principal rays are diffracted-reflected and diffracted. The proposed model was simplified assuming grazing diffraction. Additionally, the ground reflection was ignored and the constructions are considered infinite knife edges. This model is in agreement with the measured data. The limitation of this model is the deep diffraction caused by high frequencies and very high buildings.

C. Teague, P. Lilleboe, and D. Barrick, **“Estimation of HF Radar Mixed-Media Path Loss Using the Millington Method,”** *IEEE/OES (CWTM)*.

In [12] the propagation of high-frequency surface radar, when the transmitter is on the coast of a Beach is studied. Earlier works used Millington for distances of several kilometers,

in this study Millington was used for short distances. The values of the electrical parameters were chosen to give the best fit by eye to the measured data.

The measurements were carried out for dry sand, dry-wet sand and dry sand- wet sand and water. The paths were of 200 m to 300 m. All the three measurements were compared with predicted values using Millington, all of them have a good agreement, showing that the electrical parameters for the three different paths are correct.

Furthermore, a mixed-media propagation factor as an additional power loss is defined. Since when the path is only water it does not present that attenuation. Furthermore, the recovery effect is evident when the first path is greater than 50 m.

J. Yu, W. Chen, K. Yang, C. Li, F. Li, and Y. Shui, “**Path Loss Channel Model for Inland River Radio Propagation at 1.4 GHz,**” *International Journal of Antennas and Propagation*.

For a transmitter located on land and receiver over a river, in [23] the Inland model was proposed. They propose three improvements to Round Earth Loss (REL) model for open sea environment. These three improvements are replacing the equation of free space for Okumura suburban since the measured data over the water is well described by Okumura for the suburban environment. The second improvement is the addition of diffraction using finite widescreen which is a combination of multiple knife-edges in several directions because of the obstacles near the river bank as buildings or bridges. The third improvement is the mixed path methodology from ITU-R 1546. Measured data were carried out in 1.4 GHz for vertical polarization. Three scenarios were studied suburban, urban with the presence of bridges and urban with the presence of huge buildings.

Okumura Hata and ITU-R P.1546 are used to compare with the measured data. The quantitative analysis was develop using Root Mean Square Error (RMSE), Grey Relation Grade and Mean Absolute Percentage Error (GRG-MAPE), Pearson Correlation Coefficient and Mean Absolute Percentage error (PCC-MAPE). The biggest RMSE is 6.35 dB for the environment with huge buildings.

G.P.S.Cavalcante and A. Giarola, “**Optimization of Radio Communication in Media with Three Layers,**” *IEEE Transactions on Antennas and Propagation*

In [30] the electromagnetic radiation of a dipole in a media with three layers is studied using the Dyadic Green Functions (DGF). The far-field region is determined meanly by the lateral wave. The power loss for horizontal and vertical dipoles was calculated. The first layer

represents the top of the tree, the second layer is the trunk of the tree and the third layer is the soil. Measured data show agreement with DGF results.

J. Souza, F. Magno, Z. Valente, J. Costa, and G. Cavalcante, “**Mobile Radio Propagation Along Mixed Paths in Forest Environment using Parabolic Equations,**” *Microwave and Optical Technology Letters*.

In [22] a radio propagation model for the mixed path (city-forest) using Parabolic Equation (PE) method was proposed. Measurement campaigns in 900 MHz and 1.8 GHz were carried out. The measurement campaign considers a receiver inside the forest.

The PE showed coherence with measured data in a city-forest environment. It has a limitation with large propagation angles, however, the advantage is a less computational effort compared with similar techniques. To reduce the computational effort the system was reduced to a tridiagonal system. The method to solve the tridiagonal system is the implicit finite differences scheme of the Crank–Nicolson type.

After present some related works can be concluded that studies conducted on digital television do not contemplate mixed paths in the Amazon region. The mixed paths analyzed are city-forest or city-river; however, there are no studies about receivers over the river and behind the forest. In addition, the transition zone city-river was analyzed only for distances greater than 1 km. Therefore, a propagation model for the Amazon region considering city-river-forest-river is necessary as well as the analysis of the transition zone for distances less than 1 km.

Chapter 3 – Fundamentals of Radio Propagation

3.1 – Introduction

This chapter describes the radio propagation models existed in the literature for the UHF band in different scenarios as city, river, and forest. Furthermore, the technics used for the proposed model called Mixed Path, Geometrical Optics (GO) and the Uniform theory of diffraction (UTD) are also detailed.

3.2 – Radio propagation models

Radio propagation models predict the electric field that arrives at the receiver. They are divided into three groups: deterministic models, empirical models, and semi-deterministic models. Deterministic models use only theoretical methods, empirical models are based on measurements and the Semi-Deterministic models are a combination of measurements and theoretical methods. Next, a description of some radio propagation models.

3.2.1 Okumura-Hata

A radio propagation model widely used is the empirical model proposed by Okumura who makes an extensive measurement campaign for 10 years in Japan [18]. In order to facilitate the application of this model, Hata proposed simple equations to calculate path loss [31]. This model was designed for Suburban, Urban, Rural and Mixed scenarios.

The path loss for an urban scenario (L_b) considering an E.R.P (Effective Radiated Power) of 1 kW, is given by the following equation:

$$L_b = 69.55 + 26.16 \log(f_{MHz}) - 13.82 \log(h_t) - a(h_r) + (44.9 - 6.55 \log(h_t))(\log(d))^b \quad (1)$$

Electric field strength ($dB\mu V/m$) for an Urban environment is given by the following expression:

$$E = 69.82 - 6.16 \log(f_{MHz}) + 13.82 \log(h_t) + a(h_r) - (44.9 - 6.55 \log(h_t))(\log(d))^b \quad (2)$$

For distances greater than 20 km:

$$b = 1 + (0.14 + 0,000187f_{MHz} + 0.00107h_t)[\log(0.05d)]^{0.8} \quad (3)$$

where:

- f : Frequency, $150 \leq f \leq 1500$ MHz.

- h_t : Effective height of transmitter, $30 \leq h_t \leq 200$ m.
- h_r : Height of receiver, $1 \leq h_r \leq 10$ m.
- d : Distance (km)
- b : $1, d \leq 20$ km

$a(h_r)$ is the correction factor for the receiver antenna due to the environment around it, if $h_r = 1.5m$ $a(h_r) = 0$, in other cases:

Small city:

$$a(h_r) = (1.1 \log(f) - 0.7)h_r - (1.56 \log(f) - 0.8) \text{ dB} \quad (4)$$

Large city:

$$a(h_r) = 8.29 (\log(1.54 h_r))^2 - 1.1 \text{ dB}, f \leq 200\text{MHz} \quad (5)$$

$$a(h_r) = 3.2 (\log(11.754 h_r))^2 - 4.97 \text{ dB}, f \geq 400\text{MHz} \quad (6)$$

For suburban areas with small buildings and wide streets, the path loss formulation in dB is:

$$L_{sub} = L_b - 2 \left(\log \left(\frac{f(\text{MHz})}{28} \right) \right)^2 - 5.4 \quad (7)$$

For mixed path land-water, with $d < 30$ km:

$$\beta = d_1/d \quad (8)$$

$$K_{mp}(\beta) = -8\beta^2 + 19\beta \quad (9)$$

where:

- d_1 : Distance only over water.

3.2.2 Cost 231 model -Walfish-Ikegami

This model is the combination of Ikegami and Walfish-Bertoni models. The formulation for Walfish-Ikegami has three terms: free space loss (L_0), diffraction loss (L_{rt}) and dispersion since roofs until the roads (L_{rm})[28].

For LoS propagation in a street,

$$L_p = 42.6 + 26 \log(d(\text{km})) + 20 \log(f(\text{MHz})) \quad d > 0.02\text{km} \quad (10)$$

For NLoS propagation,

$$L_p = \begin{cases} L_0 + L_{rt} + L_{rm}, & L_{rt} + L_{rm} > 0 \\ L_0, & L_{rt} + L_{rm} \leq 0 \end{cases} \quad (11)$$

where:

$$L_{rm} = -16.9 - 10 \log(w_s(m)) + 10 \log(f(\text{MHz})) + 20 \log(H_B(m) - h_m(m)) \quad (12)$$

$$+ L_{ori}$$

with

$$L_{ori} = \begin{cases} -10 + 0.354 \varphi(^{\circ}), 0^{\circ} < \varphi < 35^{\circ} \\ 2.5 + 0.075(\varphi(^{\circ}) - 35^{\circ}), 35^{\circ} \leq \varphi < 55^{\circ} \\ 4 + 0.114(\varphi(^{\circ}) - 55^{\circ}), 55^{\circ} \leq \varphi \leq 90^{\circ} \end{cases} \quad (13)$$

and

$$L_{rt} = L_{vsh} + k_a + k_d \log(d(\text{km})) + k_f \log(f(\text{MHz})) - 9 \log(w_B(m)) \quad (14)$$

with

$$k_d = \begin{cases} 18, h_b > H_B \\ 18 - 15 \frac{h_b - H_B}{H_B}, h_b \leq H_B \end{cases} \quad (15)$$

$$L_{bsh} = \begin{cases} -18 \log(h_b - H_B + 1), h_b > H_B \\ 0, h_b \leq H_B \end{cases} \quad (16)$$

$$k_a = \begin{cases} 54, h_b \leq H_B \\ 54 - 0.8(h_b(m) - H_B(m)), d \geq 0.5 \text{ km}, h_b \leq H_B \\ 54 - 1.6(h_b(m) - H_B(m)), d \leq 0.5 \text{ km}, h_b \leq H_B \end{cases} \quad (17)$$

$$k_f = \begin{cases} -4 + 0.7 \left(\frac{f(\text{MHz})}{925} - 1 \right), \text{urban and suburban} \\ -4 + 1.5 \left(\frac{f(\text{MHz})}{925} - 1 \right), \text{dense urban} \end{cases} \quad (18)$$

where:

- h_b : Height of base station
- H_B : Height of building
- w_s : Width of street
- w_B : Distance between the buildings.
- h_m : Height of mobile receiver.
- φ : Angle between the incidence wave and the street.

3.2.3 Recommendation ITU-R-P.1546

Recommendation ITU-R P.1546 [17] is for propagation point-zone in the band (30 MHz-3 GHz), for distances between 0.1 km and 1000 km, based in measurement campaigns over the city and over the sea. Curves for an ERP of 1kW illustrate the measured data. The

nominal frequencies are: 100, 600 and 2000 MHz, height of transmitter (h_1) of 10, 20, 37.5, 75, 150, 300, 600 and 1200 m, height of receiver of 10 m over the ground and a percentage of time of 1%, 10% and 50 %.

The received electric field is calculated doing interpolations between the curves that are near the values that need to be estimated. For example, if the frequency is 500 MHz, equations for interpolation between the curves for 100 MHz and 600 MHz are used.

Furthermore, the recommendation according to with the scenario suggests adding the following corrections: obstacles around the transmitter, obstacles around the receiver, angle free of obstacles, tropospheric dispersion, a difference of antenna height, diffraction due to water, etc.

For a mixed path is proposed a methodology that consists in first calculate all the path as land, second calculate all the path as water and finally and interpolation between these two curves. The equations for this methodology are:

$$E = (1 - A) \cdot E_{land}(d_{total}) + A \cdot E_{sea}(d_{total}) \quad (19)$$

The interpolation factor:

$$A = A_0(F_{sea})^V \quad (20)$$

where:

F_{sea} is a relation between the distance only over the water (d_{ST}) and the total distance of the link (d_{total}).

$$F_{sea} = \frac{d_{ST}}{d_{total}} \quad (21)$$

$A_0(F_{sea})$ is defined analytically:

$$A_0(F_{sea}) = 1 - (1 - F_{sea})^{2/3} \quad (22)$$

The following expression is to calculate the value of V

$$V = \max \left[1.0, 1.0 + \frac{\Delta}{40.0} \right] \quad (23)$$

with

$$\Delta = E_{sea}(d_{total}) - E_{land}(d_{total}) \quad (24)$$

3.3 – Plane wave

Wave is a function of both space and time. A plane wave is characterized by the vector of the electric or magnetic field, for its complex wave number and its direction of propagation.

In the far-field region, in a small portion of the sphere surface, the spherical waves can be approximated as a plane wave. The far field is known as the Fraunhofer region that is the distance bigger than the distance of Fraunhofer, d_F , given by the following expression [32]:

$$d_F = \frac{2D^2}{\lambda} \quad (25)$$

where:

D : is the largest dimension of the transmitter

λ : Wave length

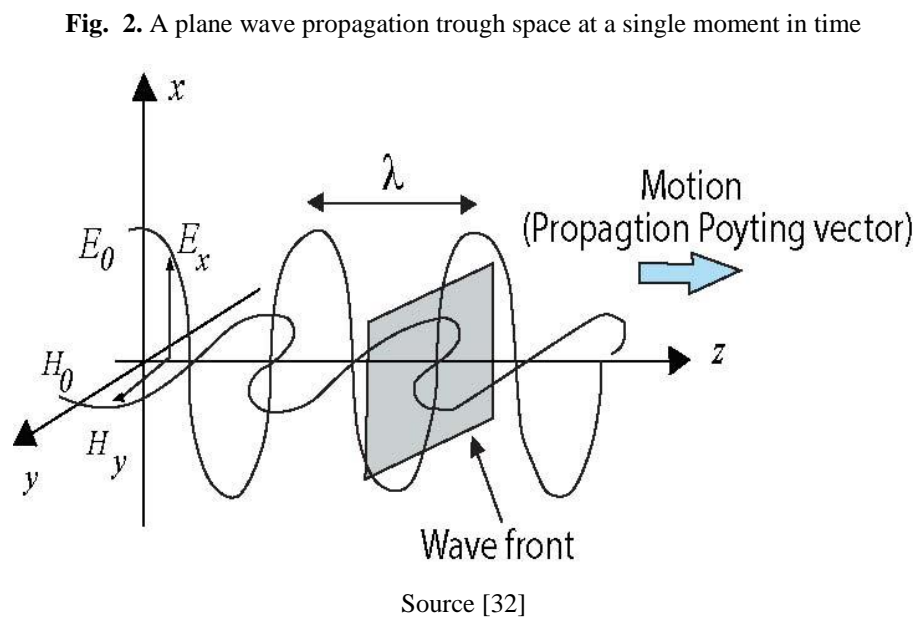


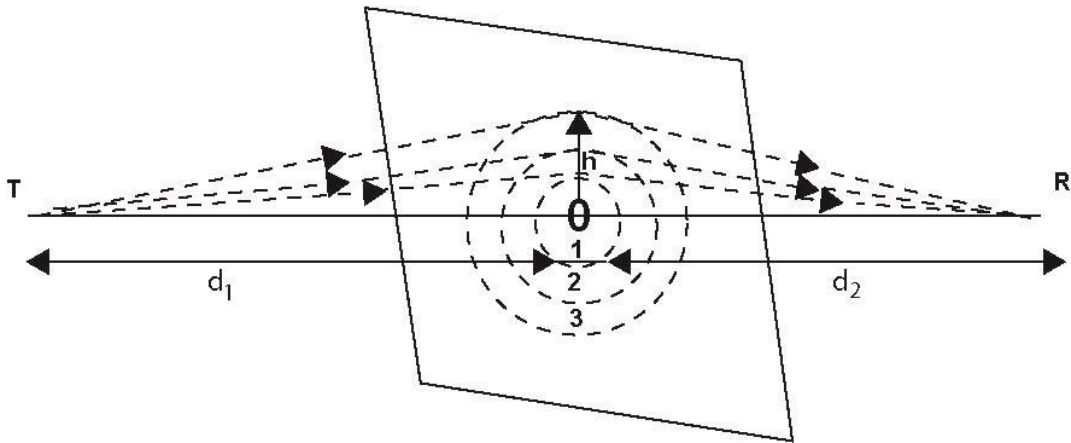
Fig. 2 shows a plane wave propagating parallel to the z -axis at time $t=0$. The electric, E , and magnetic fields, H , are perpendicular to each other and to the direction of propagation of the wave. The propagation vector is known as the Pointing vector.

3.4 – Fresnel zones

Fresnel zones allow determining the diffraction loss as a function of the path difference around an obstruction. Fresnel zones represent successive regions where secondary waves

have a path length from the transmitter to receiver which are $\frac{n\lambda}{2}$ greater than the total path length of a line of sight path illustrated in Fig 3.

Fig. 3. Successive Fresnel zones



Source [33]

The radius of n^{th} Fresnel zone circle, can be expressed in terms of λ , d_1 and d_2 :

$$r_n = \sqrt{\frac{n\lambda d_1 d_2}{d_1 + d_2}} \quad (26)$$

where:

r_n : Number of radius of Fresnel

d_1 : Distance between the transmitter and the obstacles

d_2 : Distance between the obstacle and the receiver.

This approximation is valid for $d_1, d_2 \gg r_n$.

The effect of shadowing is sensitive to the frequency as well as the location of obstructions with relation to the transmitter or receiver. Diffraction effects are neglected when the first Fresnel zone is free more or equal than 60%.

The difference between the direct path and the diffracted path is given for:

$$\Delta \approx \frac{h^2 (d_1 + d_2)}{2 d_1 d_2} \quad (27)$$

One the most used parameters to determine diffraction is the dimensionless Fresnel Kirchoff diffraction parameter v which is given by[33]:

$$v = h \sqrt{\frac{2(d_1 + d_2)}{\lambda d_1 d_2}} \quad (28)$$

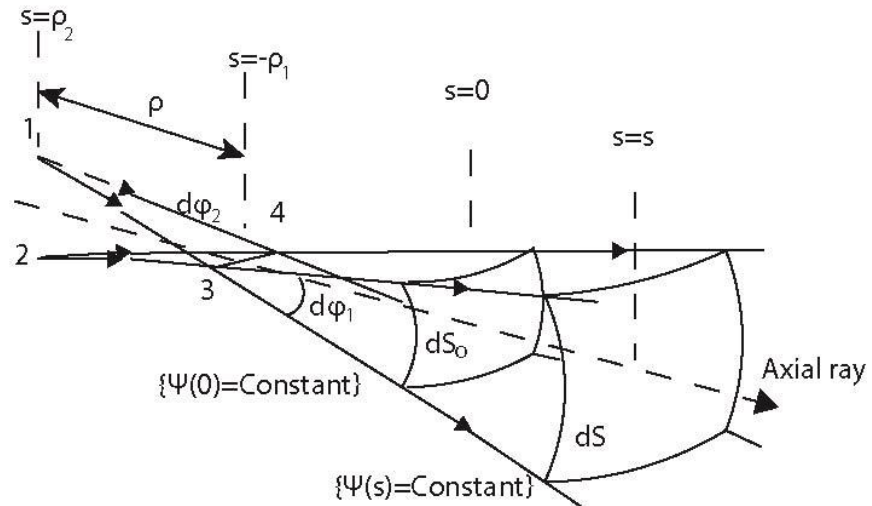
When $v \geq -0.78$, there is diffraction.

3.5 Geometrical Optics

The incorporation of such local plane wave behavior of the field allows reducing the electromagnetic wave equations to the simpler equations for the polarization, amplitude, phase and propagation path of the high frequency field. Geometrical Optics (GO) method allows determining the wave propagation for incident, reflected and refracted fields.

The transmission of the geometrical optics field for a general astigmatic ray tube is illustrated in Fig. 4.

Fig. 4. Infinitesimally narrow diverging astigmatic ray tube, for which both ρ_1 and ρ_2 are positive (ρ is the astigmatic difference)



Source [24]

In Fig. 4 the distance, p , between the focal lines is called the astigmatic difference. The reference constant phase is $\Psi(0)$, and it has principal radii of curvature ρ_1 and ρ_2 measured on the central ray. The $\Psi(s)$ surface has principal radii of curvature $(\rho_1 + s)$ and $(\rho_2 + s)$.

The expression describing the transmission of the geometrical optics (GO) field, for the general astigmatic ray tube shown in Fig. 4 is given by,

$$E(s) = E(0) \sqrt{|\rho_1 \rho_2 / (\rho_1 + s)(\rho_2 + s)|} e^{-jks} e^{-j(n-m)\pi/2} \quad (29)$$

where:

- $E(0)$: Amplitude, phase and polarization at the reference point ($s = 0$)
- s : Distance along the ray path from the reference point ($s = 0$)
- e^{-ks} : Phase shift along the ray path.
- $A(s) = \sqrt{|\rho_1\rho_2/(\rho_1 + s)(\rho_2 + s)|}$: Spreading factor which governs the amplitude variation of the GO field along the ray path
- ρ_1 and ρ_2 : the principal radii of curvature of the wave front (which is a surface) at the reference point $s = 0$. The sign convention is that a positive (negative) radius of curvature implies diverging (converging) rays in the corresponding principal plane.
- n (m): is the number of caustic lines crossed by the observer in moving from the references position $s = 0$ to the given observation point s in a direction of (opposite to that of) propagation.

3.5.1 Field of direct wave

Direct field is known as line of sight, because there is not an obstacle between the transmitter and the receiver. Electric field for direct ray, E_{LOS} , decreases with the distance as is shown in the following equation [33]:

$$E_{LOS}(R_{TR}) = \frac{\sqrt{30 P_T G_T}}{R_{TR}\sqrt{L}} e^{-jkR_{TR}} \quad (30)$$

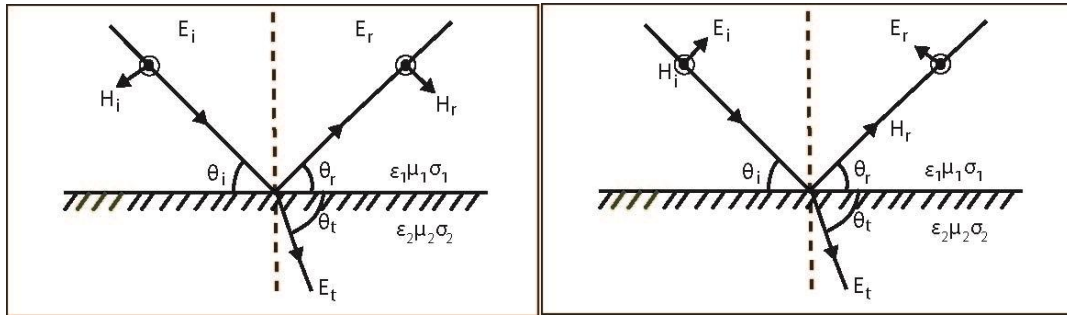
where:

- P_T : Transmission Power.
- G_T : Gain of transmitter antenna.
- L : Loss for connectors, cable, etc.
- k : Free space propagation constant [24].

3.5.2 Reflected field

When there are two media with different electrical parameters and an incident wave encounters the interface a fraction of the wave intensity will be reflected into medium 1, as can be seen in Fig. 5. Two grazing angles, θ_i , for the incident ray and θ_r for the reflected ray are also illustrated. Knowing the direction of the electric field, can be defined the wave polarization if the electric field is parallel to the incidence plane it is known as vertical polarization. When the electric field is perpendicular to the incidence plane, it is a horizontal polarization.

Fig. 5. Reflected wave for : a) Vertical polarization, b) Horizontal polarization [33]



a) E into the incidence plane

b) E perpendicular to the incidence plane

Source [33]

The formulation used to calculate the coefficient of reflection for these two polarizations are:

Vertical polarization:

$$\Gamma_V = \frac{E_r}{E_i} = \frac{\eta_2 \sin \theta_t - \eta_1 \sin \theta_i}{\eta_2 \sin \theta_t + \eta_1 \sin \theta_i} \quad (31)$$

Horizontal polarization

$$\Gamma_H = \frac{E_r}{E_i} = \frac{\eta_2 \sin \theta_i - \eta_1 \sin \theta_t}{\eta_2 \sin \theta_i + \eta_1 \sin \theta_t} \quad (32)$$

where:

η_i : Intrinsic impedance of media i .

When the first media is the free space the coefficients are:

For vertical polarization:

$$\Gamma_V = \frac{\epsilon_c \sin \theta_i - \sqrt{\epsilon_c - \cos^2 \theta_i}}{\epsilon_c \sin \theta_i + \sqrt{\epsilon_c - \cos^2 \theta_i}} \quad (33)$$

For horizontal polarization:

$$\Gamma_H = \frac{\sin \theta_i - \sqrt{\epsilon_c - \cos^2 \theta_i}}{\sin \theta_i + \sqrt{\epsilon_c - \cos^2 \theta_i}} \quad (34)$$

$$\epsilon_r = \epsilon - j60\sigma\lambda \quad (35)$$

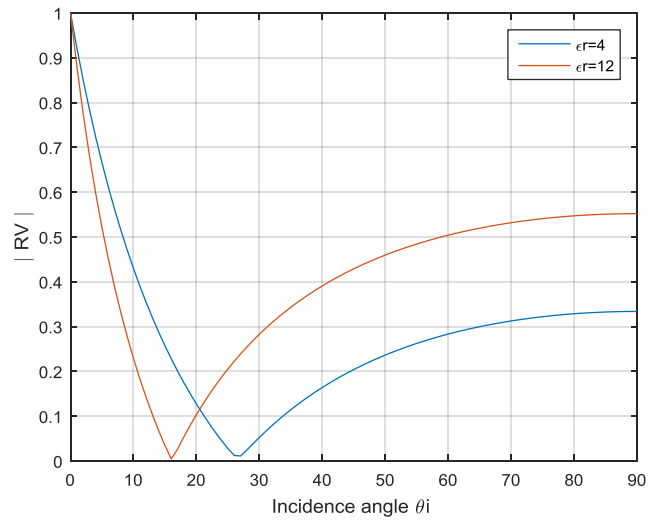
where:

- σ : Conductivity in (S/m)

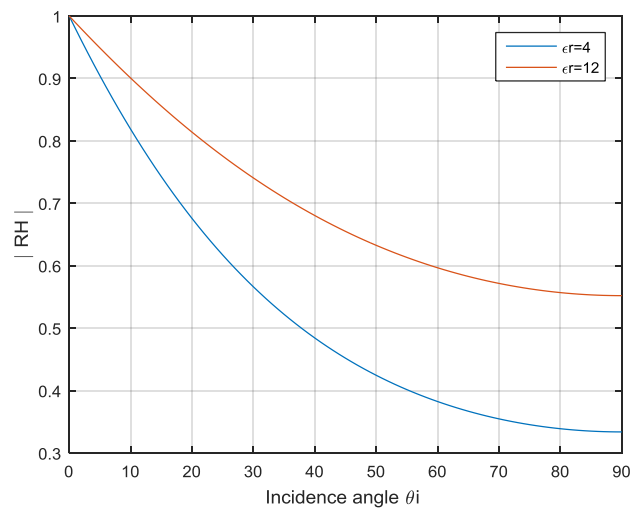
- ε : Permittivity (F/m)
- λ : Wavelength (m)

The reflection coefficients illustrated in Fig. 6 are reproduced from [33].

Fig. 6. - Reflection coefficient magnitude for a frequency of 100MHz with $\varepsilon_r=4$ and $\varepsilon_r=12$, a) Vertical Polarization and b) Horizontal Polarization



a) Vertical polarization



b) Horizontal polarization

Source [33]

The electric field for a reflective wave, E_r , can be calculated as follows:

$$E_r(R_{TR}) = E_{LOS}(R_{Tp_r}) \frac{R_{Tp_r}}{R_{Tp_r} + R_{p_rR}} \Gamma e^{-jkR_{p_rR}} \quad (36)$$

where:

- $E_{LOS}(R_{Tp_r})$: Electric field of incidence in, p_r , the incidence point of reflection (p_r is illustrated in Fig. 16).
- R_{Tp_r} : Distance between transmitter and p_r .
- R_{p_rR} : Distance between p_r and the receiver.
- Γ : Reflection coefficient.

3.5.3 Refracted/Transmitted field

Refraction happens when a wave passes from medium one to medium two, and these two media have different electrical parameters. In Fig. 7 refraction (transmission) is illustrated. Considering the first medium as free space, the following equations are to calculate the refraction/transmission coefficient:

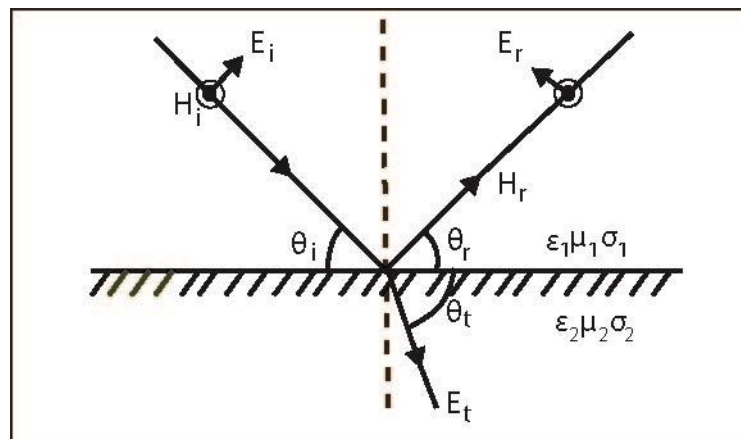
Vertical Polarization:

$$\tau_V = \frac{2\eta_2 \cos\theta_i}{\eta_1 \cos\theta_i + \eta_2 \cos\theta_t} \quad (37)$$

Horizontal Polarization

$$\tau_H = \frac{2\eta_2 \cos\theta_i}{\eta_2 \cos\theta_i + \eta_1 \cos\theta_t} \quad (38)$$

Fig. 7. Refraction of a wave



Source [33]

In order to calculate the refracted/transmitted electric field, for the present work are considered two transmissions/refractions. Then in the general formula for refraction is

introducing one more refraction coefficient. There are not considering reflections inside the forest, the expression for refracted/transmitted field, E_t , is:

$$E_t(R_{TR}) = E_{LOS}(R_{Tp_t}) \frac{R_{Tp_t}}{R_{Tp_t} + R_{p_t n} + R_{nR}} \tau_{af} \tau_{fa} e^{-jkR_{nR}} \quad (39)$$

where:

- $E_{LOS}(R_{Tp_t})$: Incidence electric field in p_t , the incidence point of transmission/refraction (p_t is illustrate in Fig.16) .
- R_{Tp_t} : Distance between transmitter and p_t .
- $R_{p_t n}$: Distance inside the forest between p_t and n , the point of incidence of refraction forest-air, illustrated in Fig. 16.

forest-air, illustrated in Fig. 16.

- R_{nR} : Distance between n and the receiver.
- τ_{af} : Transmission coefficient air-forest.
- τ_{fa} : Transmission coefficient forest-air.

Real angle of refraction/transmission

The incident and transmission/refraction angles are calculated using Snell's law, with the following equation [34]:

$$\beta_1 \sin(\theta_i) = \beta_2 \sin(\theta_t) \quad (40)$$

$$\beta = \omega \sqrt{\mu \varepsilon} \left\{ \frac{1}{2} \left[\sqrt{1 + \left(\frac{\sigma}{\omega \varepsilon} \right)^2} + 1 \right] \right\}^{1/2} \text{ rad/m} \quad (41)$$

where:

- β_1 : phase constant
- μ : permeability
- ε : Relative electrical permittivity farads/meters

From Snell's Law can be deduced that the angles are complex and do not have physical coherence. To find the real angles for the two refractions/transmissions, the following equations are used:

The attenuation constant:

$$\alpha = \omega \sqrt{\mu \varepsilon} \left\{ \frac{1}{2} \left[\sqrt{1 + \left(\frac{\sigma}{\omega \varepsilon} \right)^2} - 1 \right] \right\}^{1/2} Np/m \quad (42)$$

Real refraction/transmission angles for Air-Forest:

$$\sin \Psi_{taF} = \frac{\beta_a \sin \Psi_{iaF}}{\sqrt{(\beta_a \sin \Psi_{iaF})^2 + q_{aF}^2}} \quad (43)$$

$$M = 1 - (a_{aF}^2 - b_{aF}^2) \sin^2 \Psi_{iaF} + p_{aF}^2 \quad (44)$$

$$q_{af} = \frac{\beta_F(M) - 2\alpha_F a_{aF} b_{aF} \sin^2 \Psi_{iaF}}{\sqrt{2(M)}} \quad (45)$$

$$a_{aF} = \frac{\beta_a \beta_F}{\beta_F^2 + \alpha_F^2} \quad (46)$$

$$b_{aF} = \frac{\beta_a \alpha_F}{\beta_F^2 + \alpha_F^2} \quad (47)$$

$$p_{aF}^2 = \frac{2a_{aF} b_{aF} \sin^2 \Psi_{iaF}}{\sin 2y_{aF}} \quad (48)$$

$$\sin 2y_{aF} = \frac{A_{aF}^2}{\sqrt{1 + A_{aF}^2}} \quad (49)$$

$$A_{aF} = \frac{2a_{aF} b_{aF} \sin^2 \Psi_{iaF}}{1 - (a_{aF}^2 - b_{aF}^2) \sin^2 \Psi_{iaF}} \quad (50)$$

Real transmission angles for Forest-Air:

$$\sin \Psi_{tFa} = \frac{\beta_F \sin \Psi_{iFa}}{\sqrt{(\beta_F \sin \Psi_{iFa})^2 + q_{Fa}^2}} \quad (51)$$

$$q_{Fa} = \beta_a \sqrt{\frac{[1 - (a_{Fa}^2 - b_{Fa}^2) \sin^2 \Psi_{iFa} + p_{Fa}^2]}{2}} \quad (52)$$

$$a_{Fa} = \frac{\beta_F}{\beta_a} \quad (53)$$

$$b_{Fa} = \frac{\alpha_F}{\beta_a} \quad (54)$$

$$p_{Fa}^2 = \frac{-2a_{Fa}b_{Fa}\sin^2\Psi_{iFa}}{\text{sen}2y_{Fa}} \quad (55)$$

$$\text{sen}2y_{Fa} = -\sqrt{\frac{A_{Fa}^2}{1 + A_{Fa}^2}} \quad (56)$$

$$A_{Fa} = \frac{-2a_{Fa}b_{Fa}\sin^2\Psi_{iFa}}{1 - (a_{Fa}^2 - b_{Fa}^2)\sin^2\Psi_{iFa}} \quad (57)$$

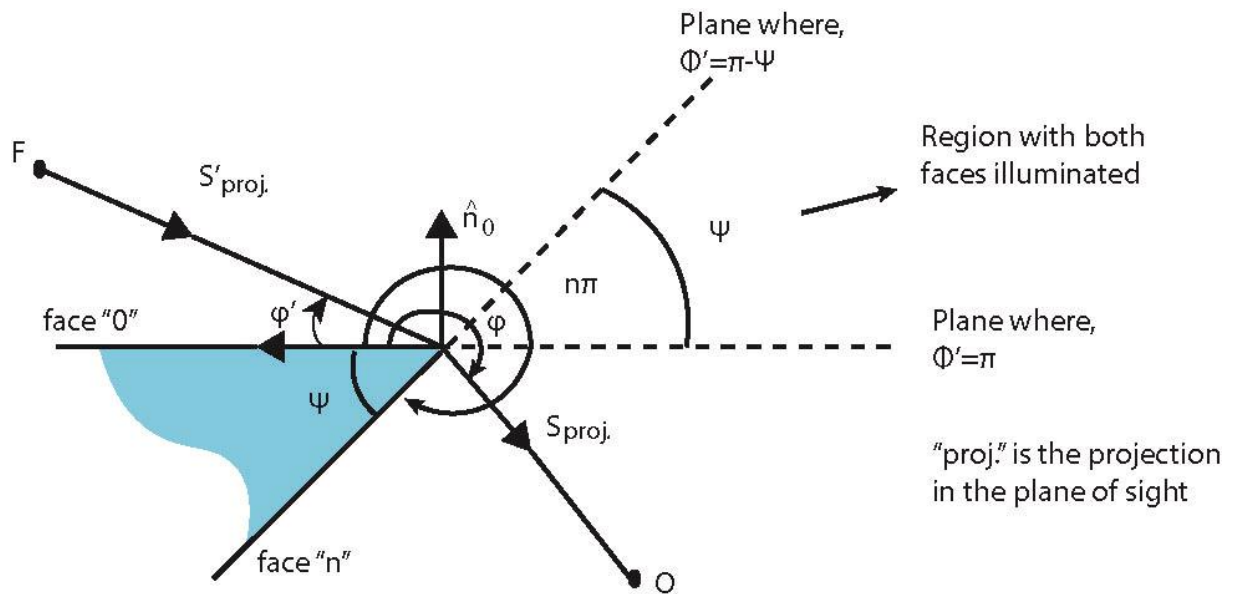
where:

- $\beta_{F,i}$ Phase constant for forest and air [35].
- α_F : Attenuation constant for forest [35].

3.6 Uniform Theory of Diffraction

Diffraction is a local phenomenon which depends on two things: 1. The geometry of the object where the incident ray for diffraction arrives, 2. The characteristics of the incident field at the point of diffraction such as: amplitude, phase and polarization.

Fig. 8. Diffracted wave



Source [36]

In Fig.8 a diffracted ray is showed for an arbitrary wedge with flat faces, Φ' is the incidence angle of diffraction, Φ is the angle formed between the face 0 and face n of the wedge. S_{proj} is the distances of diffraction and S'_{proj} is the incidence distance.

Previously diffraction formulation is studied for the General Theory of Diffraction (GTD), however, it is inaccurate in the vicinity of the shadow boundaries [24]. The Uniform

Theory of Diffraction proposes an additional term for the diffraction coefficient, known as Fresnel transition function, to solution the inaccuracy of GTD formulation. The Diffraction coefficient for 2D is[24]:

$$D_1 = G_n \frac{-e^{-j\pi/4}}{2n\sqrt{2\pi k}} \cot \left[\frac{\pi + (\phi - \phi')}{2n} \right] F[kLa^+(\phi - \phi')] \quad (58)$$

$$D_2 = G_0 \frac{-e^{-j\pi/4}}{2n\sqrt{2\pi k}} \cot \left[\frac{\pi - (\phi - \phi')}{2n} \right] F[kLa^-(\phi - \phi')] \quad (59)$$

$$D_3 = G_n \frac{-e^{-j\pi/4}}{2n\sqrt{2\pi k}} \cot \left[\frac{\pi + (\phi + \phi')}{2n} \right] F[kLa^+(\phi + \phi')] \quad (60)$$

$$D_4 = G_0 \frac{-e^{-j\pi/4}}{2n\sqrt{2\pi k}} \cot \left[\frac{\pi - (\phi + \phi')}{2n} \right] F[kLa^-(\phi + \phi')] \quad (61)$$

$$L = \frac{s s'}{s + s'} \quad (62)$$

$$a \pm (\phi \pm \phi') = 2\cos^2 \left(\frac{2n\pi N^\pm - (\phi \pm \phi')}{2} \right) \quad (63)$$

$$2n\pi N^+ - (\phi \pm \phi') = \pi \quad (64)$$

$$2n\pi N^- - (\phi \pm \phi') = -\pi \quad (65)$$

The values of N^+ and N^- , are related with the incident shadow boundary (ISB) and the reflection shadow boundary (RSB), as functions of $\phi \pm \phi'$ and n [24].

where:

- n : Used to calculated the angle of the obstacle, this work uses $n = 1.5$.
- ϕ' : Incidence angle of diffraction.
- ϕ : Angle formed between the 0 face and the diffracted ray
- L : Distance parameter that satisfies the condition of continuity of the electric field across the shadow regions. For the situation of interest (incidence of spherical waves and flat faces).
- s : Distance between the fount (F) and the point of incidence of diffraction.
- s' : Distance between point of incidence of diffraction and the observation point (O)
- N^\pm : It is an integer number that most nearly satisfies the equations (64) and (65).

The values of G_0 and G_n are used to include the grazing effects, for a finite conductivity application the values are:

$$G_0 = \begin{cases} \frac{1}{1 + \Gamma_0}, & \phi' = 0, |1 + \Gamma_0| > 0 \\ \frac{1}{2}, & \phi' = n\pi \\ 1, & \text{otherwise} \end{cases} \quad (66)$$

$$G_n = \begin{cases} \frac{1}{1 + \Gamma_n}, & \phi' = n\pi, |1 + \Gamma_n| > 0 \\ \frac{1}{2}, & \phi' = 0 \\ 1, & \text{otherwise} \end{cases} \quad (67)$$

The formulation for diffraction is the following:

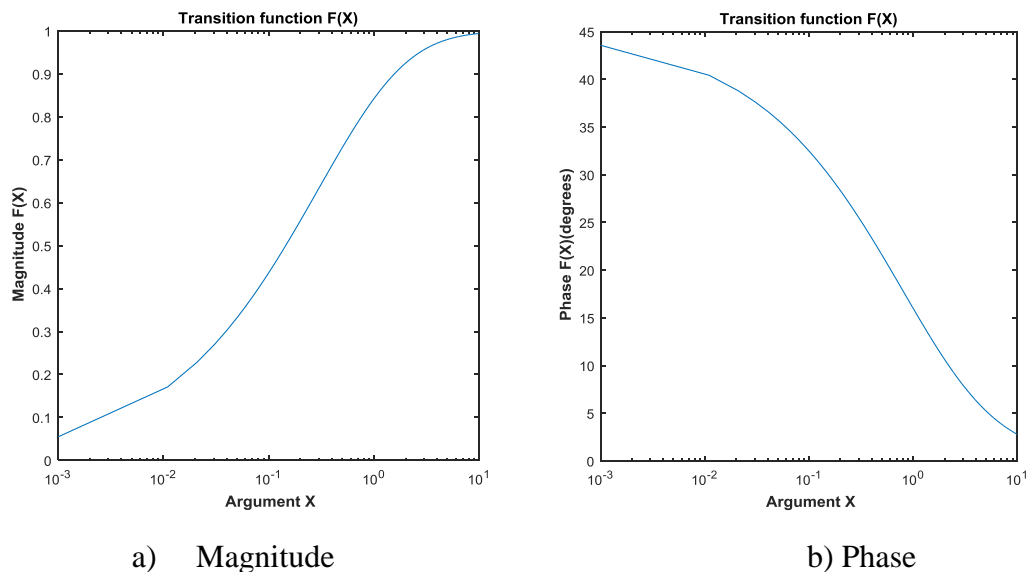
$$E_d(R_{TR}) = E_{LOS}(R_{Tb}) \sqrt{\frac{R_{Tb}}{R_{bR}(R_{Tb} + R_{bR})}} D e^{-jkR_{bR}} \quad (68)$$

where:

- $E_{LOS}(R_{Tb})$: Electric field at the point of incidence b .
- R_{Tb} : Incidence distance between transmitter and b .
- R_{bR} : Diffraction distance between b and receiver.
- D : Diffraction coefficient

In order to prove that formulation is executed with accuracy, the Fresnel transition function is reproduced from [24] and can be observed in Fig. 9.

Fig. 9. Fresnel Transition function: a) Magnitude b) Phase



Source [24]

Furthermore, in Fig. 10 the scattered field from a wedge with plane incidence using UTD diffraction coefficients [24] is shown. The parameters for calculation are the amplitude of the electric field which is 1, with $n=1.778$, $\alpha = 40^\circ$, the incidence angle of diffraction $\phi' = 55$ degrees, the distance of incidence is 1m, the frequency of 3 GHz, horizontal polarization.

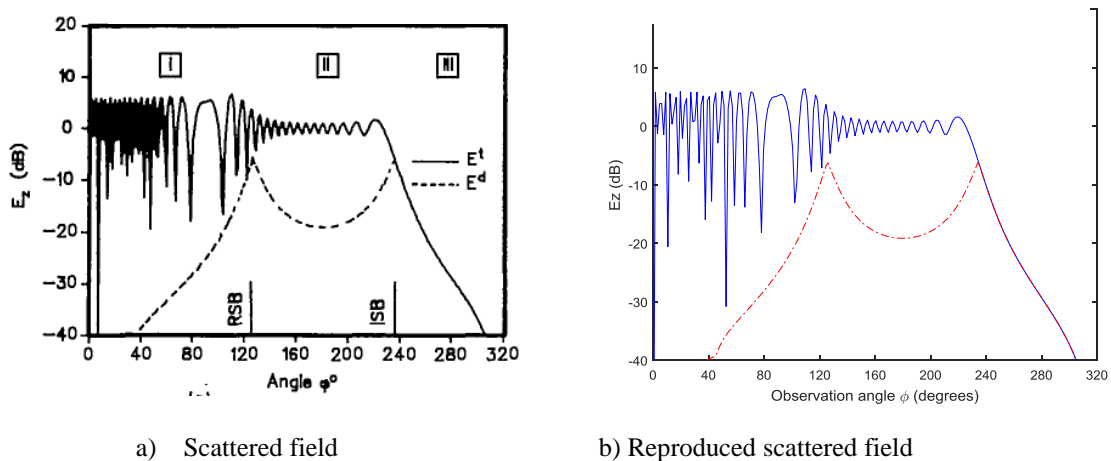
The total electric field, E^t is calculated according with the region I, II or III, which are separated for the shadow boundaries RSB and ISB. The equation is as follows

$$E_z^t = \begin{cases} E_z^i + E_z^r + E_z^d, & 0 \leq \phi < \pi - \phi' \text{ (Region I)} \\ E_z^i + E_z^r, & \pi - \phi' < \phi < \pi + \phi' \text{ (Region II)} \\ E_z^d, & \pi + \phi' < \phi \leq \pi - \alpha \text{ (Region III)} \end{cases} \quad (69)$$

where

E_z^i , is the electric field given by the direct ray, E_z^r is the reflected ray and finally E_z^d is the diffracted ray.

Fig. 10. Scattered field from a wedge with plane using UTD diffraction coefficients: a) Scattered field, b) Scattered field recalculated by the author



Source: [24]

3.7 Ray Tracing

For radio propagation and for its accuracy Ray tracing (RT) is widely used. This tool includes reflection, diffraction and refraction/transmission and another phenome that are related to the scenario in studying. For ray tracing there are two classical methods [36]:

- Shooting and Bouncing Rays (SBR) method: Consist of tracking a large number of rays launched from the transmitter antenna and their descendent rays.

- **Image Method:** This method introduces virtual sources for the reflections. These virtual sources are used for analysis purposes and give the trajectories between transmitter and receiver.

Image Method

The present study implements the image theory in order to calculate the reflected field trajectories. In Fig. 11, the image method is illustrated.

The surfaces are smooth and plane, the image method is efficient to calculate the reflected rays. The virtual source in Fig. 10 is T'. Knowing the reception point R, the reflected ray trajectory is perfectly defined. Then distances T- R' is the same distance of Reflected ray T-R.

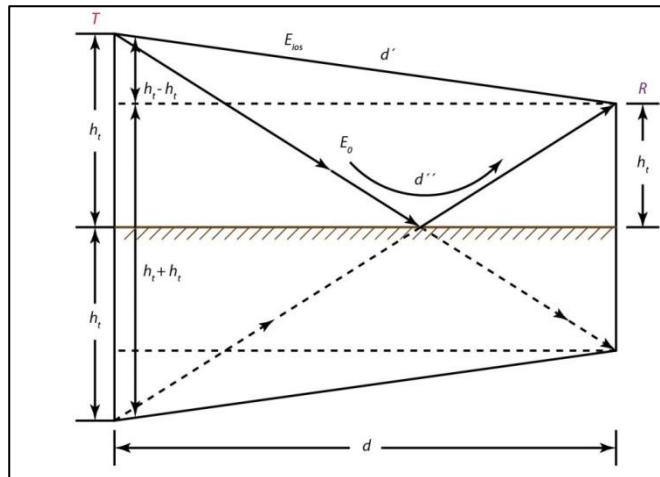
The expression two find T-R' is:

$$d_{TR'} = \sqrt{(2 * h_t)^2 + d^2} \quad (70)$$

where:

- h_t : height of the transmitter
- d : distance between transmitter and receiver

Fig. 11. Image method is used to find the difference between direct ray and reflected ray



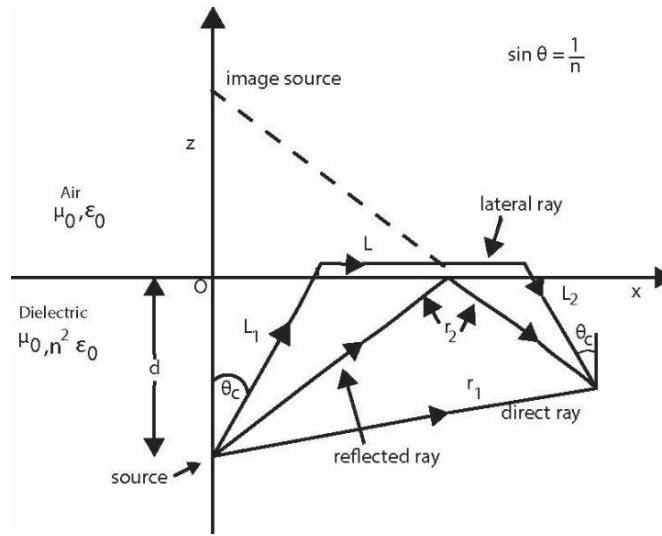
Source [33]

3.8 Lateral Wave

Tamir in 1967 presented a study about the lateral wave that is produced for a critical angle when a ray passes from a dense medium to a less dense medium. The lateral wave contributes to the total electric field that arrives at a receiver. Fig. 12 illustrates a transmitter

inside the forest which originates a refracted ray forest-air, this ray forms a critical angle which originates a lateral wave.

Fig. 12. Critical angle that produces a lateral wave .



Source [37]

The critical angle according with [38] is given by the following expression:

$$\theta_c = \sin^{-1}\left(\frac{1}{n}\right) \quad (71)$$

$$n^2 = \epsilon_1 + j60\sigma\lambda \quad (72)$$

In order to calculate the critical angle only the real part is considered

Then according with [35], the critical angle can be calculated with:

$$\theta_c = \sin^{-1}\left(\sqrt{\frac{\mu_2\epsilon_2}{\mu_1\epsilon_1}}\right) \quad (73)$$

where ,

μ_1 : permeability of forest

ϵ_1 : permittivity of forest

μ_2 : permeability of air

ϵ_2 : permittivity of air

With $\mu_1=\mu_2$

$$\theta_c = \sin^{-1}\left(\sqrt{\frac{\epsilon_0}{\epsilon_0\epsilon_{r1}}}\right) \quad (74)$$

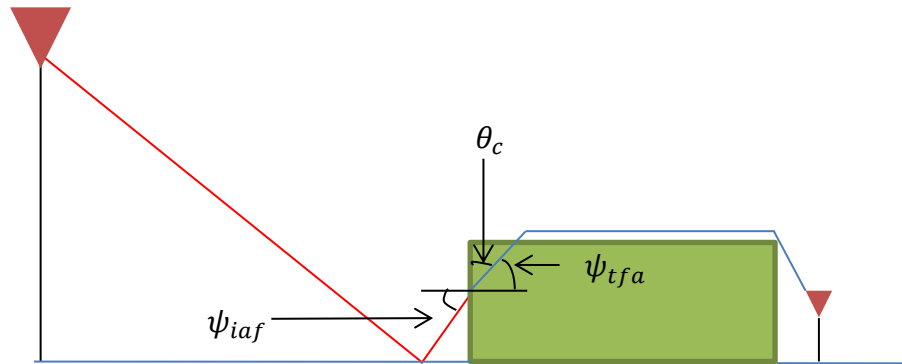
where:

ϵ_{r1} = relative permittivity of forest

With the two formulations given by [38] and [35] the critical angle depends on permittivity of the forest.

The proposed Model Mixed Path pretended to use a lateral wave in the total electric field, however the geometry does not produce the value needed for the critical angle.

Fig. 13. Critical angle for Mixed Path.



Source: Author

Using (74) with the electrical parameters for a dense forest from [19], the value for the critical angle is 61.29 degrees. Fig. 13 illustrates that the critical angle for the scenario of Mixed Path depends on the incidence angle of refraction air forest which depends on the reflection angle over the water. Then the angles formed instead the critical angle are around 88.41 and 88.68 degrees, which do not produce a lateral wave.

3.8 Final considerations

Mixed Path model uses some of the existing theory of literature, for example, reflection and diffraction coefficients. Furthermore, to ensure that existing formulation was implemented correctly some applications were reproduced from books. Ray tracing and the method of the images was also explained since these methods are used in the proposed model.

Chapter 4 – Proposed Model: Mixed Path

4.1 Introduction

For telecommunications, Amazon environments are a challenge due to the presence of rain, forests, rivers, and high temperatures. The focus of this work is to develop a radio propagation model that integrates the characteristics of the Amazon cities.

The proposed radio propagation model is called Mixed Path which uses Geometrical Optics and the Uniform Theory of Diffraction. In addition, using Mixed Path Model the electric field can be predicted for Mobile Digital Television (M-DTV) and Home Digital Television (H-DTV).

4.2 Scenario

The Mixed Path model is designed for both M-DTV and H-DTV. In Fig. 14, the scenario is illustrated with the different paths denominated as City, Water1, Forest1, Water2, and Forest2. The receivers over the rooftop building and over the ground and river level can be observed, referencing the H-DTV service and M-DTV service. In Figs. 14-16, the geometrical parameters used in calculations of the electric field are illustrated and detailed in Table I. In Fig. 16 are illustrated the ten rays used for Mixed Path model in mixed City-Water1-Forest1-Water2-Forest2 path, however in each section the number of rays is different. For example for M-DTV in the City path the maximum number of rays is eight which are the principal contributors to the total electric field.

Fig. 14. Scenario for Mixed Path model for the services of M-DTV and H-DTV.

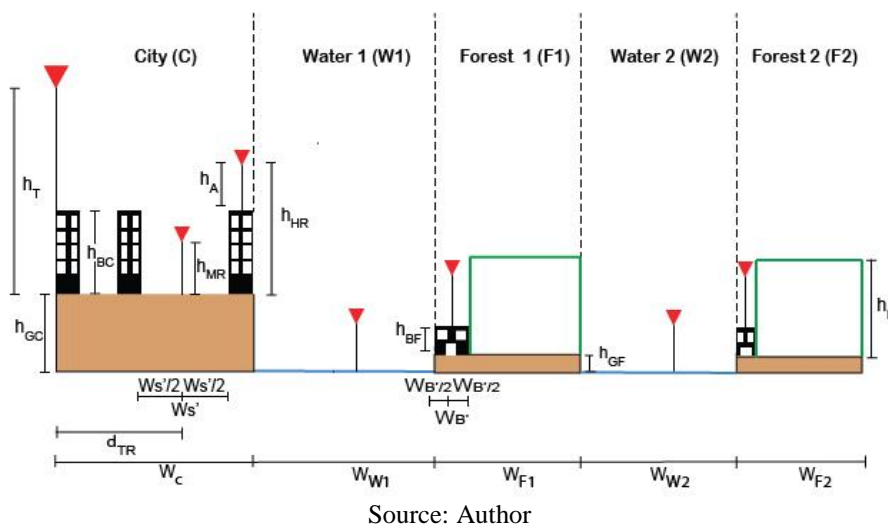
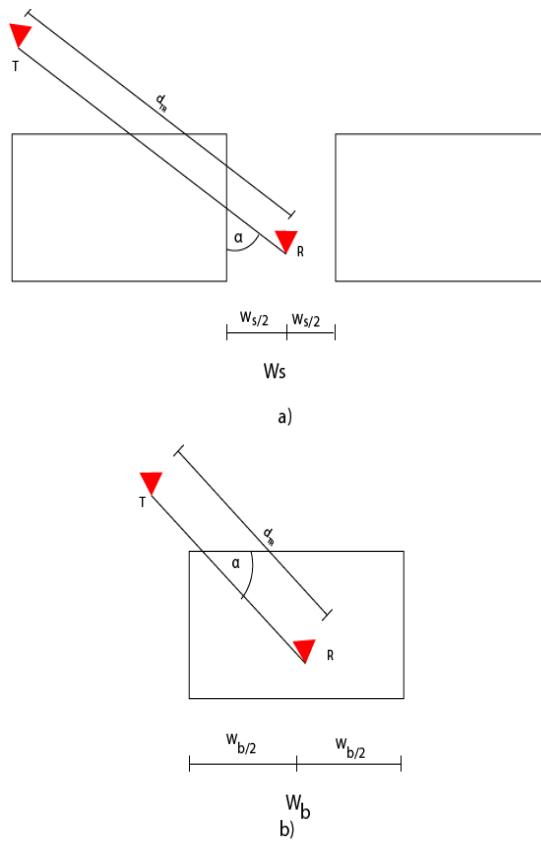
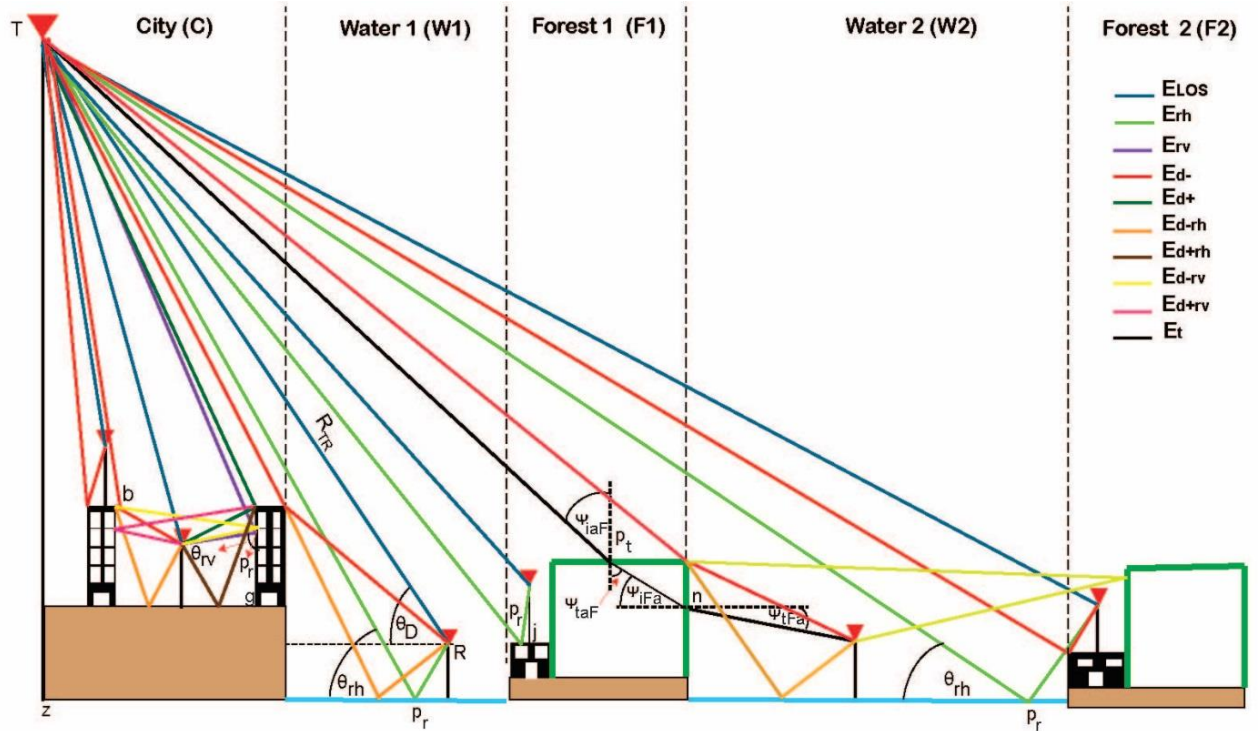


Fig. 15. Width of street and width of building.



Source: Author

Fig. 16. Rays used in Mixed Path for calculation of total electric field for M-DTV and H-DTV.



Source: Author

Table I- Parameters for Mixed Path model.

Symbol	Description
h_T	Height of transmitter over ground
h_R	Height of receiver
h_b	Height of building over ground
h_g	Height of ground
h_f	Height of forest
d_{TR}	Distance between transmitter and receiver over the ground
R_{TR}	Direct distance between transmitter and receiver
W_s'	Width of the street considering α (top view)
$W_{w1,2}$	Width of Water1 or Water2
$W_{F1,2}$	Width of Forest1 or Forest2
W_c	Width of city with constructions
W_b'	Width of the building considering α (top view).
α	Angle formed by the straight line between transmitter-receiver and the street or building (top view)
W_s	Width of the street from top view Fig. 15
W_b	Width of the building from top view Fig. 15
p_r	Incidence point of reflection.
p_t	Incidence point of transmission
b	Incidence point of diffraction
θ_{rv}	Grazing angle for reflection on a vertical surface
θ_{rh}	Grazing angle for reflection on a horizontal surface
θ_D	Angle of direct ray
ψ_{iaf}	Incidence angle for transmission air-forest
ψ_{taf}	Transmission angle for air-forest
ψ_{ifa}	Incidence angle for transmission forest-air
ψ_{tfa}	Transmission angle for forest-air
z	Point of transmitter placement
g	Point of the base of the building
n	Transmission point forest-air

4.3 Formulation

Considering GO and UTD, described in chapter 3, Mixed Path model defines a different number of rays in each section, then for M-DTV the maximum number of rays in the City is eight, over Water 1 four and over Water 2 nine. For H-DTV in the City path Mixed Path

model considers maximum 3 rays and for Forest 1 and Forest 2 maximum 4 rays. All the rays are defined in Table II and illustrated in Fig. 16.

Table II- Rays used in Mixed Path model

Symbol	Description
E_{LOS}	Line of sight.
E_{rh}	Reflection on a horizontal surface.
E_{rv}	Reflection on a vertical surface.
E_{d-}	Diffraction on the left.
E_{d+}	Diffraction on the right.
E_{d-rh}	Diffraction on the left, reflection on a horizontal surface.
E_{d+rh}	Diffraction on the right, reflection on a horizontal surface
E_{d-rv}	Diffraction on the left, reflection on a vertical surface
E_{d+rv}	Diffraction on the right, reflection on a vertical surface
E_t	Transmission through the forest.

Next, are described the rays for each path and formulations for M-DTV and H-DTV

4.3.1 Formulation for City Path for M-DTV

Mixed Path model uses maximum eight rays to calculate the total electrical field for a receiver on the City. Furthermore, the value of the Fresnel parameter is calculated to know if the first Fresnel Ellipsoid is unobstructed or not. In the City, two Fresnel parameters are considered, the first one for line of sight ray and the second one for reflected ray on the building wall.

The Fresnel parameter for line of sight, v_{CD} , is given by the following expressions,

$$W'_S = \frac{W_S}{\sin(\alpha)} \quad (75)$$

$$h_{CD} = \cos\theta_D(h_B - h_{RM} - (W'_S/2)\tan\theta_D) \quad (76)$$

$$h_{Cr} = \sin\theta_{rv}(h_B - h_{RM} - 1.5W'_S \cot\theta_{rv}) \quad (77)$$

$$v_{CD} = h_{CD} \sqrt{\frac{2 d_{TR} \cos\theta_D}{\lambda \left(d_{TR} - \frac{W'_S}{2} - h_{CD} \sin\theta_D \right) \left(\frac{W'_S}{2} + h_{CD} \sin\theta_D \right)}} \quad (78)$$

The Fresnel parameter for line of sight, v_{Cr} , is as follows,

$$v_{Cr} = h_{Cr} \sqrt{\frac{2 \left(d_{TR} + \frac{W_s'}{2} \right) \sin \theta_{rv}}{\lambda \left(d_{TR} - \frac{W_s'}{2} - h_{Cr} \cos \theta_{rv} \right) (W_s' + h_{Cr} \cos \theta_{rv})}} \quad (79)$$

Furthermore, to know if the reflected ray will be added in the total electric field, first, h_{p_rg} is calculated, it is the height between the incidence point of reflection p_r and g , illustrated in Fig. 16.

$$h_{p_rg} = \left(\frac{W_s'}{2 \tan \theta_{rv}} \right) + h_R \quad (80)$$

Then, if $h_{p_rg} < h_B$, the reflected ray can be added to the total electric field

After calculating the Fresnel parameters, the total electrical field for City is calculated considering four cases:

1) When v_{CD} and v_{Cr} are lower than -0.78 and $h_{p_rg} < h_B$, the total electric field for City is:

$$E_{\Sigma MC}(R_{TR}) = E_{LOS}(R_{TR}) + E_{rv}(R_{TR}) + E_{d-}(R_{TR}) + E_{d+}(R_{TR}) + E_{d-rv}(R_{TR}) \quad (81) \\ + E_{d-rh}(R_{TR}) + E_{d+rv}(R_{TR}) + E_{d+rh}(R_{TR})$$

2) When v_{CD} and v_{Cr} are lower than -0.78 and $h_{p_rg} > h_B$ or v_{CD} is lower than -0.78 and v_{Cr} is higher than -0.78, the total electrified for City is:

$$E_{\Sigma MC}(R_{TR}) = E_{LOS}(R_{TR}) + E_{d-}(R_{TR}) + E_{d+}(R_{TR}) + E_{d-rv}(R_{TR}) + E_{d-rh}(R_{TR}) \quad (82) \\ + E_{d+rv}(R_{TR}) + E_{d+rh}(R_{TR})$$

3) When v_{CD} and v_{Cr} are higher than -0.78 or v_{CD} is higher than -0.78 and v_{Cr} is lower than -0.78 and $h_{p_rg} > h_B$ the total electrified for City is:

$$E_{\Sigma MC}(R_{TR}) = E_{d-}(R_{TR}) + E_{d+}(R_{TR}) + E_{d-rv}(R_{TR}) + E_{d-rh}(R_{TR}) + E_{d+rv}(R_{TR}) \quad (83) \\ + E_{d+rh}(R_{TR})$$

4) When v_{CD} is higher than -0.78 and v_{Cr} is lower than -0.78 and $h_{prg} <$

h_B , the total electrified for City is:

$$E_{\Sigma MC}(R_{TR}) = E_{rv}(R_{TR}) + E_{d-}(R_{TR}) + E_{d+}(R_{TR}) + E_{d-rv}(R_{TR}) + E_{d-rh}(R_{TR}) \quad (84)$$

$$+ E_{d+rv}(R_{TR}) + E_{d+rh}(R_{TR})$$

4.3.2 Formulation for Water1 Path for M-DTV

A receiver located over Water 1 can have maximum 4 rays. In order to know if direct ray and the reflected ray over the water can be added in the total electric field are calculated Fresnel parameters for direct ray, v_{W1D} , and reflected ray, v_{W1r} . The equations to calculate the Fresnel parameter for direct ray, v_{W1D} , are:

$$d_{W1} = d_{TR} - W_C \quad (85)$$

$$h_{W1D} = \cos\theta_D (h_{BC} + h_G - h_{MR} - d_{W1} \tan\theta_D) \quad (86)$$

$$h_{W1r} = \cos\theta_{rh} (h_{BC} - h_T + W_C \tan\theta_{rh}) \quad (87)$$

$$v_{W1D} = h_{W1D} \sqrt{\frac{2 d_{TR} \cos\theta_D}{\lambda (d_{TR} - d_{W1} - h_{W1D} \sin\theta_D) (d_{W1} + h_{W1D} \sin\theta_D)}} \quad (88)$$

Fresnel parameter for reflected ray, v_{W1D} , is:

$$v_{W1r} = h_{W1r} \sqrt{\frac{2 (h_T + h_G) \cot\theta_{rh} \cos\theta_{rh}}{\lambda ((h_T + h_G) \cot\theta_{rh} - d_{TR} + h_{W1r} \sin\theta_{rh}) (d_{TR} - h_{W1r} \sin\theta_{rh})}} \quad (89)$$

Additionally, to be added in the total electric field the reflected field over the Water1, the following condition has to be accomplished, $d_{zpr} > W_C$, where, d_{zpr} is the distance between z and p_r , depicted in Fig.16.

Finally, for the total electric field in Water1, an environmental correction factor is added. This factor introduces the attenuation caused for City before that signal arrives at the receiver over Water1. The correction factor, C_{W1} , is given by de following expression:

$$C_{W1}(W_C) = E_{\Sigma MC}(W_C) - E_{LOS}(W_C) \quad (90)$$

where:

$E_{\Sigma MC}(W_C)$: Total electric field for City at a distance equal to the width of City with constructions.

$E_{LOS}(W_C)$: Electric field for Line of sight at a distance equal to the width of City.

Then total electric field over Water1 is calculated. Considering Fresnel parameters, the conditions for reflection and the correction factor, there are four cases:

1) When v_{W1D} and v_{W1r} are lower than -0.78 and $d_{zpr} > W_C$ the total electric field for Water1 is:

$$E_{\Sigma MPW1}(R_{TR}) = E_{LOS}(R_{TR}) + E_{rh}(R_{TR}) + E_{d-}(R_{TR}) + E_{d-rh}(R_{TR}) + C_{W1}(W_C) \quad (91)$$

2) When v_{W1D} and v_{W1r} are lower than -0.78 and $d_{zpr} < W_C$ or v_{W1D} is lower than -0.78 and v_{W1r} is higher than -0.78, the total electric field for Water1 is:

$$E_{\Sigma MPW1}(R_{TR}) = E_{LOS}(R_{TR}) + E_{d-}(R_{TR}) + E_{d-rh}(R_{TR}) + C_{W1}(W_C) \quad (92)$$

3) When v_{W1D} and v_{W1r} are higher than -0.78 or v_{W1D} is higher than -0.78 and v_{W1r} is lower than -0.78 and $d_{zpr} < W_C$, the total electric field for Water1 is:

$$E_{\Sigma MPW1}(R_{TR}) = E_{d-}(R_{TR}) + E_{d-rh}(R_{TR}) + C_{W1}(W_C) \quad (93)$$

4) When v_{W1D} is higher than -0.78 and v_{W1r} is lower than -0.78 and $d_{zpr} > W_C$, the total electric field for City is:

$$E_{\Sigma MPW1}(R_{TR}) = E_{rh}(R_{TR}) + E_{d-}(R_{TR}) + E_{d-rh}(R_{TR}) + C_{W1}(W_C) \quad (94)$$

4.3.3 Formulation for Water2 Path for M-DTV

In Water 2 the maximum number of rays which arrive to the receiver is nine rays. For the scenario because of the frequency a slab represents the forest. Generally, the receiver is far away from the transmitter, and then diffraction on the left of the receiver can be calculated as grazing diffraction. On the other hand diffraction on the right of the forest will be slope diffraction, it means a huge attenuation of the signal, and therefore, this ray will not contribute to the total electrical field.

First of all the Fresnel parameters are calculated for direct, reflected and diffracted ray on the right. The Fresnel parameter for direct ray in Water2 Path, v_{W2D} , is calculated as follows:

$$d_{TF1} = W_C + W_{W1} + W_{F1} \quad (95)$$

$$d_{W2} = d_{TR} - d_{TF1} \quad (96)$$

$$h_{W2D} = \cos\theta_D (h_F + h_{GF} - h_{MR} - d_{W2} \tan\theta_D) \quad (97)$$

$$v_{W2D} = h_{W2D} \sqrt{\frac{2 d_{TR} \cos\theta_D}{\lambda(d_{TR} - d_{W2} - h_{W2D} \sin\theta_D) (d_{W2} + h_{W2D} \sin\theta_D)}} \quad (98)$$

Fresnel parameter for reflected ray in Water2 path, v_{W2r} , is calculated as follows:

$$h_{W2r} = \cos\theta_{rh} (h_F + h_{GF} - h_T - h_G + d_{TF1} \tan\theta_{rh}) \quad (99)$$

$$v_{W2r} = h_{W2r} \sqrt{\frac{2 (h_T + h_G) \cot\theta_{rh} \cos\theta_{rh}}{\lambda((h_T + h_G) \cot\theta_{rh} - d_{TF1} + h_{W2r} \sin\theta_{rh}) (d_{TF1} - h_{W2r} \sin\theta_{rh})}} \quad (100)$$

The second condition for the reflected ray to be added at the total electric field over Water2 is: $d_{zpr} > d_{TF1}$, where d_{zpr} is the distance between z and p_r , illustrated in Fig. 13 for Water2.

The Fresnel parameter for ray diffracted on the right is used to know if there is slope diffraction. When the incidence ray of diffraction is diffracted on the right then, the signal is attenuated for double diffraction and it does not contribute significantly to the total electric field. The equations for v_{W2d+} the Fresnel parameter for diffracted ray on the right are:

$$d_{TF2} = W_C + W_{W1} + W_{F1} + W_{W2} \quad (101)$$

$$d_{TW1} = W_C + W_{W1} \quad (102)$$

$$d_{W2} = d_{TR} - d_{TF1} \quad (103)$$

$$\theta_{d+} = \tan^{-1}((h_G + h_T) - (h_{GF} + h_F)) / d_{TW1} \quad (104)$$

$$h_{W2d+} = \cos\theta_{d+} (d_{W2} \tan\theta_{d+} * -1) \quad (105)$$

$$v_{W2d+} = h_{W2d+} \sqrt{\frac{2 d_{TW1} \cos\theta_{d+}}{\lambda(d_{TW1} - d_{W2} - h_{W2d+} \sin\theta_{d+}) (d_{W2} - h_{W2d+} \sin\theta_{d+})}} \quad (106)$$

Another parameter to be calculated is d_g , the distance of grazing diffraction. Grazing diffraction means that the incidence angle of diffraction is zero degrees, therefore the incidence ray of diffraction is grazing the 0 surface. In the case of Water2 as forest is not a uniform height, first is calculated, Δh_f , the difference height of forest. Then when d_g , is

bigger than 1, the incidence diffraction ray is grazing the forest. For example, if d_g is 50 m, the incidence diffracted ray is grazing the surface of diffraction (forest) 50 m before it reaches the point of diffraction. The equations to calculate the grazing distance are:

$$\Delta h_f = h_{fmax} - h_{fmin} \quad (107)$$

$$d_g = \frac{\Delta h_f}{\tan(\varphi')} \quad (108)$$

$$d_g > 1 \cong \text{grazing diffraction} \quad (109)$$

where:

h_{fmax} : Maximum forest height

h_{fmin} : Minimum forest height

φ' : Incidence angle of diffraction

The incidence angle of diffraction is near zero degrees in Water 2 because the receiver is far away from the transmitter. When the parameter d_g , distance of grazing diffraction is higher than 1, it means the incidence ray of diffraction is grazing the incidence surface of the obstacle. Furthermore in [26], when the angle is near zero it is considered a grazing diffraction.

Finally, for Water2 there is an environmental correction factor, to introduce the attenuations produced by city and Water1. The equation for a correction factor, $C_{W2}(W_{C+}W_{w1})$, is:

$$C_{W2}(W_{C+}W_{w1}) = E_{\Sigma MPW1}(W_{C+}W_{w1}) - E_{LOS}(W_{C+}W_{w1}) \quad (110)$$

The expressions for total electrical field in Water2, are divided into six cases based on Fresnel parameters and condition of the reflected ray and are detailed next,

- 1) When v_{W2D} , v_{W2r} and v_{W2d+} are lower than -0.78 and $d_{zpr} > d_{TF1}$ the total electric field for Water1 is:

$$E_{\Sigma MPW2}(R_{TR}) = E_{LOS}(R_{TR}) + E_{rh}(R_{TR}) + E_{d-}(R_{TR}) + E_{d+}(R_{TR}) + E_{d-rv}(R_{TR}) \quad (111)$$

$$+ E_{d-rh}(R_{TR}) + E_{d+rv}(R_{TR}) + E_{d+rh}(R_{TR}) + E_t(R_{TR}) + C_{W2}(W_C)$$

- 2) When v_{W2D} , v_{W2r} and v_{W2d+} are lower than -0.78 and $d_{zpr} < d_{TF1}$ or v_{W2D} and v_{W2d+} are lower than -0.78 and v_{W2r} is higher than -0.78, the total electric field for Water1 is:

$$E_{\Sigma MPW2}(R_{TR}) = E_{LOS}(R_{TR}) + E_{d-}(R_{TR}) + E_{d+}(R_{TR}) + E_{d-rv}(R_{TR}) \quad (112)$$

$$+ E_{d-rh}(R_{TR}) + E_{d+rv}(R_{TR}) + E_{d+rh}(R_{TR}) + E_t(R_{TR}) + C_{W2}(W_C)$$

- 3) When v_{W2D} , v_{W2r} are lower than -0.78 and v_{W2d+} higher than -0.78 or $d_g > 1$ and $d_{zpr} > d_{TF1}$ the total electric field for Water1 is:

$$E_{\Sigma MPW2}(R_{TR}) = E_{LOS}(R_{TR}) + E_{rh}(R_{TR}) + E_{d-}(R_{TR}) + E_{d-rv}(R_{TR}) + E_{d-rh}(R_{TR}) \quad (113)$$

$$+ E_t(R_{TR}) + C_{W2}(W_C)$$

- 4) When v_{W2D} , v_{W2r} are lower than -0.78, v_{W2d+} higher than -0.78 or $d_g > 1$ and $d_{zpr} < d_{TF1}$ or v_{W2D} is lower than -0.78 and v_{W2r} and v_{W2d+} are higher than -0.78, the total electric field for Water2 is:

$$E_{\Sigma MPW2}(R_{TR}) = E_{LOS}(R_{TR}) + E_{d-}(R_{TR}) + E_{d-rv}(R_{TR}) + E_{d-rh}(R_{TR}) \quad (114)$$

$$+ E_t(R_{TR}) + C_{W2}(W_C)$$

- 5) When v_{W2D} and v_{W2r} are higher than -0.78 and v_{W2d+} lower than -0.78 or v_{W2D} is higher than -0.78 and v_{W2r} and v_{W2d+} are lower than -0.78 and $d_{zpr} < d_{TF1}$, the total electric field for Water2 is:

$$E_{\Sigma MPW2}(R_{TR}) = E_{d-}(R_{TR}) + E_{d+}(R_{TR}) + E_{d-rv}(R_{TR}) + E_{d-rh}(R_{TR}) \quad (115)$$

$$+ E_{d+rv}(R_{TR}) + E_{d+rh} + E_t(R_{TR}) + C_{W2}(W_C)$$

- 6) When v_{W2D} and v_{W2r} are higher than -0.78 and v_{W2d+} higher than -0.78 or $d_g > 1$, or v_{W2D} is higher than -0.78 and v_{W2r} is lower than -0.78 and $d_{zpr} < d_{TF1}$ and v_{W2d+} higher than -0.78 or $d_g > 1$ the total electric field for Water2 is:

$$E_{\Sigma MPW2}(R_{TR}) = E_{d-}(R_{TR}) + E_{d-rv}(R_{TR}) + E_{d-rh}(R_{TR}) + E_t(R_{TR}) \quad (116)$$

$$+ C_{W2}(W_C)$$

4.3.4 Formulation for City Path for H-DTV

In the case of H-DTV the receiver is on the houses' rooftop then, is considered to have line of sight between the transmitter and the receiver. For the City path the maximum number of rays is three, the total electric field, $E_{\Sigma HC}$, considers two cases to be calculated:

- 1) If the distance, d_{prj} , illustrated in Fig. 13, between the incidence point of reflection over the rooftop, p_r , and j is lower than $W_B'/2$, then reflected ray is added to, $E_{\Sigma HC}$,

$$d_{prj} = \frac{h_A}{\tan \theta_{rh}} \quad (117)$$

$$E_{\Sigma HC}(R_{TR}) = E_{LOS}(R_{TR}) + E_{rh}(R_{TR}) + E_{d-}(R_{TR}) \quad (118)$$

- 2) If $d_{prj} > W_B'/2$, the total electric field for City Path is,

$$E_{\Sigma HC}(R_{TR}) = E_{LOS}(R_{TR}) + E_{d-}(R_{TR}) \quad (119)$$

4.3.5 Formulation for Forest1 Path for H-DTV

In Forest 1 and Forest 2 are used maximum 4 rays. For Forest1, the Fresnel parameter is used to know if the reflected ray on water is being diffracted for the house on the border of the river. It is calculated using the following expressions:

$$h_{HF1r} = \cos \theta_{rh} (d_{TR} \tan \theta_{rh} - (h_{BF} + h_{GF})) \quad (120)$$

$$W_B' = \frac{W_B}{\sin \alpha} \quad (121)$$

$$v_{HF1r} = h_{HF1r} \sqrt{\frac{2h_{HR} \cos^2 \theta_{rh}}{\lambda(h_{HR} - \sin \theta_{rh} d_{TR} + h_{HF1r} \sin^2 \theta_{rh}) (d_{TR} - h_{HF1r} \sin \theta_{rh})}} \quad (122)$$

After, calculating the Fresnel parameter, v_{HF1r} , then two cases are possible, as detailed next,

- 1) If $v_{HF1r} < -0.78$, total electric field in Forest1, $E_{\Sigma HF1}$, is:

$$E_{\Sigma HF1}(R_{TR}) = E_{LOS}(R_{TR}) + E_{rhH}(R_{TR}) + E_{rhW1}(R_{TR}) + E_{d-}(R_{TR}) \quad (123)$$

where:

- $E_{rhH}(R_{TR})$: Reflected field over the rooftop of the houses

- $E_{rhW1}(R_{TR})$: Reflected field over Water1
- 2) If $v_{HF1r} > -0.78$, total electric field in Forest1, $E_{\Sigma HF1}$, is:

$$E_{\Sigma HF1}(R_{TR}) = E_{LOS}(R_{TR}) + E_{rhH}(R_{TR}) + E_{d-}(R_{TR}) \quad (124)$$

4.3.6 Formulation for Forest2 Path for H-DTV

For Forest2, the Fresnel parameter determines if the house on the border of the river is diffracting the reflected ray. The expressions to calculate it are as follows,

$$h_{HF2r} = \cos\theta_{rh}(d_{TR} \tan\theta_{rh} - (h_{BF} + h_{GF})) \quad (125)$$

$$v_{HF2r} = h_{HF2r} \sqrt{\frac{2h_{HR} \cos^2\theta_{rh}}{\lambda(h_{HR} - \sin\theta_{rh}d_{TR} + h_{HF2r}\sin^2\theta_{rh})}} \quad (126)$$

$$(d_{TR} - h_{HF1r}\sin\theta_{rh})$$

For Forest2 there are two cases for the total electric field, $E_{\Sigma HF2}$, described as follows,

- 1) If $v_{HF2r} < -0.78$,

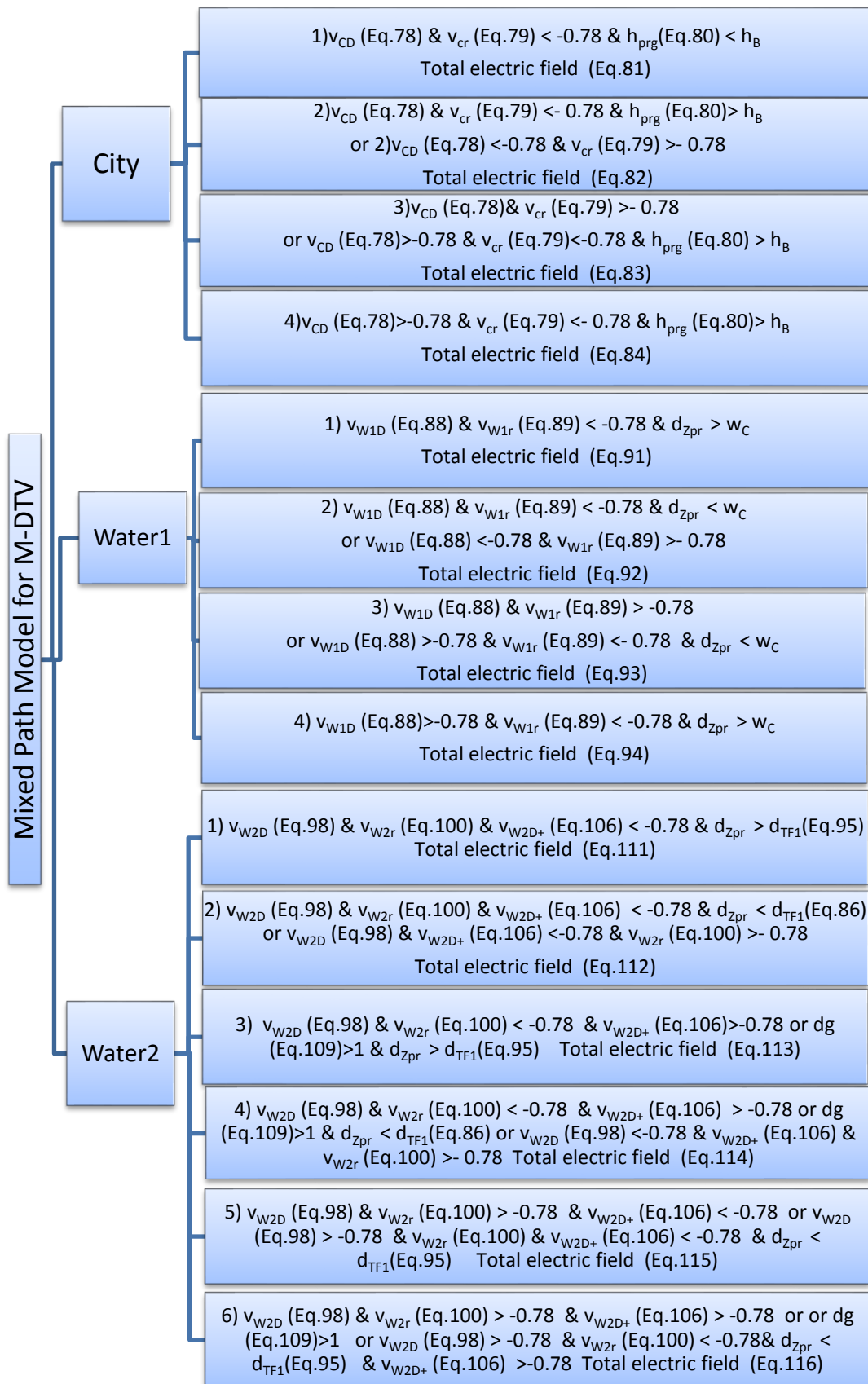
$$E_{\Sigma HF2}(R_{TR}) = E_{LOS}(R_{TR}) + E_{rhH}(R_{TR}) + E_{rhW2}(R_{TR}) + E_{d-}(R_{TR}) \quad (127)$$

where:

- $E_{rhW2}(R_{TR})$: Reflected field over Water2
- 2) If $v_{HF1r} > -0.78$,

$$E_{\Sigma HF2}(R_{TR}) = E_{LOS}(R_{TR}) + E_{rhH}(R_{TR}) + E_{d-}(R_{TR}) \quad (128)$$

4.3.7 Summary of Mixed Path model formulation for M-DTV



This summary has all the equations and conditions to implement Mixed Path model.

In the case of the City, as described before, four cases are considered in order to calculate the total electric field. The first case evaluates if the Fresnel parameter is lower than -0.78 , then Direct ray and reflected ray are not obstructed and all the eight rays are added to the total electric field. In the second case even when the Fresnel parameter for the reflected ray is lower than -0.78 , h_{prg} is higher than h_B , and there is not surface of reflection, then in the total electric field the reflected ray is not added. The third case is when the Fresnel parameters are higher than -0.78 , then the total electric field is the addition only of diffracted rays. In the fourth case, the Fresnel parameter of direct ray is higher than -0.78 and the Fresnel parameter of reflected ray is lower than -0.78 and h_{prg} is lower than h_B , as a consequence the total electric field does not consider only the direct ray.

For Water 1 and Water 2, as the same as in City, the Fresnel parameters are evaluated in order to add or not the direct ray or reflected ray or both in the total electric field.

4.4 Final considerations

In this section was presented Mixed Path model formulation. City path uses eighth rays, Water1 uses four rays and a correction factor because of the attenuation caused by City, Water2 uses nine rays and the correction factor because of attenuation caused by City and Water1. The first Fresnel zone has to be unobstructed to add the direct and/or reflected ray in the total electric field. Finally, the Mixed Path model formulation predicts the electric field for mixed City-river-forest- path.

Chapter 5 – Results of the proposed model

5.1 Introduction

The formulation of Mixed Path uses parameters such as the height of antennas, the height of buildings, permittivity and conductivity of the materials, the width of the city, etc. To know the sensibility of the model some parameters are modified and evaluated.

For Mixed Path are of special interest parameters as the level of the river, electrical constants of forest and transition zone. Since these parameters are part of the contributions of this work for the mixed city-river-forest path not studied before.

5.2 Analysis of Mixed Path model parameters

In order to evaluate the influence of the Mixed Path model parameters in the total electric field, some of them take different values. For example, the values for width of the street are varied from 6 to 18 meters. The parameters to be evaluated are the following,

W_s	Width of the street from top view Fig. 16.
α	Angle between the straight-line transmitter-receiver and the street or building (top view).
h_B	Height of building over ground.
W_c	Width of City.
h_T	Height of transmitter over ground.
h_R	Height of receiver.
h_W	Height of water.
ψ_{iaf}	Incidence angle for air-forest.
ϵ_B, σ_B	Electrical parameters for building: permittivity, conductivity, respectively.
ϵ_w, σ_w	Electrical parameters for water: permittivity, conductivity, respectively.
ϵ_f, σ_f	Electrical parameters for forest: permittivity, conductivity, respectively.

First of all, are established the values for calculation of electric field with Mixed Path model, these values are in Table III.

Table III- Values for parameters used in Mixed Path model

Values of Parameters		
$P_t = 6000 W$	$G_R = 2.15 \text{ dBi}$	$L = 1.4 \text{ dB}$
$f = 521.142 \text{ MHz}$	$h_{GC} = 7 \text{ m}$	$h_T = 114.58 \text{ m}$
$h_{MR} = 4 \text{ m (City)}$ $h_{MR} = 5 \text{ m (Water)}$	$h_{BC} = 15 \text{ m}$	$h_{GF} = 2 \text{ m}$
$h_A = 3 \text{ m}$	$h_{BF} = 3 \text{ m}$	$h_F = 18 \text{ m (R1 and R2)}$
$h_F = 21 \text{ m (R3)}$	$\alpha = 9^\circ \text{ (R1)}$	$\alpha = 12^\circ \text{ (R2 and R3)}$
$\alpha(\text{anulli}) = 10^\circ$	$W_B = 10 \text{ m}$	$W_C(R1) = 1.68 \text{ km}^*$
$W_C(R2) = 1.4 \text{ km}^*$	$W_C(R3) = 1.5 \text{ km}^*$	$W_S = 10 \text{ m}$
$W_{w1}(R1) = 3.338 \text{ km}$	$W_{w1}(R2) = 3.375 \text{ km}$	$W_{w1}(R3) = 1.88 \text{ km}$
$W_{F1}(R1) = 3.87 \text{ km}$	$W_{F1}(R2) = 3.045 \text{ km}$	$W_{F1}(R3) = 1.079 \text{ km}$
$\epsilon_b = 7 \text{ (building [39])}$	$\sigma_b = 0.0437 \text{ S/m (building[39])}$	$\epsilon_w = 80 \text{ (water [40])}$
$\sigma_w = 0.05 \text{ S/m (water[40])}$	$\epsilon_f = 1.3 \text{ (forest[19])}$	$\sigma_f = 0.03 \text{ mS/m (forest [19])}$
$\epsilon_s = 2.7 \text{ (street [19])}$	$\sigma_s = 0.04 \text{ S/m (street [19])}$	

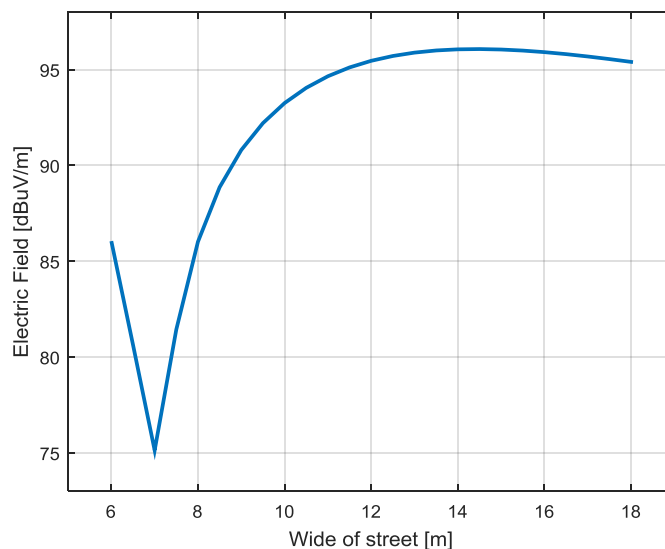
* In the case of Belem of Pará, the City path has 1.7 km of length. The values in Table III are different because was considered a length of the city where the constructions end for each Radial. It is important because the length of the city gives us the distance of the point of diffraction for the transition zone city-river.

Next, the parameters mentioned before are evaluated giving different values.

1) Width of street.

The values of the width of the street are between 6 and 18 meters. In Fig. 17 can be observed the results for a receiver located at a distance of 3km in City.

Fig. 17. Rays used in Mixed Path for calculation of total electric field for M-DTV and H-DTV.



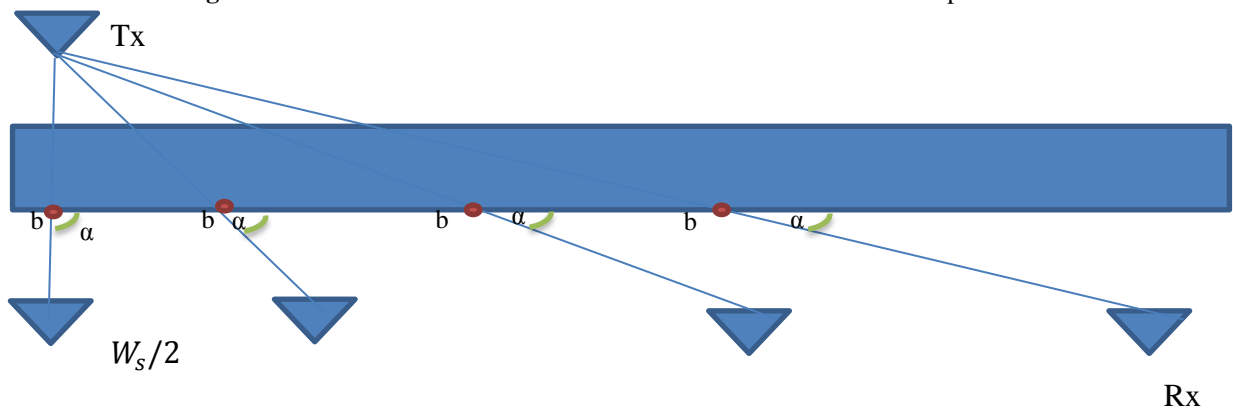
Source: Author

Then Fig 17 illustrate that for a street between 6 and 9 meters, the values of the electric field are lower than for a street of 10 m because the diffraction is stronger for narrow streets than for wide streets. For a street between 10 and 18 meters, the electric field has a soft variation. Then for wide streets, the Electric field is higher than for narrow streets.

2) Angle α

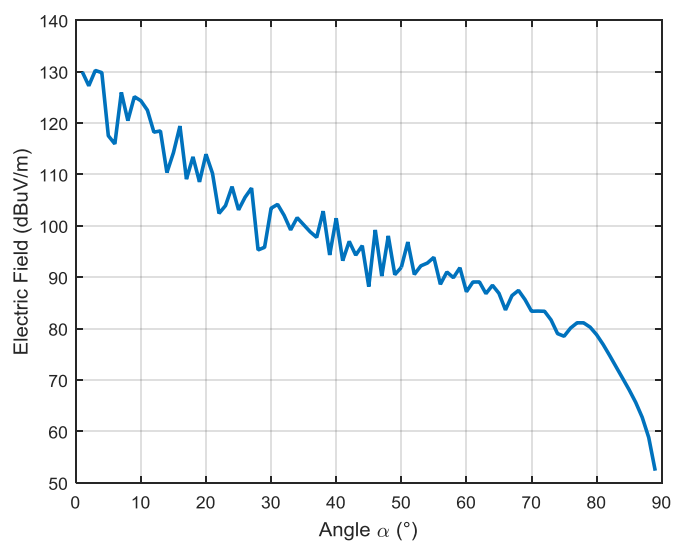
This parameter considers a receiver on the center of the street. Then the variation of the angle indicates the position of the receiver in relation with, b , the point of diffraction as illustrated in Fig.18 from a top view. The decreasing of the angle α indicates that the distance between transmitter and receiver increases and the receiver is getting far from the diffraction point.

Fig. 18. Variation of α when the receiver is in the same street from a top view.



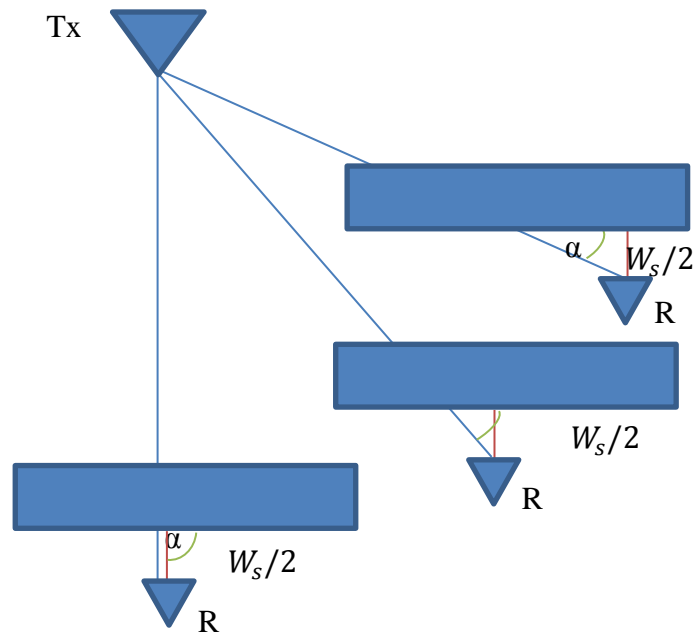
Source: Author

Fig. 19. Electric field for the variation of alpha when the receiver is in the same street.



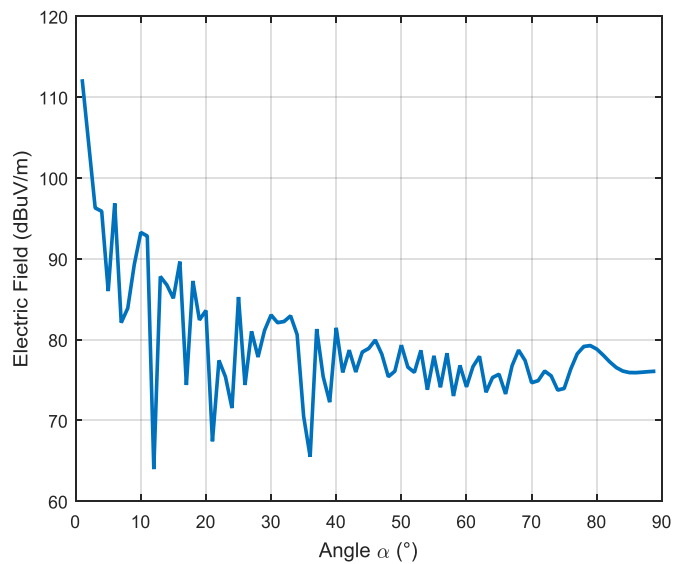
Source: Author

Fig. 20. Variation of angle α using the same distance between transmitter and receiver from a top view.



Source: Author

Fig. 21. Angle α vs Electric field.



Source: Author

Fig. 19, shows that with the increase of the angle α the electric field is decreasing, because with big angles only diffracted rays contribute to the total electric field. On the other hand, for small angles receiver can have line of sight ray as a contributor because the receiver is far from the obstacle.

For a constant distance between transmitter and receiver, while α has different values, it means that the receiver has different positions, as Fig. 20 illustrates.

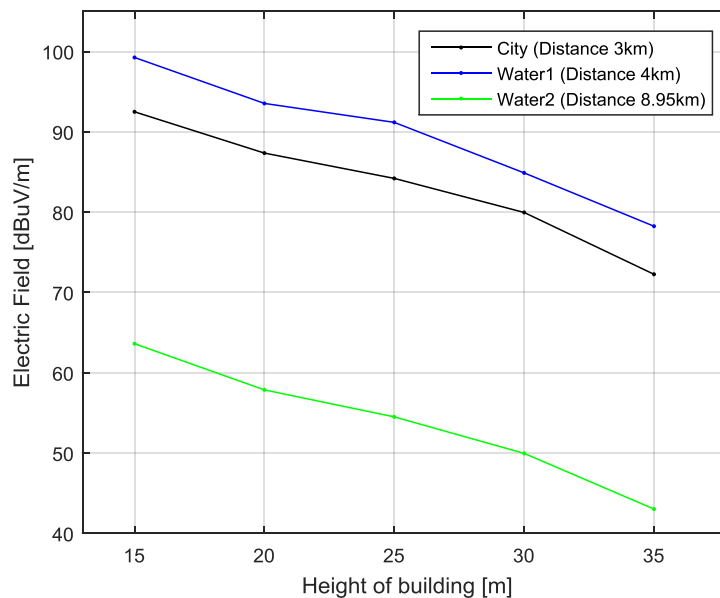
In Fig. 21, for angles up 45 degrees different rays reach the receiver, therefore, the signal presents significant increasing and attenuation. However, for angles higher than 45 degrees the signal shows a soft decreasing because only diffracted rays reach the receiver.

1) Height of building over the ground

Three different distances are used to evaluate the influence of the building's height in the received electric field, 3km for a receiver in the city, 4 km for a receiver over Water1 and 8.95 km for a receiver over Water2.

Fig. 22 illustrates that the signal decreases as the height of the buildings increases for the three different receivers. The receiver in the City path is surrounded by buildings; therefore, the signal is lower than the signal received in Water1, which considers buildings only on the left of the receiver.

Fig. 22. Height of building vs Electric field.



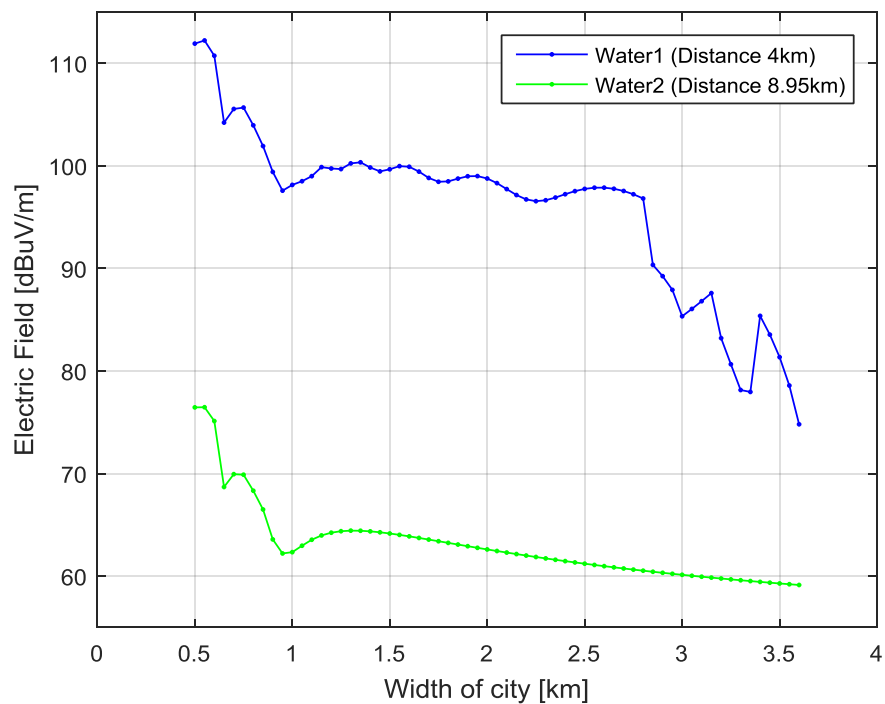
Source: Author

2) Width of city

This parameter is the total length of the city in the mixed city-river-forest path. Results for the receivers over Water 1 and over Water 2 show that the values of electric field decrease

with the width of the City. For Water 1 the receiver is fixed at 4 km from the transmitter, therefore when city width increases it means city is getting near to the receiver located over water, and then the receiver enters in the shadow zone. In the case of Water2 when the City width increases the value of the correction factor increases and electric field is lower than for Water 1.

Fig. 23. Width of the city vs Electric field.



Source: Author

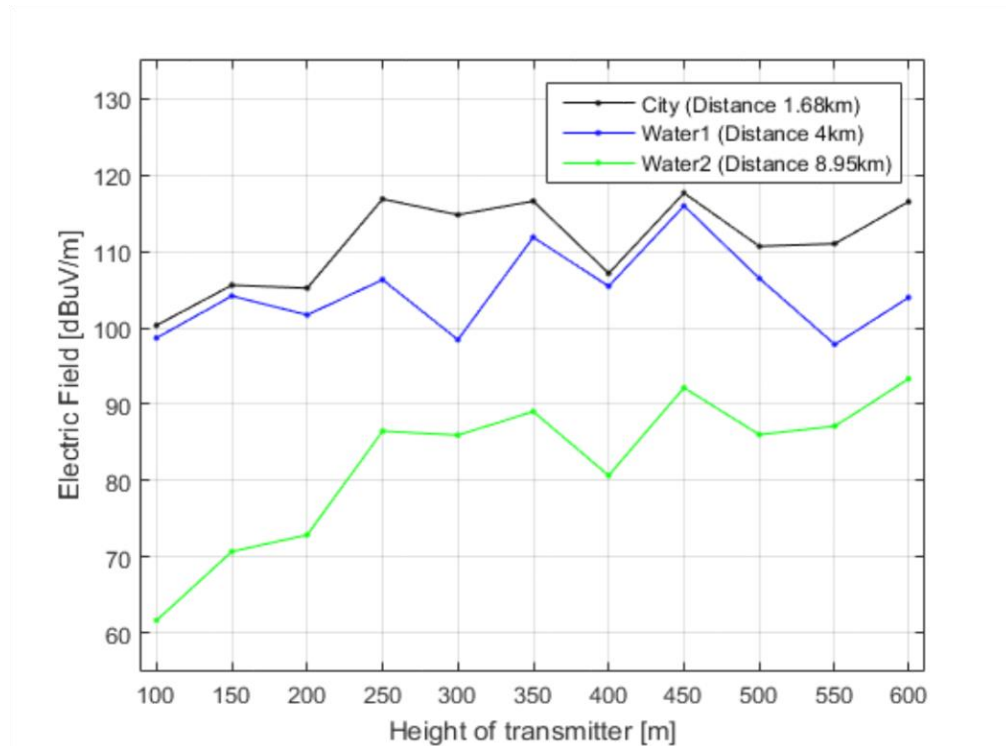
3) Height of the transmitter antenna

For Fig. 24, in three different positions is located the receiver, the first in the city, the second over Water1 and the third over Water2. For the three positions is calculated the electric field using different values of the transmitter height. The increasing of the transmitter height allows having more rays to contribute in the total electric field. However, when the direct ray exists is not advisable to increase the transmitter height because the distance between the transmitter and receiver increases, therefore, the electric field decreases.

For a receiver in the City in Fig.24, when the transmitter is higher than 300 m, a reflected ray is the principal contributor of the total electric field. The reflected ray for

different transmitter heights has similar values because the distances are similar. In some occasions the addition is not in phase, for a transmitter of 400 m, 500 m and 550 m which have lower values. For the receiver of Water1 and Water2, diffracted rays are the principal contributors to the total electric field and for a transmitter of 400m, 500m and 550m the rays are added in opposite phases.

Fig. 24. Height of transmitter antenna vs Electric field.

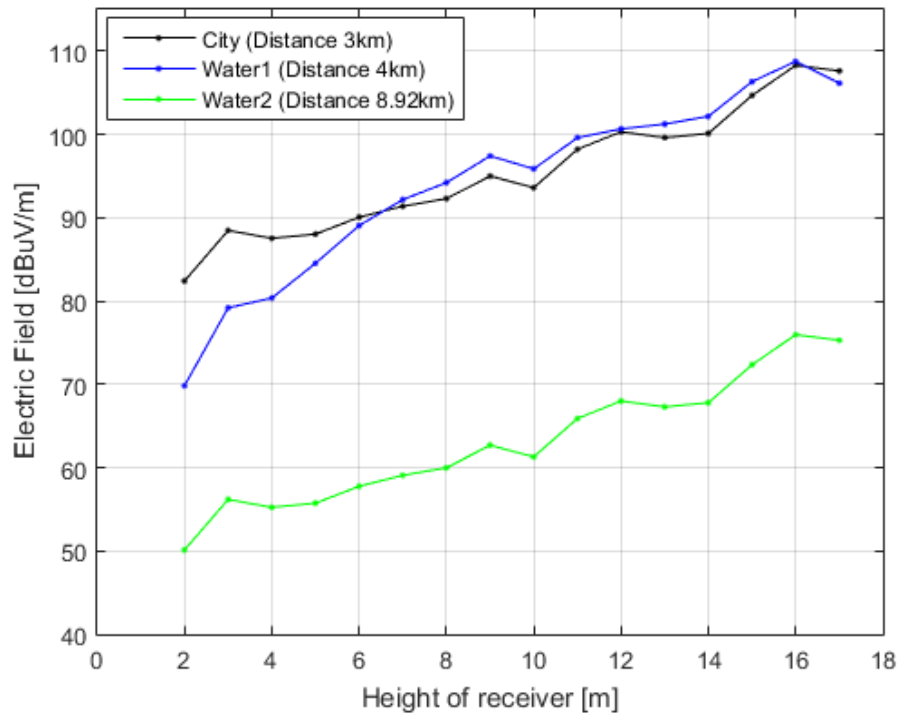


Source: Author

4) Height of receiver antenna

The first receiver is in the city, the second receiver is over Water1 and the third receiver is over Water2. In Fig. 25 for higher receivers is illustrated higher electric field, because of the direct ray. The receiver height values are from 2 to 17 meters, and the height of the buildings is 18 m since the receiver in this model is considered to be lower than the constructions. Some values of the electric field are lower even when the receiver is higher because of the adding in opposite phase of the rays. A receiver over Water1 has higher values than a receiver on the City for some receiver's height because; the diffraction is only on the left of the receiver.

Fig. 25. Height of receiver antenna vs Electric field.



Source: Author

5) Level of Water for H-DTV

A receiver on the border of the forest is analyzed when the level of water decreases in 3 meters. The decreasing of the river level is the increasing of the transmitter and receiver heights.

According to ABNT 1506, the minimum value of the electric field for Digital television is 54.54 dBuV/m and the maximum value is 111 dBuV/m or more. Then, considering the river level the best receiver antenna height is calculated using an optimization tool. Furthermore, in the calculation of the total electric field is included the cable loss.

In order to know the best height of the receiver antenna to obtain the highest electric field was used a Genetic Algorithm function from Matlab. The objective function is also implemented in Matlab and uses equations (123) and (124) for total electric field in Forest 1. A population of 50 samples and 50 generations were used. The ranges [Xmax Xmin] are the levels of ground of city from 7 to 10 meters in variation of 0.25 m and the ground of the island from 2 to 5 meters. This is because when the level of the river is zero the level of the ground is 7 m for city and 2 m for the forest and when the level of the river decreases 3 meters the level of the ground in city is 10 m and 5 m for the forest. The ranges [Ymax Ymin] are the

height of the antenna from 1 m to 15 m. The objective is to maximize the electric field to be equal or higher than 109 dBuV/m.

Fig. 26. Values electric field vs receiver antenna height from 9.65 m to 12.2m.

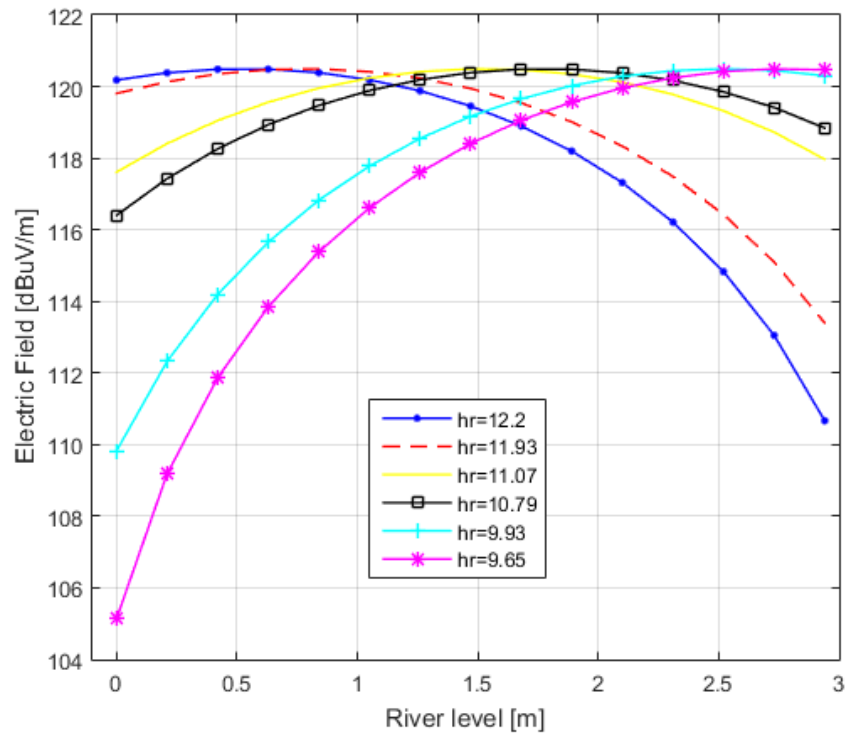
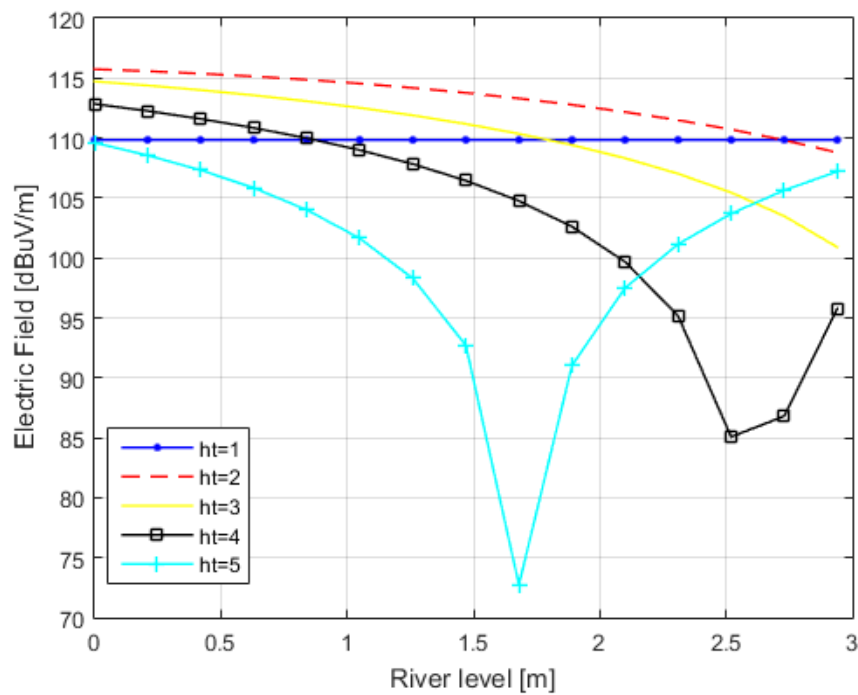


Fig. 27. Values electric field vs receiver antenna height from 1 m to 5 m.



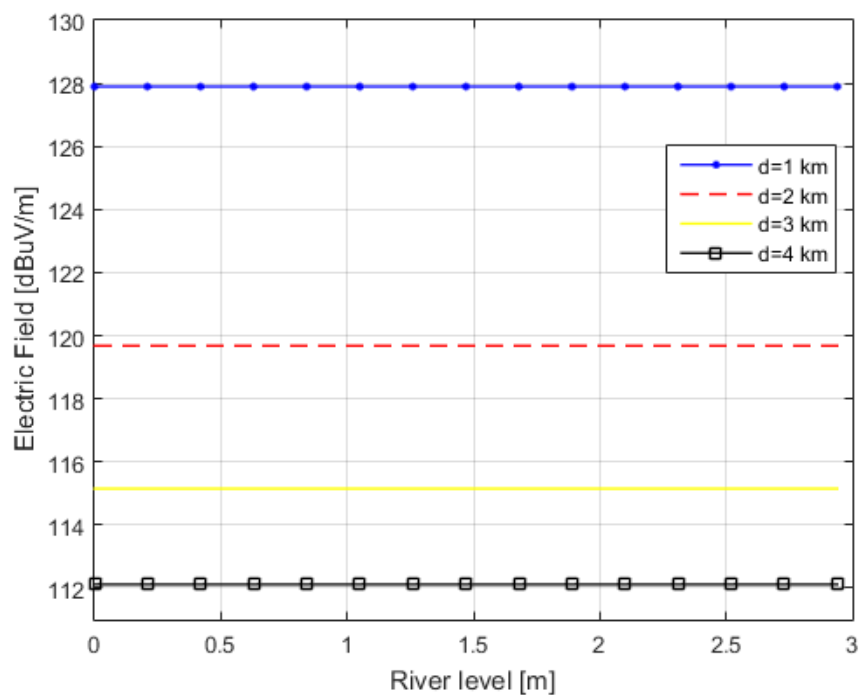
Source: Author

First is calculated the best height of the receiver antenna for each river level and 13 results are obtained, after from these results are calculated the best height of the receiver antenna for all the rivers levels. In Fig. 26 the better antennas heights are shown for a fixed receiver at 5 km. The best height of the receiver antenna is 11.07 m. Then a receiver antenna of 11 m has a minimum value of 115 dbuV/m and the cable loss is 3 dB.

Other receiver antennas heights were evaluated, from 1 m to 5 m, we can conclude from Fig. 27, that a receiver of 5 m is the worst height for a receiver. However, an antenna of 2 m height produces the maximum value of 115 dbuV/m and the minimum value 108 dbuV/m, these are values around the maximum value, then this solution is not the best but it is the cheaper solution.

For a situation where the receiver is in line of sight with the transmitter, for different distances the height of the antenna is 1 m, as can be observed in Fig. 28.

Fig. 28. Values of electric field for a receiver antenna of 1 m height in different distances.



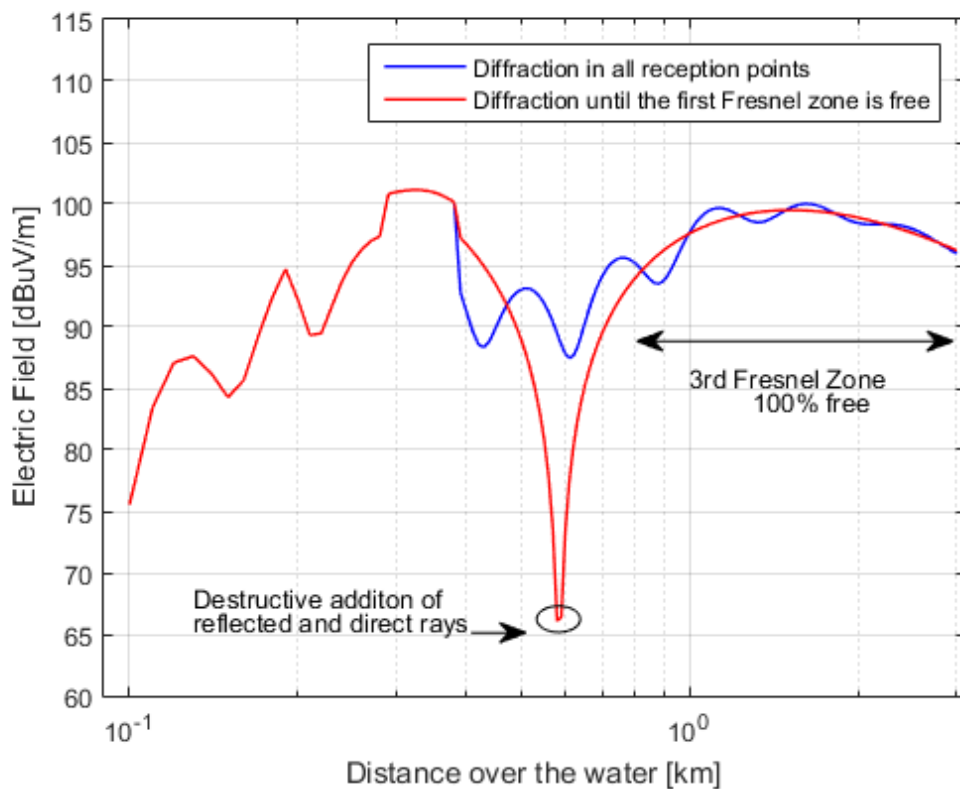
Source: Author

6) Distance over the water

A receiver is evaluated moving away from the city. In Fig. 29 the blue line illustrates that at all reception points is added the diffracted ray. In the case of the red line the diffracted ray is not added for distances greater than 0.4 km.

In addition, the arrow in Fig. 29 indicates that for distances greater than 0.8 km the third zone of Fresnel is unobstructed. Therefore, the diffracted ray is not more a significant contributor and the values represented with the blue and the red lines are similar. In other words, after the transition zone, a direct ray and a reflected ray are enough to represent the signal over the river.

Fig. 29. Distance over the water vs Electric field.



Source: Author

7) Level of water for M-DTV

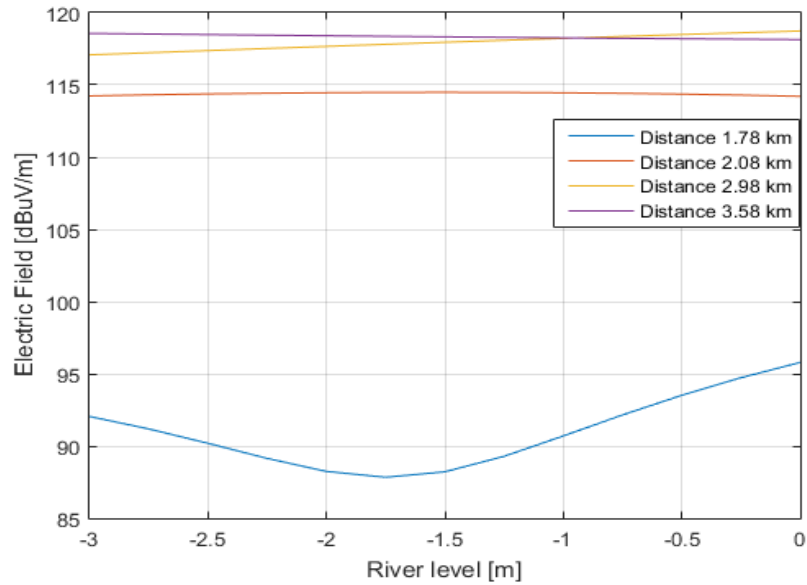
In Fig. 30, was evaluated the variation of the water level for a receiver of 5 m height, where different distances are represented, considering a city length of 1.68 km. For 1.78 km, the variation of the signal is more significant because it is close to the city. In the three remaining cases, the electric field value is almost constant for different river level values.

In Fig. 31, are illustrated the results for a receiver of 10 m height. The electric field values in Fig. 30 are greater than the values in Fig. 29 because of the receiving antenna height. However, only for a distance of 2.08 km when the river decreases between 2.3 m and 3 m, the signal attenuates up to 8 dB. At the distance of 1.78 km, the variation of the electric

field strength is of a maximum of 5 dB. The variation in these two distances can be attributed to the fact that they are close to the city. In the other cases, the signal remains constant with the variation of the river level.

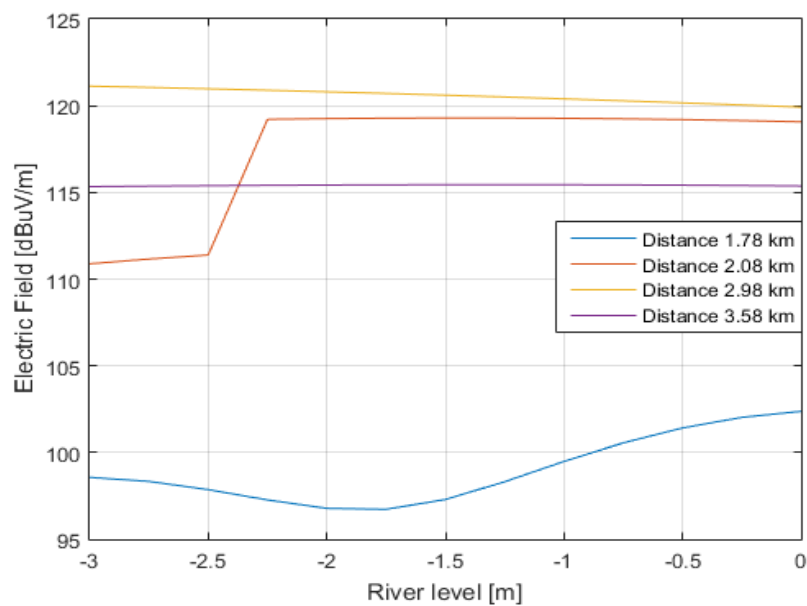
Comparing the results of Fig. 27 and Fig. 30, the water level influences the signal variation in up 28 dB for H-DTV, unlike for M-DTV where the maximum variation is 8 dB.

Fig. 30. Level of water for a 5 m receiver height over the water vs Electric field.



Source: Author

Fig. 31. Electric field vs level of water for a 10 m receiver height



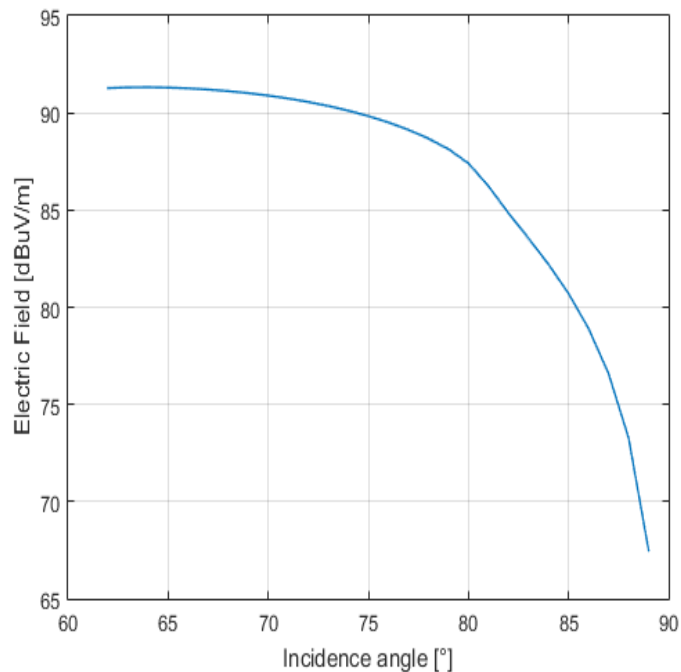
Source: Author

8) Incidence angle of forest

In Fig. 32 is illustrated the received signal for a receiver of 4 m height and different values of incidence angle. The width of the city is 1km, the river width is 1km and the width of the forest is 1.980 km. Then the electric field is low for high values on incidence angles.

Furthermore, from Table IV for higher incidence angles lower transmitted angles. Then for an incidence angle close to 90 degrees, the transmitted ray reaches receivers for greater distances. For lower incidences angles the transmitted ray reaches receivers near the forest.

Fig. 32. Electric field vs incidence angle Forest-Air.



Source: Author

Table IV- Angle of incidence Forest-Air and transmitted angle forest ar

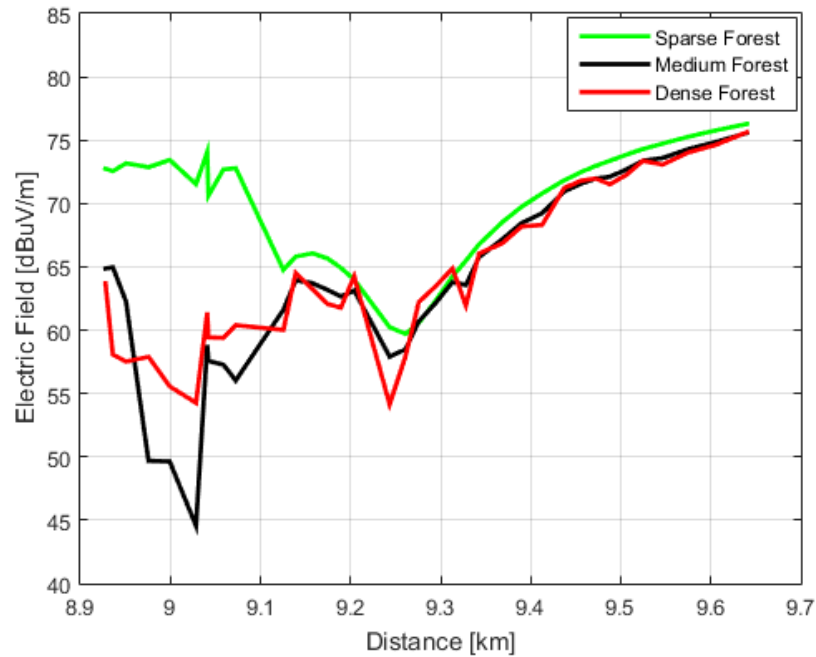
Incidence angle ar- forest [°]	89	88	87	86	77	76	75
Transmitted angle forest-ar [°]	74.58	74.87	75.36	76.07	88.80	88.94	89.05

9) Electrical parameters at the forest

In [19] the forest electrical parameters are: for a sparse forest $\sigma = 0.03mS/m$ and $\varepsilon = 1.01$, for a medium forest $\sigma = 0.1mS/m$ and $\varepsilon = 1.1$ and for a dense forest $\sigma = 0.3mS/m$

and $\varepsilon = 1.3$. In Fig. 33 the results are for a receiver located behind the forest and over Water2. For distances up to 9.1 km, the received electric field value is higher for the sparse forest than for the medium and the dense forest. In Figs. 34-36 for the different types of the forest is presented the value of the amplitude of each ray that contributes in the total electric field.

Fig. 33. Electrical parameters for forest vs Electric field.



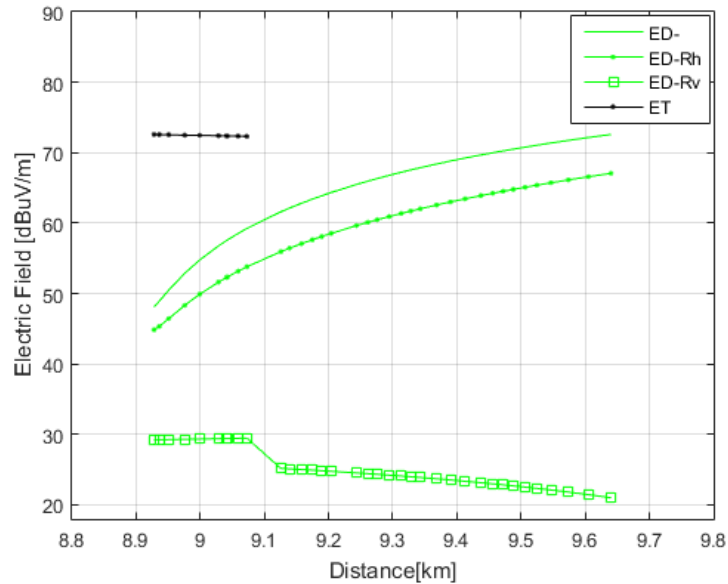
Source: Author

In Fig. 34, the transmitted field, E_T , exists for distances lower than 9.1 km, the amplitude of this ray is 73 dBuV/m, then the total electric field is higher in the first points of reception over water 2 for a sparse forest. After 9.1 km only diffracted rays exist, the diffracted ray, E_{D-} , and diffracted reflected ray on the water, E_{D-Rh} , have significant values however the diffracted reflected ray on the forest, E_{D-Rv} , has low values that do not contribute to the total electric field. The diffracted ray and diffracted reflected ray on the water, have values that are increasing with the distances because, the values of the diffracted coefficients are higher when $\phi - \phi'$ produce values near π , it means is near the shadow boundaries. In this case, the incidence angle of diffraction, ϕ' , has low values around 1° , and ϕ has values a little higher than 180° .

For a medium forest in Fig. 35, the E_T , is only in the three first points of reception with lower values than for a sparse forest, 64 dBuV/m. Furthermore, the first points for E_{D-} and

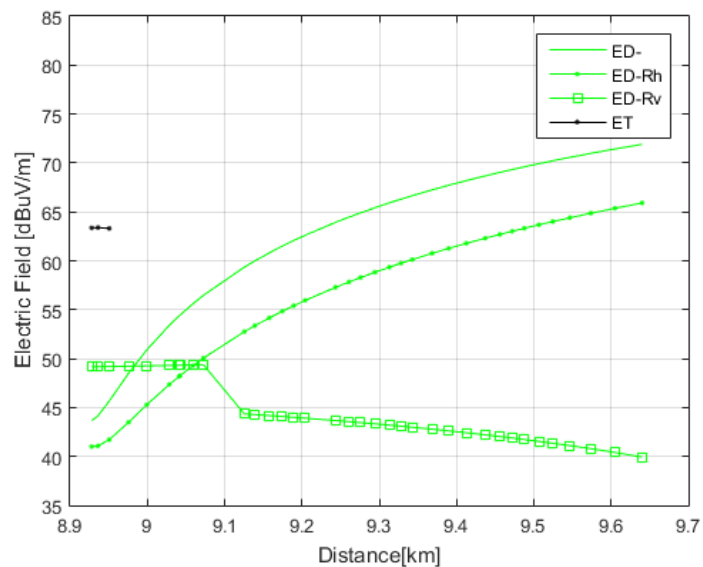
E_{D-Rh} , have lower values than for sparse forest, when distances increase the values of the electric field are similar to a sparse forest but still lower.

Fig. 34. Amplitude of each ray of total electrical field for sparse forest.



Source: Author

Fig. 35. Amplitude of each ray of total electrical field for medium forest.



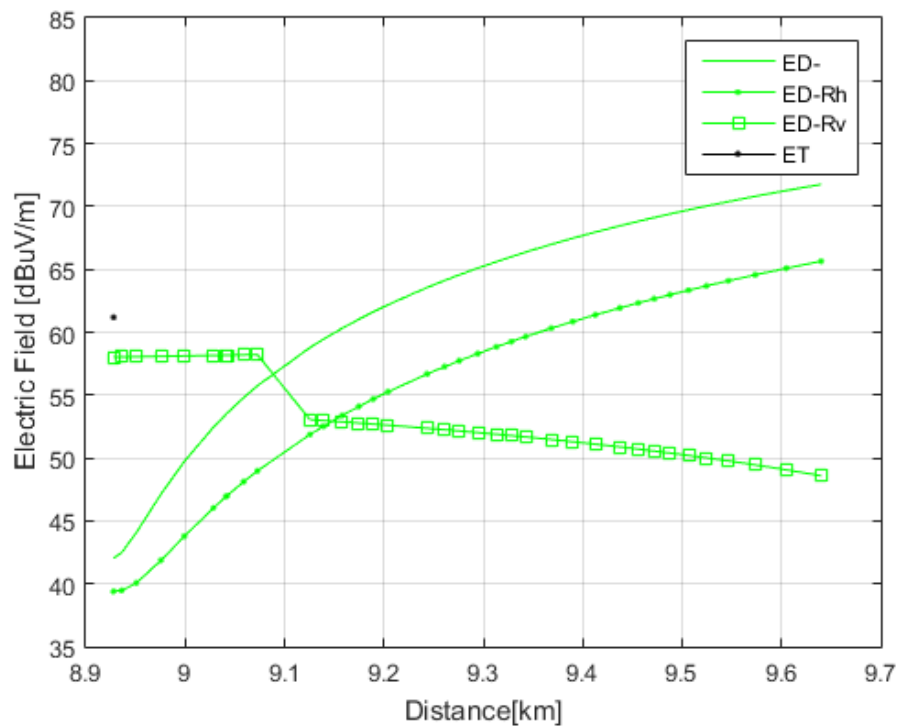
Source: Author

On the other Hand in the same Fig. 35, the values of E_{D-Rv} , are higher than the values for a sparse forest, because with the higher permittivity the signal returns to the receiver and

for a sparse forest most of the signal cross the forest. Before 9.1 km the values of E_{D-Rv} , are higher because the angles of diffraction $\phi - \phi'$ are near the value of π , after 9.1 km only E_{D-} and E_{D-Rh} contributes to the total electric field. For Radial 2 the values of E_{D-Rv} , are added in the opposite phase, for this reason, before 9.1 km it has the lowest values comparing the three types of forest.

The transmitted electrical field arrives only to one point of reception for a dense forest in Fig. 36. The values of E_{D-Rv} , are higher than for a medium forest and for distances lower than 9.1 km the addition with the other rays is in phase, then the electric field value is higher than for a medium forest. The values of E_{D-Rh} and E_{D-} , are similar to the values of a medium forest and are the principal contributors to the total electric field after 9.1 km of distance.

Fig. 36. Amplitude of each ray of total electrical field for dense forest.



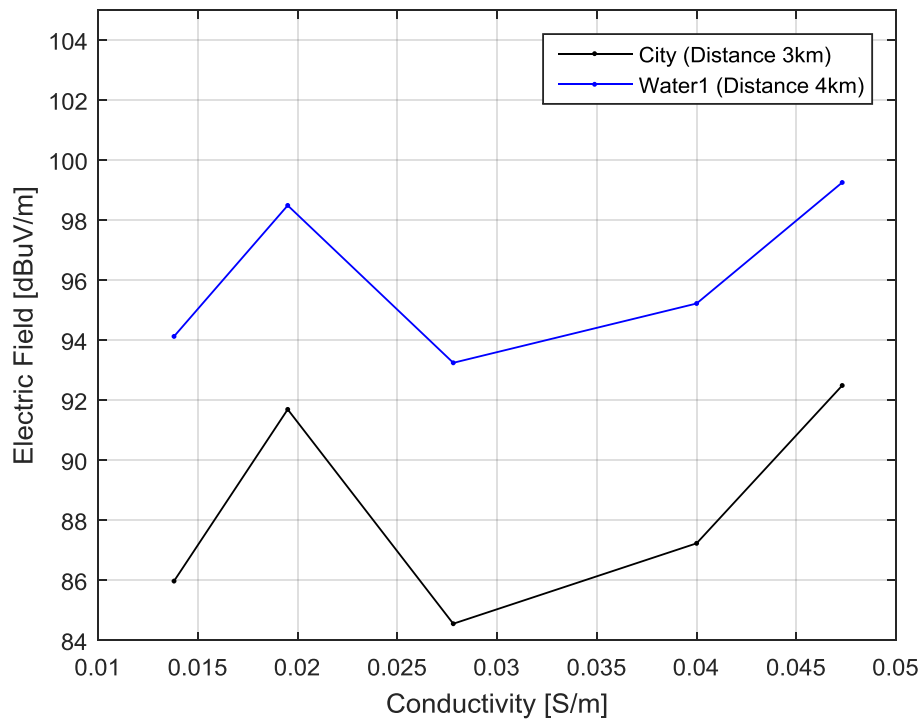
Source: Author

10) Electrical parameters of buildings for city

The values of conductivity and permittivity of 5 types of concrete are detailed In Table V. In Fig. 37 the results are for a receiver located in the city at a distance of 3 km and another receiver located on Water1 at a distance of 4km. The electric field on the city has lower values than electric field over the water because in the city the receiver is surrounded by

constructions while the receiver over the water has constructions only in the transition zone. The difference between heavy concrete and light concrete is 8 dB in the city and 7 dB over water. Then, the electric field is higher when the permittivity has higher values, as the cases of the street and heavy concrete from Table V.

Fig. 37. Electrical parameters for buildings vs Electric field.



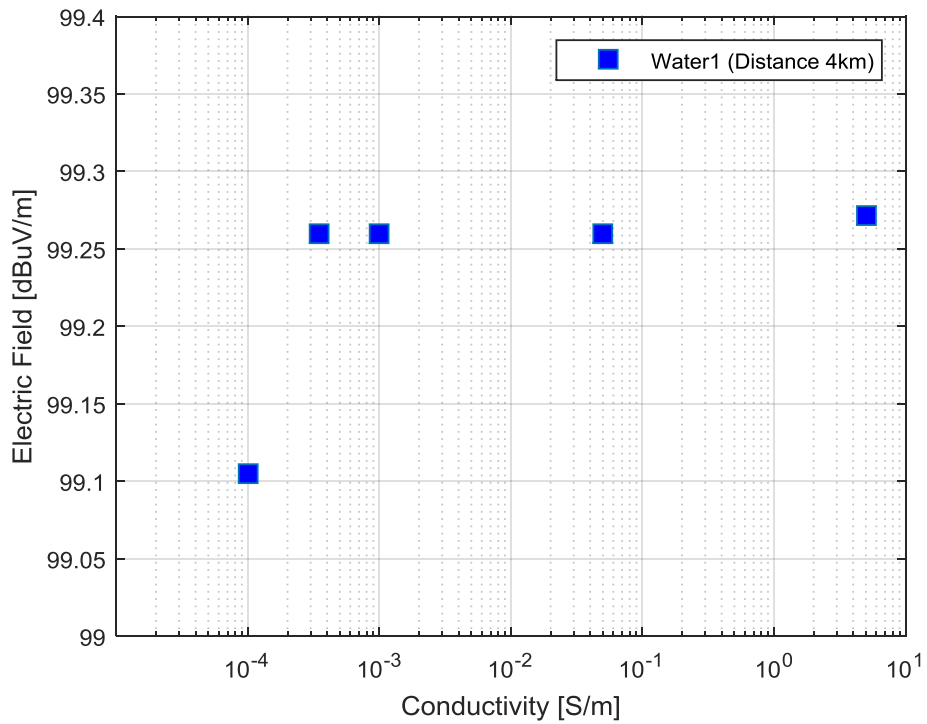
Source: Author

Table V- Electrical parameters for different types of concrete [39]

Material	Conductivity	Permittivity
Aerate concrete	0.0138	2.5
Street	0.0195	6
Light concrete	0.0278	2
Reinforced concrete	0.04	2.7
heavy concrete	0.0473	7

11) Electrical parameters water

Five different electrical parameters of water from [40], [41] detailed in Table VI are analyzed. The receiver is 4m height and it is at a distance of 4km. In Fig. 37, the electric field is practically the same for all types of water with permittivity 80. For ice, the electric field is different in 0.1 dB.

Fig. 38. Electrical parameters for water vs Electric field.

Source: Author

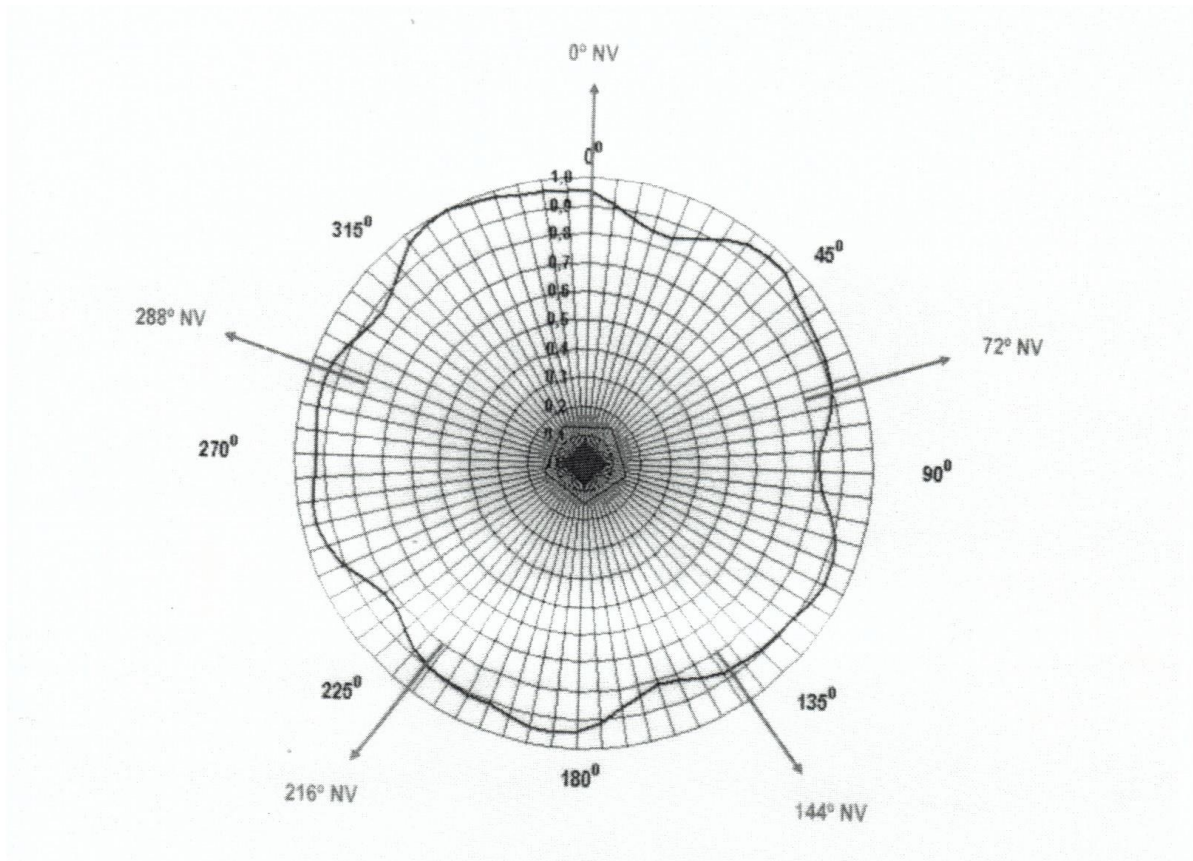
Table VI- Electrical parameters for water

Material	Conductivity	Permittivity
Fresh water Amazon	$3.5e-4$	80
Fresh water Amazon	$1e-3$	80
Sea	5	80
Fresh Water	$5e-2$	80
Ice	$1e-4$	3

12) Radiation pattern of transmitter and receiver antennas

For Digital television, the polarization of the antennas most of the times is horizontal. At homes, the common external antenna is a log periodic. In Figs. 39 and 40 are exhibited the radiation patterns of a transmitter antenna and a log periodic antenna respectively.

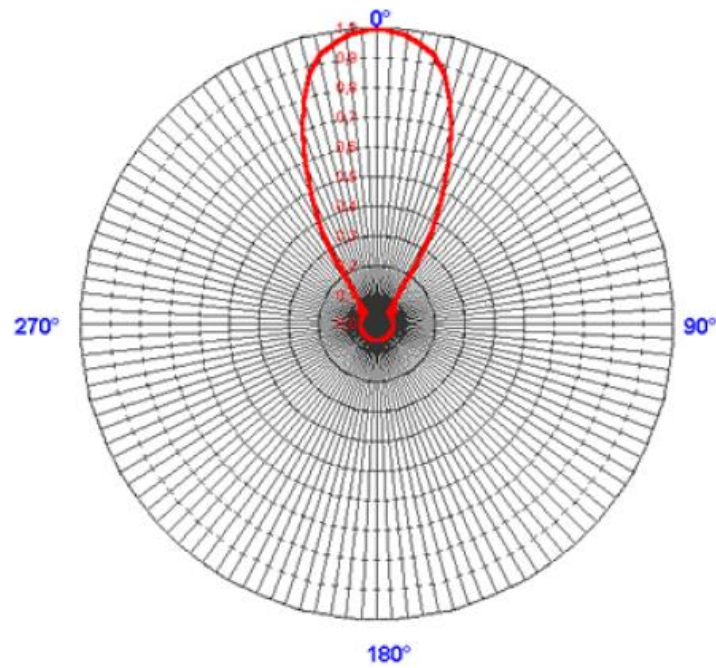
Fig. 39. Radiation Diagram of Transmitter Antenna.



Source: Broadcaster technical documentation.

Fig. 40. Radiation Diagram of Receiver Antenna.

Channels: 14 - 59

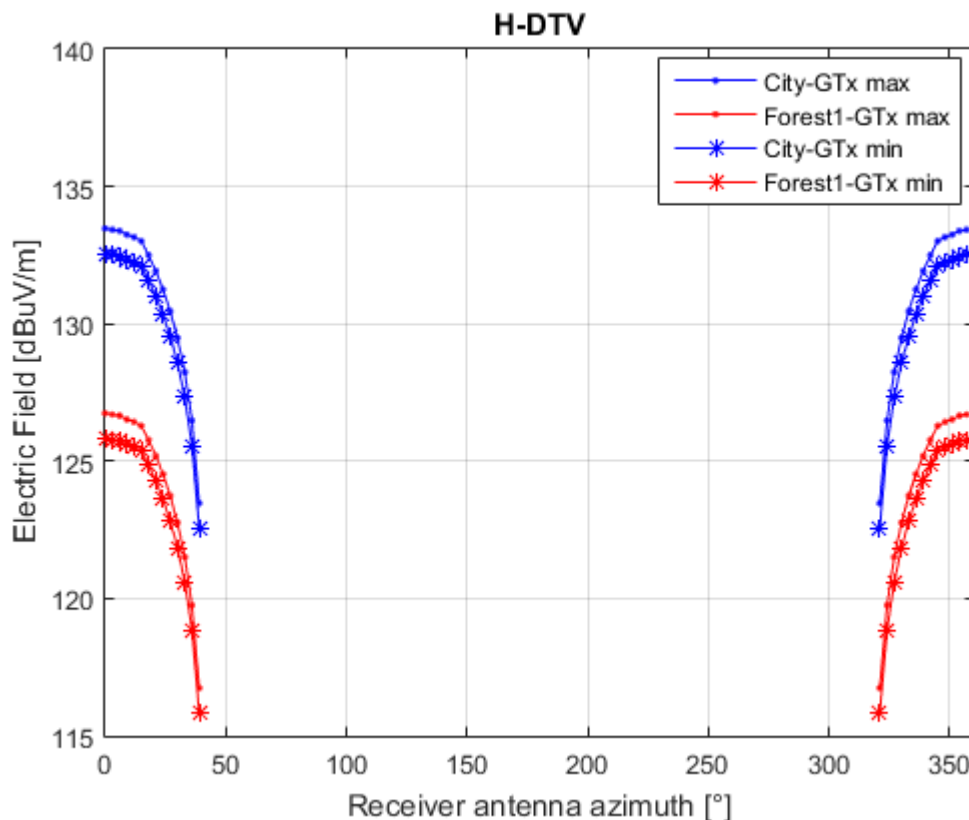


Source: Datasheet of log periodic Antenna

An analysis of the received electric field is realized for a fixed position of the receiver but rotating the receiver antenna 360°. The transmitter antenna is considering to have the maximum gain for 330° of azimuth with 13.25 dBi and minimum gain in 160° of azimuth with 12.33 dBi. The receiver antenna has its maximum gain of 12 dBi in 0° and its lowest value at 39° of 2 dBi. In Fig. 41 are shown the results for the maximum and the minimum gain of the transmitter antenna. The receiver is in the city and over forest1 at a distance of 1.68 km and 8 km respectively. When both antennas have their maximum gain in city electric field reaches the value of 133.5 dBuV/m and in Forest1 126 dBuV/m. In contrast when both antennas have their lowest gain in city electric field is 122.6 dBuV/m and in the forest is 115.8 dBuV/m.

Furthermore, for a receiver antenna with its maximum gain pointing the lowest gain of the transmitter antenna, the user receives 132 dBuV/m, this value is higher than the maximum value recommended for receivers in the ABNT 1506.

Fig. 41. Electric field vs azimuth of transmitter antenna



Source: Author

5.3 Measurement Campaign

In order to validate the Mixed Path model, two measurement campaigns were carried out in Belém of Pará for a digital TV station. The first measurement campaign was developed only in a suburban environment, with distances of up to 20 km as shown in Fig. 42. There were 37 points of measurement. The reception antenna had a height of 4 m, horizontal polarization, a gain of 5 dBi and was omnidirectional.

The second measurement campaign was carried out in three types of environments, as shown in Fig. 43. The first environment is the city, the measured points are close to the river bank, the second environment is over the river and the third environment is over the river behind the forest. The reception antenna had a height of 4 m in the city and 5 m over the water. The gain of the antenna was 2.15 dBi with horizontal polarization and omnidirectional.

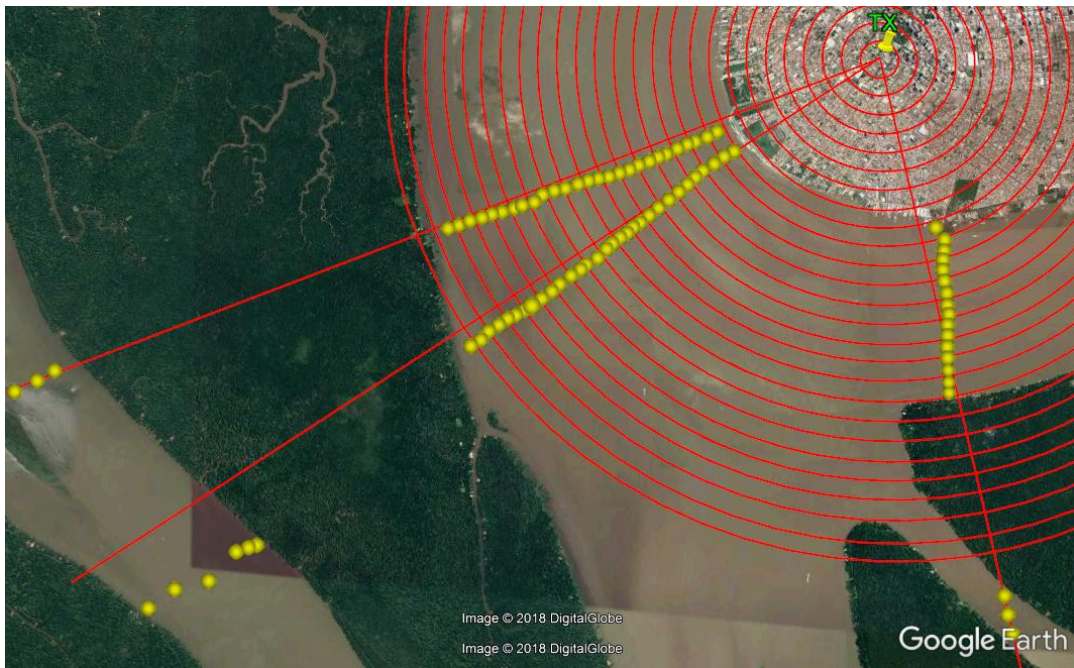
The transmission system was the same for the two measurement campaigns. The central frequency of transmission was 521 MHz, with a bandwidth of 6 MHz. The height of the transmitter antenna was 114.58 m over the ground level and the antenna gain was 13.25 dB. The Effective Radiated Power (ERP) was 49.32 dB. In Belem 352 points distributed in three radials were collected in the measurement campaign, 15 in the city, 212 over the river and 125 over the river behind the forest.

Fig. 42. Reception points for the first measurement campaign in City.



Source: Google Earth

Fig. 43. Reception points for the second measurement campaign for City-River-Forest-River.



Source:Google Earth

A spectrum analyzer ANRITSU was used to collect power reception, GARMIN'S GPS 12 MAP Personal NavigatorTM was used to take the geographic coordinates. In the case of points over the water, measurements were constant, in a speed of 11 km/h. For all the measurement points the receiver antenna was rotated to obtain the maximum power reception.

In Figs. 44-47, is shown the environment of the second measurement campaign and part of the equipment used for it.

Fig. 44. City-river path in Belém of Pará.



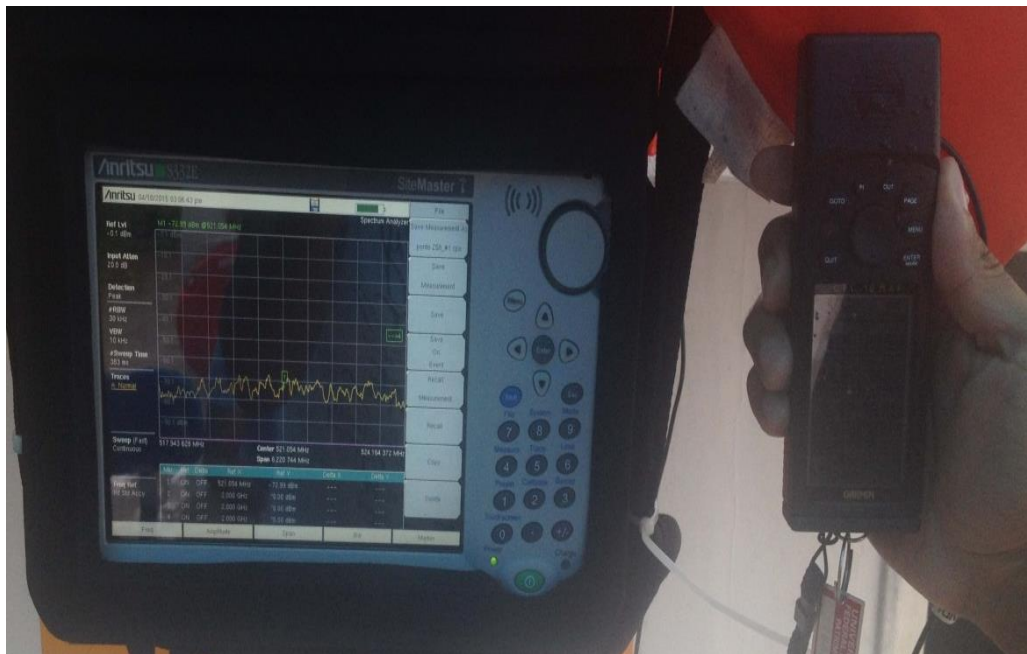
Source:Author

Fig. 45. River-Forest path in Belém of Pará.



Source:Author

Fig. 46. Spectrum analyzer and GPS.



Source:Author

Fig. 47. Receiver antenna over Curupira Ship.



Source: Author

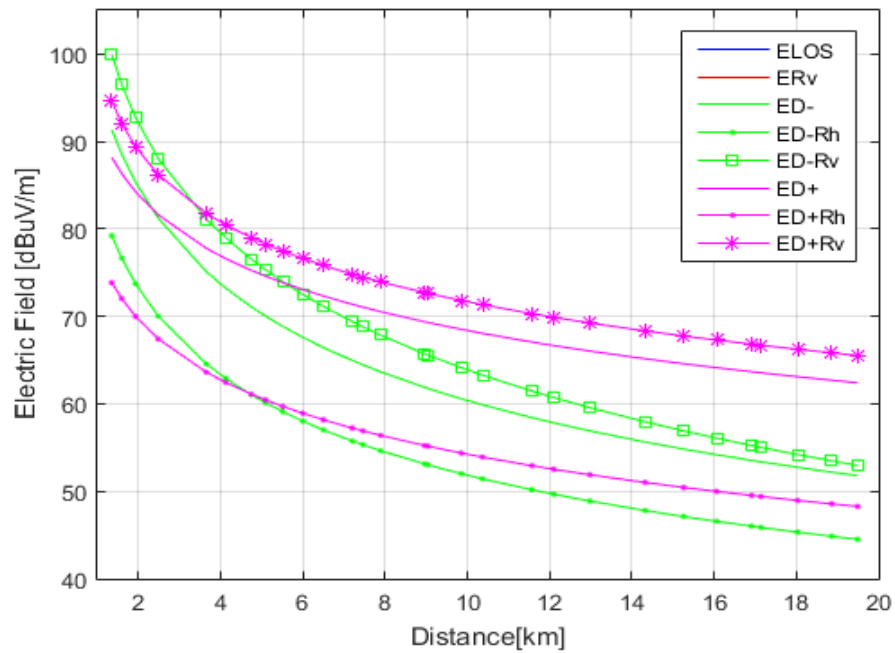
5.4 Results for Mixed Path model

Four different environments are evaluated to validate Mixed Path model. For M-DTV and H-DTV is evaluated the mixed City-Water1-Forest1-Water2-Forest2 path. For M-DTV data is analyzed in radials and annuli. For H-DTV data is analyzed only in radials. Below are detailed the results.

5.4.1 Results for M-DTV City

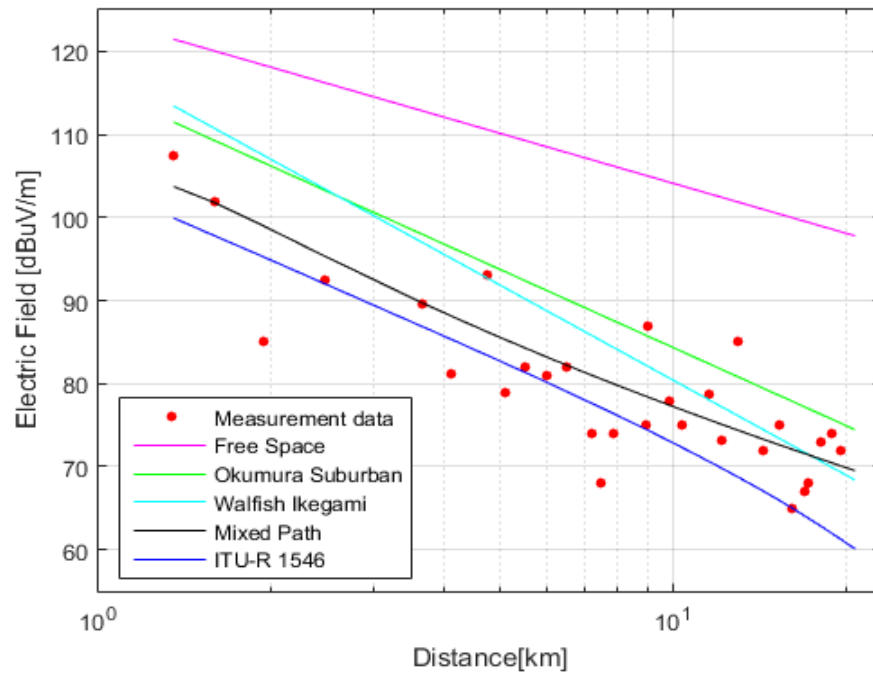
First of all, for a receiver located in the city are calculated the results. Fig. 48 illustrates the amplitude of each ray which contributes to the total electric field for Mixed Path model. For distances lower than 3 km the higher amplitude is for, E_{D-Rv} , the diffracted ray on the left reflected on the wall of the building. Diffracted rays reflected on the buildings, E_{D-Rv} and E_{D+Rv} have the higher values, because of the angles of diffraction, ϕ and ϕ' , the subtraction of $\phi - \phi'$, have values near π , then the values of electric field are higher than E_{D-} and E_{D+} . The lowest electric field is given by Diffracted reflected ray on the street. Then for this case of study the rays which are the principal contributors are the diffracted on the right.

Fig. 48. Electric field amplitude of each ray for total electric field in City



Source:Author

Fig. 49. Results of different Radio Propagation models over Belém City for M-DTV.



Source:Author

After the calculation of electric field using Mixed Path model for M-DTV, are compared the results with three radio propagation models which are Okumura Hata, ITU-R P.1546-5 and COST 231-Walfish Ikegami, depicted in Fig.49.

The parameters for the calculations are in Table III. Furthermore, measured data were organized in annuli of 200 m to have a uniform scenario.

In Fig. 49, the free space model gives the reference of the maximum values that the electric field can reach. Okumura Hata and Walfish Ikegami show higher values than the data measured in the first 10 km because, in the case of Okumura, it is an empirical model that was designed based on the characteristics of Tokyo and in the case of Walfish Ikegami it does not consider the electrical parameters in the calculations. For distances greater than 10 km, all the models are approximate to the measured data because it is a residential area without large buildings.

On the other hand, ITU-R1546 presents approximate but lower values compared to the measured data, due to ITU-R P. 1546 considers higher constructions than Belem. ITU-R 1546-5 determines 20 m height and Belem has an average of 15 m height for a suburban area. Mixed Path model manages to show an average of the measured values because it considers both the electrical parameters of the environment and the average height of the constructions.

5.4.2 Results for M-DTV City-Water1-Forest1-Water2

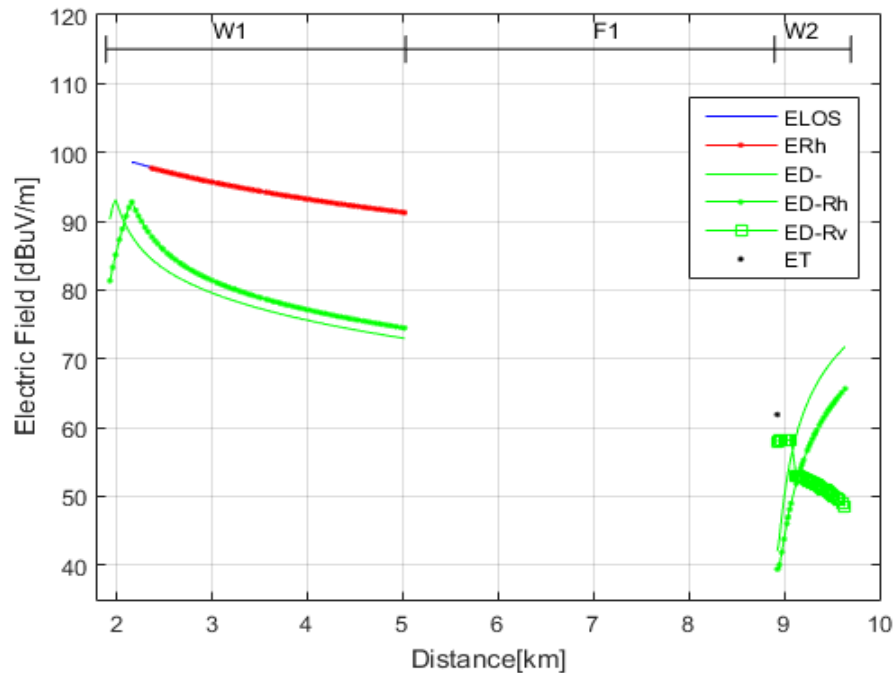
Radial 1

The transmitter is in the city, and the receiver is over Water1 and over Water2. The parameters used for the calculations are in Table III. First, in Fig. 50 the amplitude of each ray is illustrated, the principal rays are E_{LOS} and E_{Rh} , then E_{D-} has the highest values in the first reception points after that E_{D-Rh} has the higher values of the diffracted rays. E_{D-Rh} , has higher values than E_{D-} because the diffraction is near the shadow boundary, in other words, $\phi - \phi'$, have values near π . For Water2, E_T is only for the first point of reception, E_{D-} and E_{D-Rh} , are increasing with the distance because the subtraction of the angles of diffraction $\phi - \phi'$ is getting values near π . The first values of E_{D-Rv} , contribute in the total electric field and are higher for distances up to 9 km because the angles of diffraction are near the shadow boundary.

After the calculation of electric field using Mixed Path model, in Fig. 51, the results are compared with measured data and two models of radio propagation, Okumura Hata and ITU-

R P.1546-5. In Water1 for distances up to 2.5 km measured data shows lower values than for bigger distances, this is because it is the transition zone (city-water) and is affected by constructions near the river border.

Fig. 50. Electric field amplitude of each ray for total electric field calculated for Radial 1 over Water1 and Water2.



Source: Author

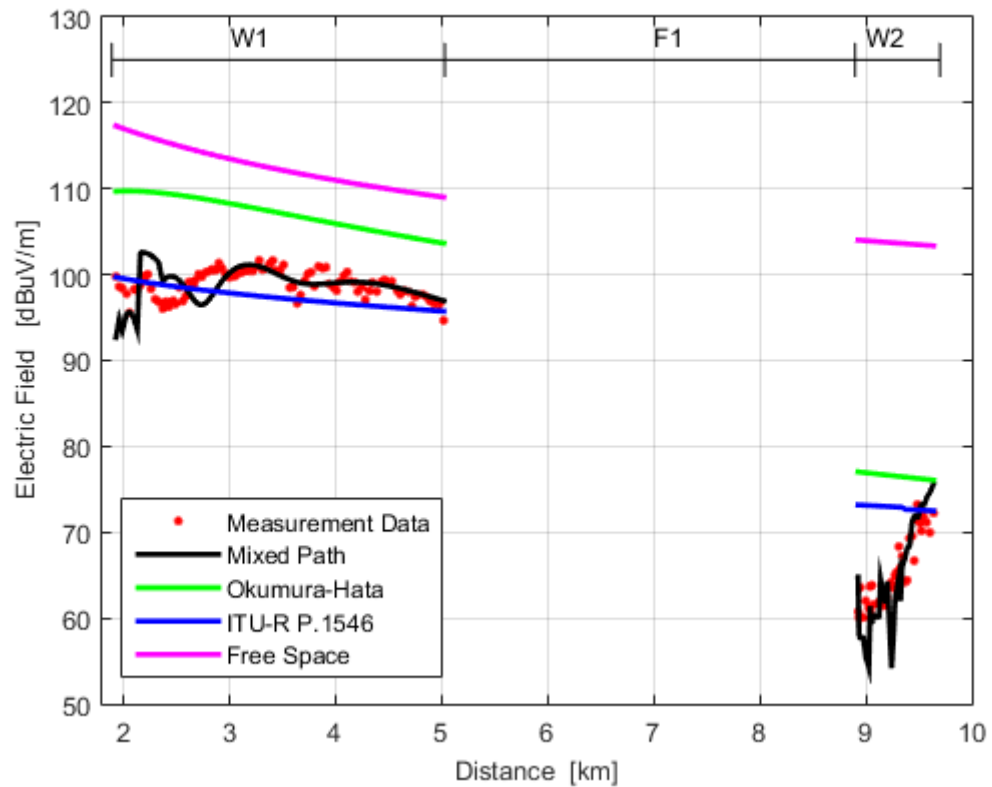
Okumura Hata and ITU-R P.1546 were calculated using the mixed path corrections of each model. In the case of Okumura Hata, the correction aims to increase the value of the electric field because there are no obstacles over the water. Consequently, the electric field values obtained with Okumura Hata are greater than measured data over Water1. ITU-R P.1546-5 has similar values to the measured data; however, this model does not represent the recovery effect of the signal in the transition zone.

Mixed Path model has a good agreement with measured data and predicts the electric field in the transition zone. It is because Mixed Path model considers constructions on the border of the river and the interaction of the principal rays in amplitude and phase.

Okumura Hata model and ITU-R. P.1546-5 are not designed to calculate electric field over a river and behind a forest (Water2), therefore, to calculate the electric field values with Okumura Hata and ITU-R1546, the factor for vegetation attenuation of ITU-R P.833 was added. Fig. 51 depicts that Mixed Path model predicts the diffraction in the first points of reception behind the forest and the increasing of the signal when the distances increases. As

conclusion, Mixed Path model is in good agreement with measured data over Water1 and over Water2, estimating the diffraction effects caused by the constructions in the city and for the forest.

Fig. 51. Results for Radial 1 over Water 1 and over Water 2.



Source: Author

Between each radio propagation model and the measurement, data was calculated the Root Mean Square Error. In Table VII, are presented the RMSE results, first for reception points over each path Water1 or Water2, and second for all the reception points over Water1 and Water2. Mixed Path model presents the lowest RMSE, for the two paths separated and the two paths together. ITU-R1546 has a good agreement with measurement data only for Water2. However, Okumura-Hata and ITU-R P.1546 have high RMSE values for Water2, because these models are not for mixed paths including forest.

The electrical parameters for the forest in Belem of Para were calculated to minimize the RMSE for Mixed Path model. It was possible using a Genetic Algorithm from Matlab.

The objective was to obtain the less RMSE between measurement data and predicted data using Mixed Path model.

From Tamir [38] , were obtained the range of values for conductivity and permittivity used in AG algorithm. The RMSE values calculated with the new electrical parameters for the forest are presented in Table VII. However, RMSE is reduced only in 0.2 dB, that is similar to the RMSE obtained with electrical parameters from literature.

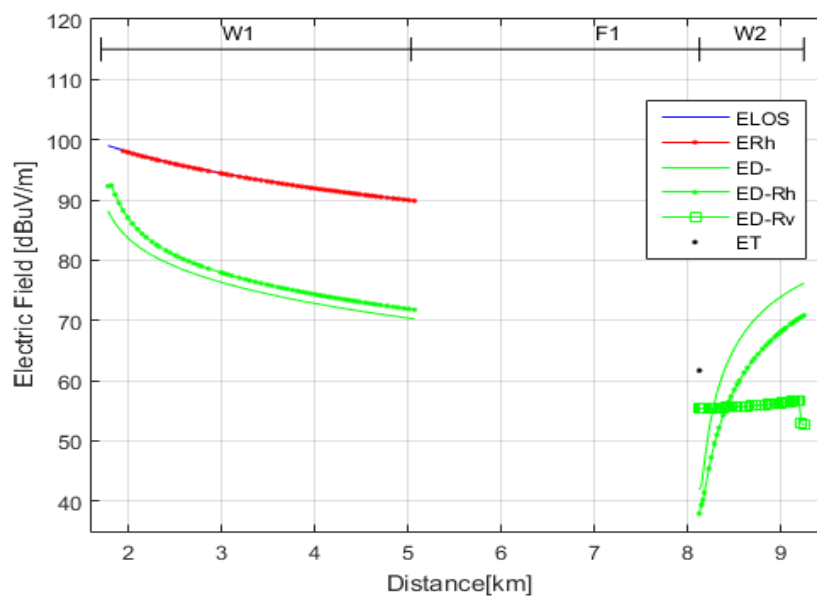
Table VII. RMSE for Radial 1- M-DTV

	Radial 1 RMSE [dB]		
	Water1	Water2	Water1-Water2
Mixed Path	2.1	3.66	2.63
Okumura-Hata	8.57	11.94	9.65
ITU-R P.1546	2.33	8.57	4.97
Mixed. Path ($\epsilon_f = 1.4$)	2.1	3.46	2.56

Radial 2

First of all the amplitude of each ray that contributes in the total electric field are illustrated in Fig. 52.

Fig. 52. Electric field amplitude of each ray for total electric field calculated for Radial 2 over Water1 and Water2.

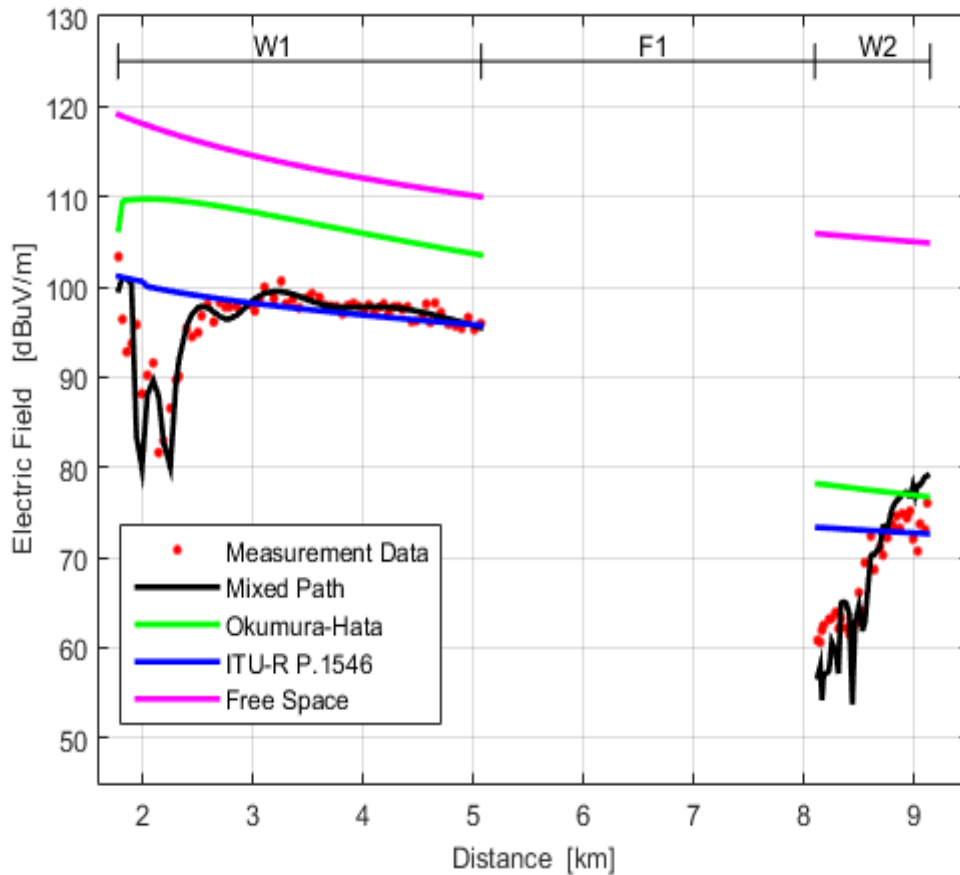


Source: Author

In contrast with Radial 1 over Water1, Fig. 52 illustrates that the values of E_{D-} , have a different amplitude in the first points of reception. On the other hand, the values of E_{D-Rh} , are higher than E_{D-} , due to the value of the angles of diffraction. For Water2 only one point of reception receives E_t , then the value of E_{D-} and E_{D-Rh} are the principal contributors, however, E_{D-Rh} , is the principal contributor in the first points of reception over Water2.

After showing the amplitude of the principal rays for Mixed Path model, Fig. 53 presents the total electric field. Furthermore, Okumura Hata, ITU-R P. 1546-5 and Mixed Path model are compared. The transition zone is different from Radial 1, then the interaction of the phase of the rays that arrive at the receiver is important. In contrast with Radial 1, the width of the city for Radial 2 is 1.4 km. In addition, in Fig. 52, Okumura Hata presents higher values than the measured data and ITU-R P.1546 has similar values to the measured values over Water1. Nonetheless, it does not follow the values in the transition zone. For Water2, Okumura Hata and ITU-R. P.1546 have higher values than measured data for distances up to 8.7 km.

Fig. 53. Results for Radial 2 over Water 1 and over Water 2.



Source: Author

The values of RMSE, as expected from Fig. 53, are the lowest for Mixed Path model, for each path separately and when Water1 and Water2 together. For Radial 2, ITU-R. P.1546-5 has a bigger RMSE value than for Radial 1 because of the transition zone in Water1. In the case of Water2, only Mixed Path has a low RMSE value. The optimized values of the electrical parameters of forest improve the RMSE for Water2 in 0.05 dB according to Table VIII.

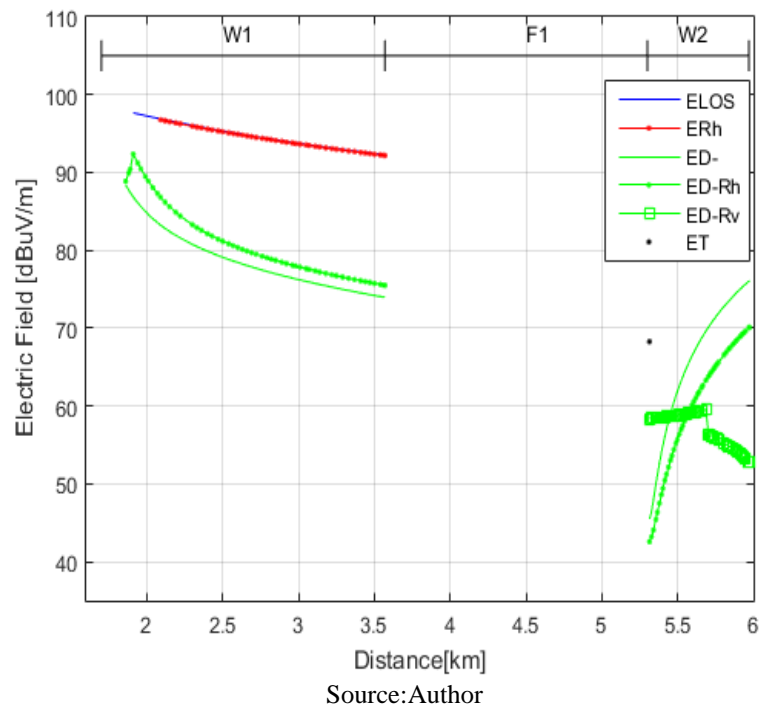
Table VIII. RMSE for Radial 2- M-DTV

	Radial 2 RMSE [dB]		
	Water1	Water2	Water1-Water2
Mixed Path	2.78	3.91	3.24
Okumura-Hata	12	10.26	11.39
ITU-R P.1546	4.9	7.025	5.78
Mixed Path ($\epsilon_f = 1.4$)	2.78	3.86	3.22

Radial 3

For Radial 3 the distances over Water1 and over Water2 are lower than for Radial 1 and Radial 2.

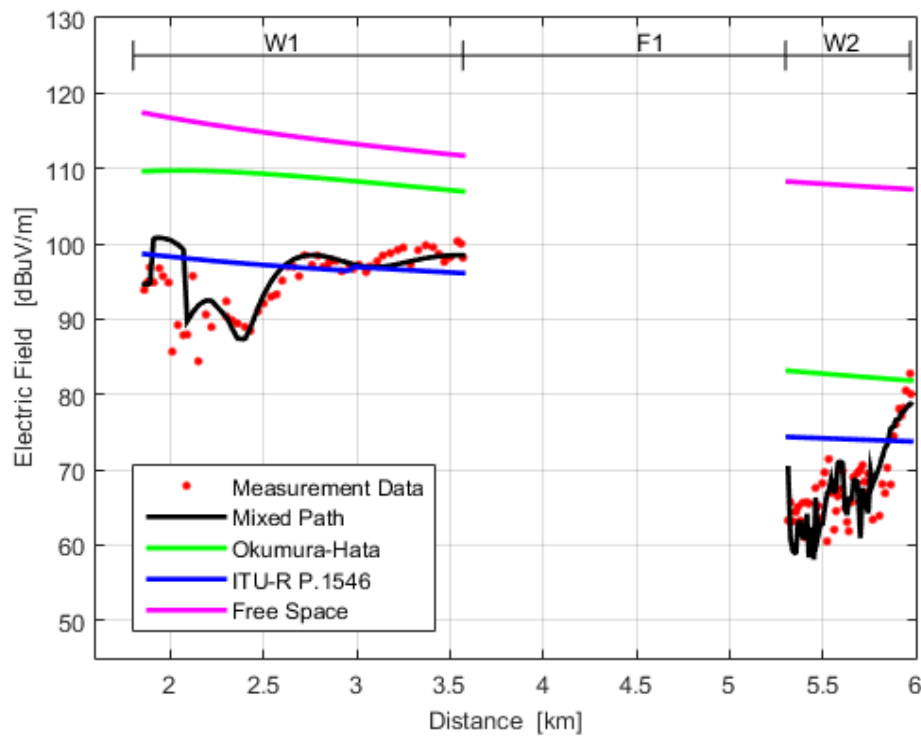
Fig. 54. Electric field amplitude of each ray calculated for Radial 3 over Water1 and Water2.



Furthermore, the forest is the shortest with 1.079 km of length, but the trees are taller than for Radial 1 and Radial 2. From Fig. 54, can be observed that the principal rays are E_{LOS} and E_{Rh} . For distances up to 2.5 km consider as the transition zone, diffracted rays influence the total electric field. For Water2, the behavior of each ray is similar to Radial 1 and Radial 2, there is only one point of reception for E_t , the E_{D-Rv} is the principal contributor in the first points of reception. After the addition of E_{D-} , E_{D-Rh} and E_{D-Rv} forms the total electric field.

In Fig. 55, Mixed Path model results are compared with measured data and predicted values using Okumura Hata and ITU-R P.1546-5. In Figure 54, as for Radials 1 and 2, Okumura Hata shows values higher than the measured values and ITU-R1546 presents values similar to those measured but does not model the transition zone. The Mixed Path model for Radial 3 uses a different parameter with respect to Radial 2, the width of the city, which in this case is 1.55 km, the width of the city varies in all three radials because for this parameter it is considered where the constructions finish and not where the city ends, since sometimes the constructions finish before arriving at the edge of the river. Again, the Mixed Path model is the one that presents the greatest coherence between the measured data and the predicted data.

Fig. 55. Results for Radial 3 over Water 1 and over Water 2.



Source: Author

In Table IX, the RMSE values for Mixed Path model are higher than in Radial 1 and Radial 2. However, they are in coherence with measurement data. The values of RMSE are

higher because the measurements in Radial 3 were carried out in front of a port, then the transition zone is not exactly as the evaluated with Mixed Path model. The presences of boats can modify the receiving electric field since the Mixed Path model considers only constructions of concrete on the border. Mixed path model has the lowest RMSE value, showing that it is valid for mixed path formed by City-River-Forest.

The optimized values of the electrical parameters of forest improve the RMSE for Water2 in 0.19 dB according with Table IX.

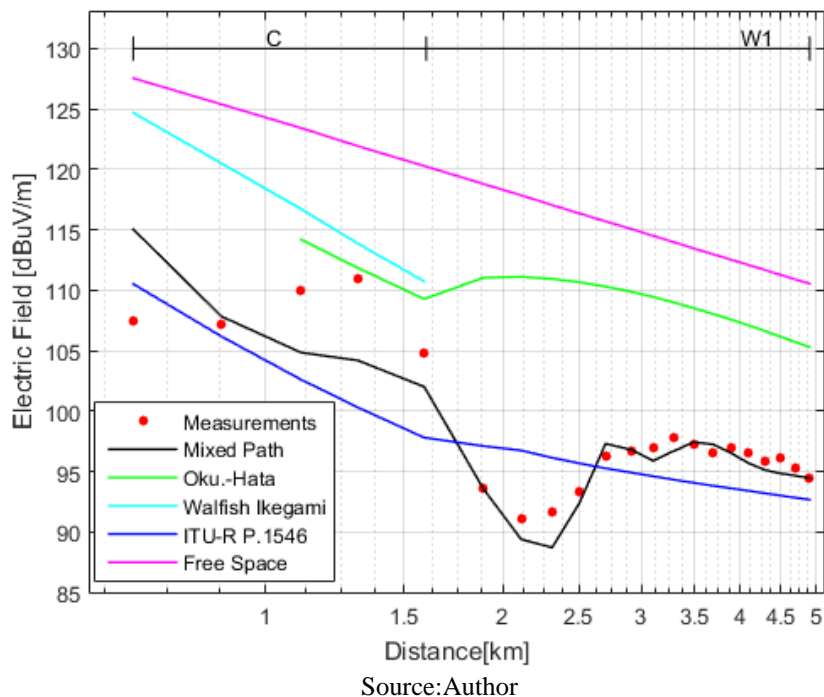
Table IX. RMSE for Radial 2- M-DTV.

	Radial 3 RMSE [dB]		
	Water1	Water2	Water1-Water2
Mixed Path	3.63	3.88	3.76
Okumura-Hata	14.51	15.62	15
ITU-R P.1546	5	8.22	6.73
Mixed Path ($\epsilon_f = 1.4$)	3.63	3.69	3.66

Annuli of City-Water1

In order to have a uniform scenario Annuli was used for distances of 200 meters as shown in Fig. 56. The annuli were not made for Water2 because the width of the forest was different for each radial.

Fig. 56. Results in annuli for Mixed Path



In Fig. 56 the measured data on the city present low values at small distances because there are buildings around the transmitter and near the measurement points. In the City path, the Walfish Ikegami model presented higher values than the measured data, in the case of Okumura-Hata values are from 1 km, these values are similar to the measured values. ITU-R P.1546 presents similar values to the measured data; however, it does not happen for the values of the transition zone. Mixed Path values are in agreement with the measured data.

The values of RMSE for all the radio propagation models are in Table X, Mixed Path model shows the lowest values among the radio propagation models evaluated for the three situations, radials, annuli, and city path. The average error for Mixed Path model in Radials is 3.4 dB, follow by ITU-R. P-1546, however, ITU-R 1546 does not predict values in good agreement with the transition zone city-water and forest-water.

Table X-RMSE for M-DTV

RMS Error [dB] for MDTV				
	Mixed Path	Okumura	Walfish Ikegami	– ITU-R P.1546
R1	2.56	9.65	-	4.97
R2	3.22	11.39	-	5.78
R3	3.66	15	-	6.73
Average Radials	3.15	12	-	5.82
Annuli	2.7	12.5	10.6*	4.3
City	6.17	10.7	8.8	7.0

*Walfish Ikegami was evaluated only in City, as Fig. 11 shows.

In order to know the attenuation caused by forest, Table XI compares the values of electric field calculated with Mixed Path for the first point behind the forest and the electric field calculated in the city in similar distances. The received electric field behind the forest is around 20 dB lower than electric field received in the city in similar distances.

Table XI- Comparison between electric field from City and Water2

City		Water2	
Distance [km]	Electric Field [dBuV/m]	Distance [km]	Electric Field [dBuV/m]
8.96	78	8.93 (R1)	58
7.89	80	8.12 (R2)	57
5.32	84	5.51 (R3)	58

5.4.2 Results for H-DTV

In the case of H-DTV Mixed Path model was compared with ITU-R P.1546-5 for rural areas. ITU-R P.1546-5 and Mixed Path values are greater than the Free Space (LOS) values as can be seen in Figs. 45 and 46. In the theory of two rays, there is an interference zone where the electric field values are higher or lower than LOS values. This zone of interference occurs for distances lower than the breakpoint distance. With the following equation is calculated the classical breakpoint distance [33]:

$$d_{b1} = \frac{4h_t h_r}{\lambda} \quad (129)$$

In literature there are several proposed equations for the break point distance, one developed for microcellular environments, is given by the following equation[42]:

$$d_{b2} = \frac{8.41 h_t h_r}{\lambda} \quad (130)$$

In [43], it is stated that in distances equal to:

$$d_{b3} = \frac{12 h_t h_r}{\lambda} \quad (131)$$

The value of the electric field is equal to the electric field in free space, for greater distances than d_{b3} the electric field is always smaller than the electric field in free space.

To calculate the break point distance, the receiver in the city for H-DTV is 18 m high and 6 m in Forest1 and Forest2. Therefore, using (129) the classical breakpoint distances are 14.2 km for the city and 4.7 km for Forest1 and Forest2. We can deduce that the city is in the interference zone and Forest1 and Forest2 are no longer in the interference zone. On the other hand, using (130) the break point distance for Forest1 e Forest2 is 10 km and with (131) the break distance point is 15 km. Therefore, they would be in the interference zone. Another explanation for the values greater than free space is the contribution of the diffracted beam on the corner of the building, the same one that is being added constructively to the direct beam.

In Figs. 57 and 58, the first point on Forest1 and Forest2 has a higher value due to the contribution of the reflected ray. In the case of ITU-R P.1546 the values on Forest1 and Forest2 are low and different from Mixed Path, because the recommendation considers grazing diffraction, this explains the low values.

In Fig. 59, for Radial 3 as well as Radial 1 and 2, the Mixed Path model values are higher than the LOS values. On the other hand ITU-R P.1546 for rural environments has similar results in the three Radials in the City Path but not in Forest1 and Forest2. The values In Forest1 and Forest2 are lower than the Mixed Path values. Additionally, in the Radial 3 for

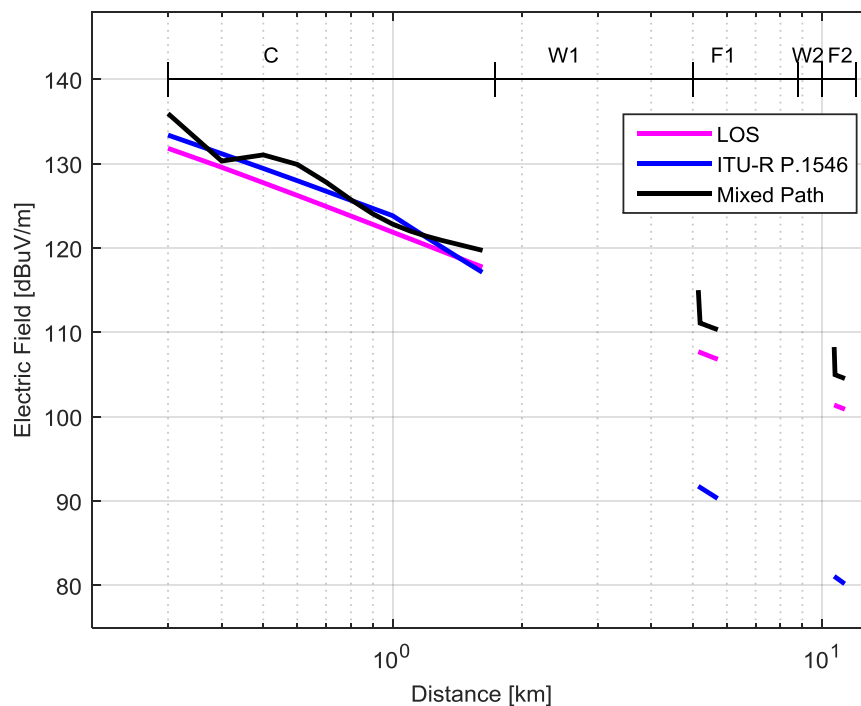
Forest1 Mixed Path model shows that the first reception point has a low value because the direct and reflected rays are in opposition of phase.

Mixed path model RMSE values are compared with ITU-R P.1546 RMSE values for rural areas in Table XII. The City Path shows low RMSE values, then Mixed Path and ITU-R P.1546 have similar values. The mixed City-Water1-Forest1-Water2-Forest2 path presents a high RMSE values because ITU-R P.1546 considers a non-line of sight reception with constructions of 10 m and Mixed Path considers line of sight.

Table XII- RMS Error for H-DTV

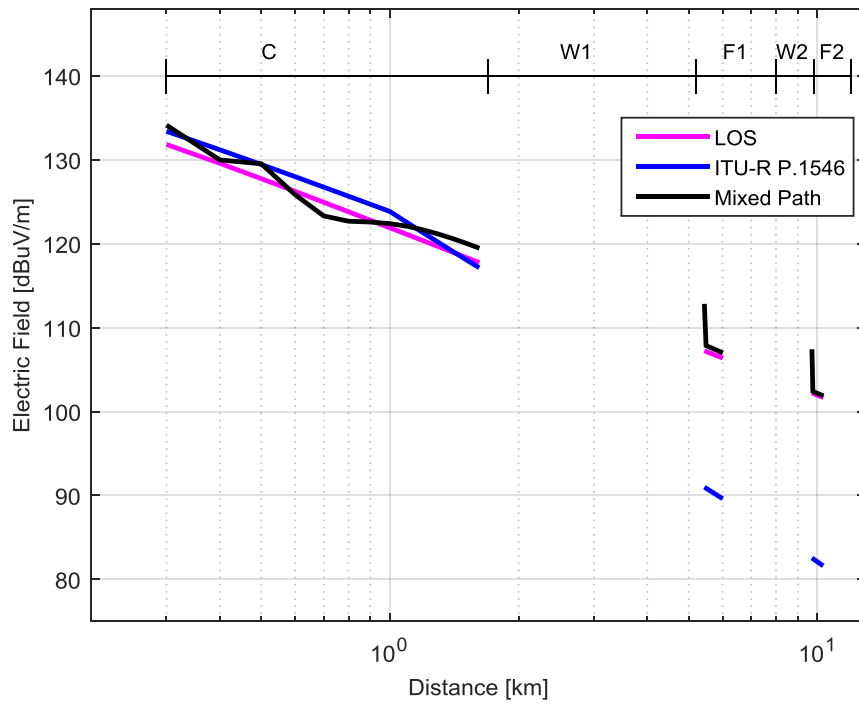
RMS Error [dB] for H-DTV				
Path	Radial 1	Radial 2	Radial 3	Average
Only City	1.4	1.8	1.3	1.5
Complete Path	19.5	16.7	15.1	17.1

Fig. 57. Radio propagation models results for H-DTV - Radial 1.



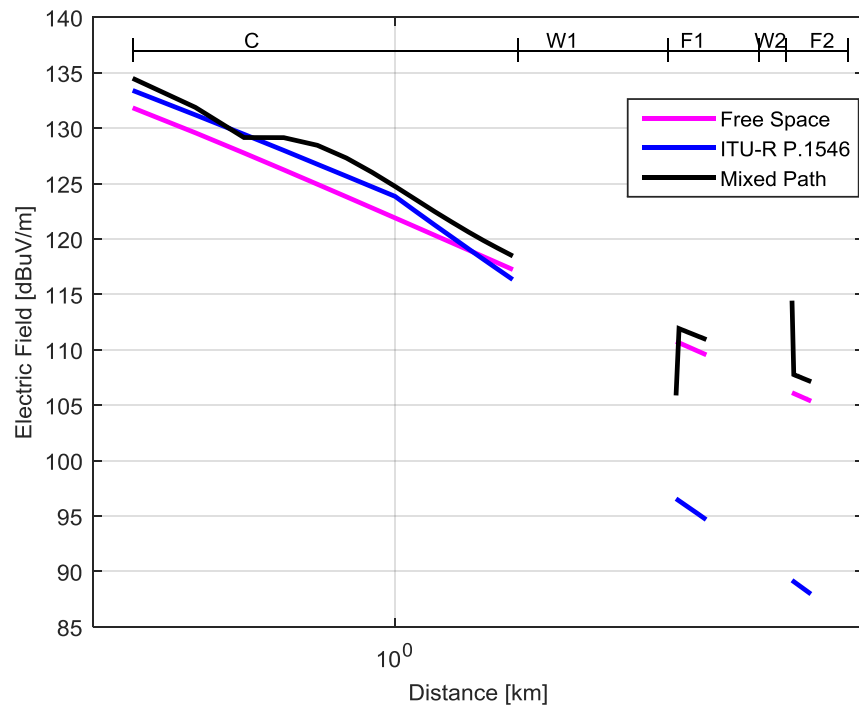
Source: Author

Fig. 58. Radio propagation models results for H-DTV - Radial 2.



Source: Author

Fig. 59. Radio propagation models results for H-DTV - Radial 3.



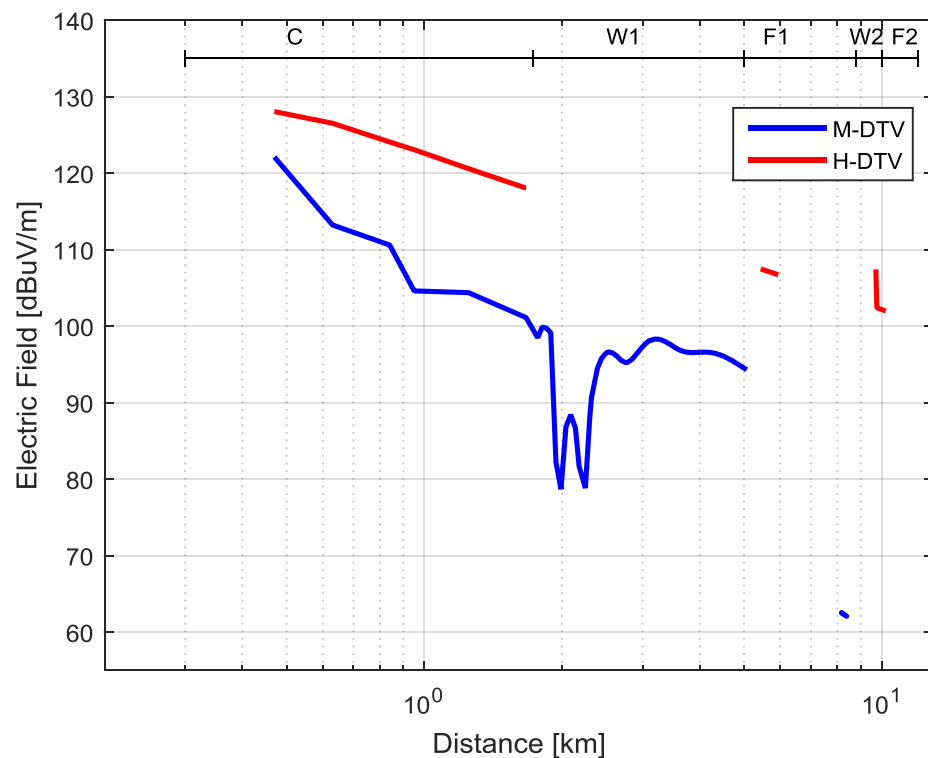
Source: Author

5.4.3 Comparison between H-DTV and M-DTV

Fig. 60 illustrates the total electric field values corresponding to Radial 2 for M-DTV and H-DTV. The electric field values for mixed City-Water1-Forest1-Water2-Forest2 path are estimated. The values of the electric field for H-DTV are higher than for M-DTV since H-DTV has a line of sight in all the reception points.

The electric field for M-DTV is calculated in City and over the Water1 and Water2, as shown in Fig. 59. For H-DTV, the electric field is calculated in City and on the border of Forest1 and Forest2. Then, the electric field for M-DTV is up to 19 dB less than the electric field for H-DTV in City path.

Fig. 60. Comparison of Mixed Path model results for Radial 2 between M-DTV and H-DTV.



Source: Author

5.5 Final Considerations

Mixed Path model for M-DTV parameters such as electrical parameters of forest affects the signal especially for distances near the forest. For H-DTV the level of the river can attenuate or increase the received signal, in order to avoid this variation for a receiver at a distance of 5 km the ideal antenna height is 11 m. The results for Mixed Path model are in agreement with measurement data in Belém of Pará.

Chapter 6 – Conclusions and Future Works

Dense forest and wide rivers characterize the Amazon Region. Then Mixed Path model can be used to plan or improve the coverage of radio telecommunication systems in mixed path environments for the UHF Band.

The range of frequencies of Digital TV can penetrate dense forests with kilometers of length, then it allows to study the signal behavior in the Amazon Region. Mixed Path model calculates electric field for a receiver at home (H-DTV), with a fixed external antenna. Furthermore, with the growing use of mobile devices, it was considering to design a model for mobile digital television) M-DTV, evaluating the propagation over rivers. Then Mixed Path model predicts the electric field for H-DTV and M-DTV.

The proposed model considers a scenario formed by City-Water1 –Forest1- Water2-Forest2. Forest produce more attenuation than buildings in City, for similar distances a receiver behind the forest receives an electric field around 20 dB lower than a receiver in the City.

GO and UTD are the technics used for Mixed Path model. M-DTV uses maximum nine rays based on the line of sight, reflection, diffraction, and refraction. In the case of HDTV are used maximum four rays: line of sight, reflection on the rooftop, reflection on the water and diffraction.

In order to incorporate the attenuation caused by City over Water1, in the total electric field is added an environmental correction factor. Measurement data in a mixed path in Belém-Pará validates the environmental correction factor.

The transition zone City-Water1 for M-DTV presents attenuation that depends on the height of the buildings in the city. The interaction of diffracted rays from the city and reflected rays over water are significant in the transition zone. After the transition zone, the main rays are the direct ray and reflected ray from the water.

The predicted values for H-DTV show higher values than the estimated values for M-DTV. In the City, the difference is up 19 dB, because H-DTV is calculated considering line of sight.

The electric field calculated for different electrical parameters of forest, show that for the reception points near the forest a sparse forest has higher electric field because of the transmitted ray that reaches the receiver, for medium forest the transmitted ray reaches maximum three reception points and for a dense forest transmitted ray reaches only one reception point. For points that are far from forest, the three types of forests have similar

values, for a sparse forest the diffracted reflected signal does not contribute to total electrical field, in the case of medium forest and dense forest diffracted reflected rays from forest contributes to the total electrical field specially in the first points of reception.

The Angle α is calculated from a top view to know the location of the receiver, the electric field decreases with the increase of the angle. For angles higher than 45 degrees with a constant distance the variation of the signal is around 4dB.

The increasing of the city width means the decreasing of the signal for a receiver in a constant distance since when the city is closer to the receiver, the city attenuates the signal.

The analysis of receiver and transmitter antennas height shows that signal has a tendency of increasing when the antennas height increases. Only when receiver is in line of sight with the transmitter, increasing the height of the transmitter antenna decreases the strength of the signal because the distance between transmitter and receiver increases.

For incidence angle air-forest, the electric field decreases with the increase of the incident angle. However, not all the incidence angles air-forest produce a ray transmitted from forest to air.

The level of the river affects the signal for a fixed receiver on the border of the Forest I at a distance of 5 km between transmitter and receiver. The best height of the receiver antenna is 11 m, at this height antenna receives the highest electric field even when the level of the river changes. On the other hand, for a receiver at 5 km of distance, the signal is attenuated more than 30 dB for 5 m height antenna when the level of the river decreases 1.6 m. Furthermore, for different distances between 1km and 5 km, the signal is stable for an antenna of 1 m height, with a minimum electric field around 109 dB μ V/m. The value of 109 dB μ V/m or greater is the maximum electric field for Digital TV according to ABNT 1506.

For M-DTV, for a 4 m receiver height, the signal does not present significant variation with the variation of the river level.

Mixed Path model presents the lowest average RMS error (3.15 dB) in relation to Okumura (12 dB) and ITU-R P.1546 (5.82dB) for Radials. Furthermore, Mixed Path for Annuli has an RMS error of 2.75 dB, Okumura (12.5 dB), ITU-R P.1546 (4.3 dB) and Walfish-Ikegami (10.6 dB). However, Walfish Ikegami was evaluated only in the city. Finally, the Mixed Path model has the best agreement for a mixed path in the Amazon region.

For future works, in order to validate the Mixed Path model for H-DTV, different measurement campaigns will be carried out in Belém of Pará considering the different positions for the reception antenna over the rooftop of the buildings. Furthermore, knowing

that Belem has at the center of the city high buildings between 20 and 30 floors, in the total electric field for H-DTV a diffracted ray can be added.

Additionally, Mixed Path model can add more rays in order to predict the electric field for higher frequencies, for example, 3.5 GHz. The goal is to calculate the dense forest attenuation since 3.5 GHz is the frequency for the fifth generation of mobile communications for outdoor scenarios. Then a tool to predict the electric field is fundamental in order to look for solutions to reduce attenuation and have good coverage. Then measurement campaigns near a dense forest in large and small scale will be carried out in Belem of Pará.

References

- [1] V. Britos and D. Simões, *To understand digital TV: technology, economy and society in the 21st century(in portuguese)*, Intercom, Brazil, Sao Paulo. 2011.
- [2] Teleco, *Analogical TV switch off*, Internal Report. Teleco, Brazil, 2018 (http://www.teleco.com.br/tvdigital_desligamento_novidades.asp). .
- [3] Teleco, *Broadcasting Brazil*,. Internal Report. Teleco, Brazil, 2016 (<http://www.teleco.com.br/nrtv.as>).
- [4] ABNT, ABNT NBR 15604: Digital Television-Receivers (in portugues),Norm, Brazil, Oct. 2017.
- [5] G. Filho, L. Leite, and C. Batista, “Ginga-J: The procedural middleware for the Brazilian digital TV system,” *Journal of the Brazilian Computer Society*, vol. 13, no. 1, March 2007, pp. 47–56.
- [6] W. Zhongyuan, R. Jin, and G. Junping, “Finite Mixture Noise Models for Mobile Digital Television Channel on Urban Terrestrial Broadcasting,” *IEEE Transactions on Broadcasting*, vol. 53, no. 4, Dec.2007, pp. 738–745.
- [7] Z. Wang, R. Jin, and Y. Jin, “Path Loss Prediction for Mobile Digital TV Propagation Under Viaduct,” *IEEE Transactions on Broadcasting*, vol. 57, no. 1, June. 2010, pp. 37–45.
- [8] B. Witvliet, “Mixed-Path Trans-Horizon UHF Measurements for ITU-R.P1546 Propagation Model Verification”, *Antennas and Propagation in Wireless Communications (APWC), IEEE-APS Topical Conference*, Torino, Italy, Sep. 2011.
- [9] J. Ong, H. Yan, S. Rao, and G. Shanmugam, “Indoor DTV Reception: Measurement Techniques,” *IEEE Transactions on Broadcasting*, vol. 50, no. 2, June. 2004,pp. 192–199.
- [10] J. Cavalcante, G. Siqueira, and R. Silva, “UHF Digital TV Radio Propagation Measurements: Fixed Reception Coverage Studies,” in *SBMO/IEEE MTT-S International Microwave and Optoelectronics Conference Proceedings*, Brazil, Dec. 2007.
- [11] J. Yan and J. Bernhard, “Investigation of the Influence of Reflective Insulation on Indoor Reception in Rural Houses,” *IEEE Antennas and Propagation Letters*, vol. 10, May 2011, pp. 423–426.
- [12] C. Teague, P. Lilleboe, and D. Barrick, “Estimation of HF Radar Mixed-Media Path Loss Using the Millington Method,” *IEEE/OES Eleventh Current, Waves and Turbulence Measurement (CWTM)*, St. Petersburg, FL, USA , May 2015.

- [13] C. Bourlier and G. Kubické, "Ground Wave Propagation Along an Inhomogeneous Rough Surface in the HF Band: Millington Effect for a Flat Earth," *IEEE Transactions on Geoscience and Remote Sensing*, vol. 49, no. 4, Aprl.2011, pp. 1374–1382.
- [14] G. Apaydin and L. Sevgi, "Numerical Investigations of and Path Loss Predictions for Surface Wave Propagation Over Sea Paths Including Hilly Island Transitions," *IEEE Transactions on Antennas and Propagation*, vol. 58, no. 4, Jan.2010, pp. 1302–1314.
- [15] G. Apaydin and L. Sevgi, "FEM-Based Surface Wave Multimixed-Path Propagator and Path Loss Predictions," *IEEE Antennas and Wireless Propagation Letters*, vol. 8, no. 3, Aug. 2009, pp. 1010–1013.
- [16] L. Sevgi, "A Mixed-Path Groundwave Field-Strength Prediction Virtual Tool for Digital Radio Broadcast Systems in Medium and Short Wave Bands," *IEEE Antennas and Propagation Magazine*, vol. 48, Oct.2006, pp. 19–27.
- [17] ITU-R, "Recommendation ITU-R P.1546-5: Method for point-to-area predictions for terrestrial services in the frequency range 30 MHz to 3000 MHz," 2013.
- [18] Y. Okumura and Et al., "Field Strength and Its Variability in VHF and UHF Land-Mobile Radio Service," *Review of the Electrical Communications Laboratory*, vol. 16, Oct.1968, pp. 9–10.
- [19] D. Cardoso and G. Calvacante, "A k-Ray Model For Mobile Systems in Environments With Abrupt Terrain Discontinuities.," in *Antennas and Propagation Society International Symposium*, 1996, vol. 2, pp. 1226–1229.
- [20] ITU-R, "Recommendation ITU-R P.833-9: Attenuation in vegetation," 2016.
- [21] G.P.S. Cavalcante, D. Rogers, and A. Giarola, "Radio Loss in Forests Using a Model with Four Layerd Media," *Radio Science*, vol. 18, no. 5, Sep. 1983, pp. 691–695.
- [22] J. Souza, F. Magno, Z. Valente, J. Costa, and G. Cavalcante, "Mobile Radio Propagation Along Mixed Paths In Forest Enviroment Using Parabolic Equation," *Microwave and Optical Technology Letters*, vol. 51, no. 4, Feb. 2009, pp. 1133–1136.
- [23] J. Yu, W. Chen, K. Yang, C. Li, F. Li, and Y. Shui, "Path Loss Channel Model for Inland River Radio Propagation at 1 . 4 GHz," *International Journal of Antennas and Propagation*, vol. 2017, Jan. 201, p. 1-15.
- [24] D. McNamara, C. Pistorius, and J. Malherbe, *The Uniform . Geometrical Theory of Diffraction*. Artech House, London,UK, 1990.
- [25] R. Luebbers, "Finite Conductivity Uniform GTD Versus Knife Edge Diffraction in Prediction of Propagation Path Loss.," *IEEE Antennas and Propagation*, vol. AP-32, no. 1, Jan. 1984, pp. 70–76.
- [26] F. Ikegami, S. Yoshida, T. Takeuchi, and M. Umehira, "Propagation Factors Controlling Mean Field Strength on Urban Streets," *IEEE Transactions on Antennas & Propagation*, vol. 32, no. 8, Aug. 1984, pp. 822–829.
- [27] J. Walfisch and H. Bertoni, "A Theoretical Model of UHF Propagation in Urban Environments," *IEEE Transactions on Antennas and Propagation*, vol. 36, no. 12, pp. 1788–1796, 1988.
- [28] COST 231, "Propagation prediction models," *Digital Mobile Radio Towards Future Generation Systems COST. 231 Final Report*, Brussels, Belgium, 1999.
- [29] N. A. Pérez García *et al.*, "Improved ITU-R model for digital terrestrial television propagation path loss prediction," *Electronics Letters*, vol. 53, no. 13, Jun. 2017, pp. 832–834.
- [30] G.P.S.Cavalcante and A. Giarola, "Optimization of radio communication in media with three layers," *IEEE Transactions on Antennas and Propagation.*, vol. 31, no. 1, Jan. 1983, pp. 141–145.
- [31] M. Hata, "Empirical Formula for Propagation Loss in Land Mobile Radio Services," *IEEE Transactions on Vehicular Technology*, vol. VT-29, no. 3, Aug. 1988, pp. 317–